The Pennsylvania State University
The J. Jeffrey and Ann Marie Fox Graduate School

ENTANGLEMENT IN ISOLATED QUANTUM SYSTEMS WITH NON-ABELIAN SYMMETRIES

A Dissertation in
Physics
by
Rishabh Kumar

Submitted in Partial Fulfillment
of the Requirements
for the Degree of

Doctor of Philosophy

May 2025

The dissertation of Rishabh Kumar was reviewed and approved by the following:

Eugenio Bianchi
Associate Professor of Physics
Dissertation Advisor, Chair of Committee

Marcos Rigol
Professor of Physics

Bangalore S. Sathyaprakash
Elsbach Professor of Physics and Professor of Astronomy and Astrophysics

Donghui Jeong
Professor of Astronomy and Astrophysics

Irina Mocioiu
Associate Professor of Physics
Director of Graduate Studies

Abstract

Entanglement lies at the heart of quantum mechanics, serving as a defining feature that sets quantum systems apart from their classical counterparts. When two or more subsystems interact, the resulting correlations cannot be fully explained by conventional classical theories, a phenomenon quantified by the concept of entanglement entropy. Many physical systems possess additional structures in the form of symmetries—ranging from simple charge conservation (Abelian) to more sophisticated gauge or rotational symmetries (non-Abelian). These symmetries impose constraints on both the dynamics and the entanglement structure. The study of properties of entanglement in such systems is grouped under the name symmetry-resolved entanglement. In Abelian cases, the total charge of a system splits neatly between subsystems and the reduced density matrix for a subsystem is block diagonal in the symmetry labels, making the analysis of symmetry-resolved entanglement straightforward. For non-Abelian symmetries, though, charges need not simply add or subtract, and this enriches the structure of entanglement considerably.

This thesis explores the role of entanglement in isolated quantum systems, focusing particularly on those systems which possess a rich symmetry structure, namely a non-Abelian symmetry. We introduce a general framework for understanding such symmetry-resolved states, showing how the Hilbert space decomposes into irreducible representations that carry distinct symmetry labels. A crucial idea here is the notion of subalgebras of observables that respect the underlying symmetry. For a given non-Abelian symmetry group G, this subset of observables remains invariant under its actions. This helps in redefining the notion of a subsystem in a manner that respects the symmetry and eventually leads to a reduced density matrix that is block-diagonal in the symmetry labels but continues to reflect internal entanglement. This leads to the concept of symmetry-resolved entanglement entropy, which quantifies accessible entanglement in an isolated quantum system in the presence of a symmetry. Focusing on compact, semisimple Lie groups, we derive exact formulas for the average and the variance of the typical

entanglement entropy for the ensemble of random pure states with fixed non-Abelian charges. By developing exact formulas for symmetry-resolved entropy and studying their asymptotic behavior for typical symmetry-resolved states, we offer a unifying perspective on how entanglement intertwines with the notions of eigenstate thermalization and chaos in quantum systems with nontrivial symmetries. Compared to the Abelian scenario, the local structure and non-Abelian symmetry together give rise to new phenomena. In particular, we find an asymmetry in the entanglement entropy upon interchanging the subsystems, which we illustrate explicitly through the calculation of the Page curve in an $SU(2)$-symmetric many-body model.

This framework deepens our understanding of the universal features of entanglement and opens new avenues for exploring how symmetry constrains and structures quantum correlations—relevant not only for fundamental theory but also for experimental platforms aiming to harness entangled states for quantum technologies. We propose multiple future applications ranging from quantifying entanglement in quantum gravity to studying the role of symmetry-resolved entanglement in the context of non-Abelian eigenstate thermalization.

Table of Contents

List of Figures

List of Tables

List of Symbols

Symbols from Quantum Physics

$\mathcal{H}$ Hilbert space.

$|\psi\rangle$ State wavefunction.

Π Projection operator.

ρ Density matrix.

$\rho_{\mathcal{A}}$ Reduced density matrix for subsystem A.

S_A Entanglement entropy for subsystem A.

S_{GA} G-local entanglement entropy.

S_{KA} K-local entanglement entropy.

$\langle S_A \rangle$ Typical entanglement entropy.

(ΔS_A) Variance around the typical entropy.

Symmetries & Algebras

G Symmetry group.

T^a Symmetry generators.

Q_k Casimir operator.

η^{ab} Cartan–Killing metric.

$\mathcal{A}$ Algebra of observables.

$\{.\}'$ Commutant of an algebra.

$\{.\}''$ Double commutant of an algebra.

$\mathcal{Z}$ Center of an algebra.

$\mathcal{A}_K$ Kinematical observables.

$\mathcal{A}_G$ G-invariant observables.

Many-Body System Symbols

N Number of particles (system size).

N_A Subsystem size (region A).

$\mathcal{H}^{(1/2)}$ One spin-$\frac{1}{2}$ Hilbert space.

$\mathcal{H}_N$ Many-body Hilbert space.

$\vec{S}_n$ Spin at site n.

S_n^i ith spin component.

σ^z Pauli Z-matrix.

$\vec{\sigma}$ Pauli matrices vector.

$\epsilon^{ij}{}_k$ Levi–Civita symbol.

$\vec{J}$ Total spin operator.

j Total spin quantum number.

$j_{\min}$, $j_{\max}$ Min/max total spin.

$\vec{L}$ Local total spin operator in A.

ℓ Subsystem spin quantum number.

$\ell_{\min}$, $\ell_{\max}$ Min/max subsystem spin.

$f = \frac{N_A}{N}$ Subsystem fraction.

$s = \frac{2j}{N}$ Spin density.

$t = \frac{2\ell}{N_A}$ Subsystem spin density.

Acknowledgments

This thesis would not have been possible without the support, guidance, and encouragement of numerous individuals who have accompanied me on this journey.

I would like to begin by expressing my deepest gratitude to my advisor, Prof. Eugenio Bianchi. He has always encouraged me to explore different ideas and his unwavering support has been instrumental throughout my graduate journey. His door was always open, whether it was for last-minute feedback on presentations or lively discussions on physics or any other topic under the sun. His cheerful demeanor and ever-present smile along with his kind and empathetic nature truly set him apart, and I feel incredibly fortunate to have had such an understanding mentor by my side.

I would also like to thank my committee members, Prof. Marcos Rigol, Prof. Bangalore S. Sathyaprakash and Prof. Donghui Jeong, whose valuable comments, insightful questions and constructive suggestions have improved my work in many ways. Their perspectives coming from their expertise in different areas of physics motivated me to think deeply about broadening the scope of my work.

I am also immensely thankful to Prof. Pietro Dona, who I believe has had a significant impact on my journey as a scholar. From diving into the intricacies of our research project to navigating through academic life, Pietro has been a valuable source of support. I would also like to express my gratitude towards Sean Prudhoe for his leadership and Prof. Sarah Shandera for her support during our work extending the KAQ framework. I would also like to extend my gratitude to my mentors at my undergrad institution, Prof. V. Ravishankar and Prof. Joyee Ghosh for sharing knowledge and perspectives on physics and academic life and motivating me to pursue higher studies.

A special note of appreciation goes to my wonderful roommates and friends, Anirban, Aviral and Ish. From cooking sessions to movie nights, they made my day-to-day life infinitely more enjoyable. Their help and moral support in figuring out both academic and personal challenges were invaluable. I fondly thank Mark, who has been an amazing friend from the very first day of grad school to the last,

whether hanging out, talking about life, or playing tennis and badminton. I would like to specially thank Erick for his friendship and for inviting me to play football (soccer) on the weekends and going out of his way to drive me there. I am also truly grateful for Monica's friendship and for her moral support and mentorship while facing academic challenges. I would also like to express my appreciation towards my friends and fellow IGC mates: Luis, Arnab, Neev, Mauricio, Chaosong, Daniel, and Samarth for being there when I needed them and always providing useful feedback on my work. I would like to acknowledge the support shown by Anirban and Manan during my job search for which I am forever grateful. The trinity of Divya, Becca and Ruobing deserves a special mention for being an amazing host to numerous parties and get-togethers. I would also like to thank members of my cohort: Le, Max, Kokkimedes, Da, Dan, Ziggy and Gavin for all the fun times.

I shall be forever grateful to the Department of Physics at Penn State for their support throughout my journey. The teaching opportunities really helped me improve my communication and presentation skills. Furthermore, I truly appreciated the various sports facilities and opportunities for outdoor adventures provided by Penn State. These provided the perfect balance between work and leisure. I would be remiss in my acknowledgements if I did not appreciate the foundation of my academic journey at my undergrad institution, Indian Institute of Technology, Delhi, and my school, The Mother's International School.

I owe my heartfelt thanks to my family for their love and faith in my aspirations. To my parents, Shikha and Shakti, your support, encouragement, and advice have given me the confidence to follow my dreams. Your sacrifices and belief in my abilities have been a constant source of motivation. To my brother, Smayan, thank you for spending time with me playing games and watching YouTube, reminding me of the importance of balance and perspective. You will always be special.

Finally, I would like to thank my better half in the true sense, Tanvi, for sticking with me all these years through thick and thin. You have never failed in motivating me and reminding me of my capabilities. Even though the time we spend together has always been limited, I have cherished every moment of it. Your love and support throughout this journey have been my source of strength and meant a lot to me.

This work was carried out with support from the National Science Foundation via Grant Nos. PHY-1806428 and PHY-2207851 as well as support from ID# 62312 grant from the John Templeton Foundation, as part of the project "The Quantum Information Structure of Spacetime" (QISS). The opinions expressed in this work are those of the author and do not necessarily reflect the views of either the National Science Foundation or the John Templeton Foundation. During my initial years, I was supported by the Bert Elsbach Graduate Fellowship in the Department of Physics for which I am very grateful. I am also thankful for the

Edward M. Frymoyer Honors Scholarship in the Department of Physics which I received in 2021 and 2022. I would like to thank the American Physical Society (APS) and the Braslau Family for supporting my trip to the APS March Meeting 2022 through the Braslau Family Travel Grant. I would also like to thank the Blaumann Foundation for support to participate in the QISS 2023 School where preliminary results of this thesis were first presented.

Chapter 1
Introduction

Entanglement can be seen as the hallmark of complex quantum systems. When the constituents of a system come into contact, they establish correlations that cannot be explained in terms of classical physics: they become entangled. This phenomenon has been put to use in many areas of interest like the study of thermalization in isolated quantum systems [1–3] and, as we will see in the next chapter, entanglement has been a central tool in the attempts to understand question of information loss in the evaporation process of black holes through Hawking radiation [4]. Remarkably, new phenomena arise from the interplay of entanglement, symmetries and constraints that a system can have [5]. In this thesis, we investigate these aspects in detail.

1.1 Entanglement and Typical States

The Hilbert space of any complex quantum system composed of multiple subsystems can be expressed as a tensor product of the Hilbert spaces corresponding to each subsystem. For simplicity, consider a bipartite system with two subsystems A and B. Then its Hilbert space can be expressed through the decomposition $\mathcal{H} = \mathcal{H}_A \otimes \mathcal{H}_B$, where $\mathcal{H}_A$ and $\mathcal{H}_B$ are the Hilbert spaces of subsyems A and B respectively. Given a pure state $|\psi\rangle$ of the system, we can quantify the entanglement of this state by considering the reduced density matrix, $\rho_A = \mathrm{tr}_B(|\psi\rangle\langle\psi|)$ and evaluating its von Neumann entropy, given by $S_A = -\mathrm{tr}_A(\rho_A \log \rho_A)$. S_A is often referred to as the entanglement entropy of the state. Interestingly, one can show that $S_A = S_B$ for a bipartite system in a pure state [6].

It is important to note that here we assume we know the complete structure of the system through the structure of its Hilbert space $\mathcal{H}$ and through that of its constituents $\mathcal{H}_A$ and $\mathcal{H}_B$. When such a system evolves without any interaction with its external environment, it is called an isolated quantum system. In such a system, the dynamics is governed by the Schrödinger equation, leading to unitary evolution that preserves the system's total energy as well as its quantum information. A key area of study in isolated quantum systems is the approach of its observables to thermal equilibrium, a process known as thermalization [1–3]. In classical systems, thermalization is often explained through ergodic dynamics, where the system explores all accessible microstates over time. However, in isolated quantum systems, the mechanism of thermalization is more intricate, where systems starting in a non-thermal state can end up in a thermal state under the influence of certain types of Hamiltonians. In these systems, the late-time properties of the entanglement entropy of pure states has been argued to be key to understanding thermalization in quantum systems [7], as it assumes the role the thermodynamic entropy for these systems. A related phenomenon is that of quantum chaos, where one studies quantum systems whose classical analogs exhibit chaotic behavior [8]. While classical chaos is characterized by sensitive dependence on initial conditions and exponential divergence of nearby trajectories, quantum systems do not have trajectories in phase space due to the uncertainty principle. As a result, quantum chaos explores how chaotic dynamics manifest in the underlying quantum regime, often focusing on the statistical properties of observables, energy levels, and eigenstates [9–12].

One of the ideas central to these phenomena is that of typical states and their entanglement [13–20]. For a given (high-dimensional) Hilbert space, a typical state is one which is randomly sampled from a known probability distribution on this space. The behavior of entanglement entropy in typical eigenstates of quantum-chaotic hamiltonians is consistent with Page's formula [21] and is characterized by the volume-law, i.e. the leading contribution to the entanglement entropy scales linearly with volume of the subsystem [13, 22]. An effective way to see the trend in the entanglement of typical states for multiple bipartitions of the same system is through the Page curve. The notion of Page curve for random states without constraints was first introduced in [21] motivated by the information puzzle in black

hole evaporation [4, 23, 24]. We look at Page's formula and curves in more detail in Chapter 2.

1.2 Symmetry-resolved Entanglement: Abelian Symmetries

So far, the discussion has hovered around general isolated quantum systems. However, physically motivated systems often possess additional structure in the form of symmetries. The role of symmetries in understanding the fundamentals of physical systems has been instrumental. Symmetry-breaking in quantum field theory, solutions to Einstein's equations argued on the basis of symmetries in general relativity and the study of topological materials in condensed matter physics are only a few examples of many such successful endeavors. In the context of isolated quantum systems, symmetries play a fundamental role as they result in conservation laws and constraints for physical quantities, including the entanglement entropy. The study of entanglement for quantum systems with a symmetry has been given the name of symmetry-resolved entanglement, and was introduced in [25–27]. A similar notion, the accessible entanglement entropy in the presence of symmetries and superselections rules, has been discussed in [28–34]

Most of the work in this area has been focused on quantum systems with Abelian symmetries like number conservation or charge conservation [35–64], (see [65] for a review). Consider a system composed of two parts A and B, with the total charge operator $Q = Q_A + Q_B$. We define the eigenstates $|\psi_q\rangle$ of the charge Q as symmetry-resolved states satisfying $Q|\psi_q\rangle = q|\psi_q\rangle$. For Abelian symmetries, as the total charge q is conserved, for every eigenvalue q_A of Q_A the corresponding eigenvalue of Q_B is fixed as $q_B = q - q_A$, which is why the Hilbert space for this system can be decomposed in the following manner

$$\mathcal{H}^{(q)} = \bigoplus_{q_A} \left(\mathcal{H}_A^{(q_A)} \otimes \mathcal{H}_B^{(q-q_A)} \right). \tag{1.1}$$

Note that, as $\left[|\psi_q\rangle\langle\psi_q|, Q\right] = 0$, we can show that the reduced density matrix com-

mutes with the charge in A, i.e., $[\rho_A, Q_A] = 0$. Note that the number of possible values of q_A is bounded by $dim(\mathcal{H}_A)$, which is why Q_A has a degenerate spectrum and can be decomposed into sectors corresponding to different charges as $Q_A = \oplus_{q_A} q_A \mathbb{I}_{n^{(q_A)}}$ where $n^{(q_A)}$ is the degeneracy of the eigenvalue q_A. Therefore, the reduced density matrix takes the block-diagonal form $\rho_A = \oplus_{q_A} p^{(q_A)} \rho_A^{(q_A)}$ with each block of definite charge q_A having probability $p^{(q_A)}$.

1.3 Symmetry-resolved Entanglement: Non-Abelian Symmetries

For non-Abelian symmetries the condition $q = q_A + q_B$ is not satisfied and the reduced state ρ_A has non-vanishing correlations for different values of q_A. This prevents us from using the above methodology to arrive at a block diagonal structure for the reduce state ρ_A. To illustrate the new aspects that arise in the presence of a non-Abelian symmetry, consider, for instance, a composite system that is invariant under the non-Abelian symmetry group $SU(2)$, with generators $\vec{J} = \vec{J}_A + \vec{J}_B$. Clearly, here a symmetry-resolved state cannot be a simultaneous eigenstate of the components J^x, J^y, J^z as these observables do not commute. The only simultaneous eigenstates have $\vec{J}^2 = 0$. Even if we were to diagonalize only a set of commuting observables such as $\vec{J}^2$ and J^z, we still face the issue that the non-Abelian charges are not additive over subsystems as, for instance, $\vec{J}^2 \neq \vec{J}_A^2 + \vec{J}_B^2$.

To facilitate understanding of the ideas that follow, we use a concrete example of a system of N spin-1/2 particles with $SU(2)$ invariant Hamiltonian. Our mathematical analysis only requires the symmetry group G, and the Hamiltonian is used here simply to provide a physical motivation. For instance, we can consider the random Heisenberg Hamiltonian [66,67]

$$H = \frac{1}{\sqrt{N}} \sum_{\substack{n,m=1 \\ n<m}}^{N} c_{nm}\, \vec{S}_n \cdot \vec{S}_m \;+\; \mu\, \vec{J}^2\,, \qquad \text{with} \quad \vec{J} = \sum_{n=1}^{N} \vec{S}_n, \tag{1.2}$$

where the coupling constants c_{nm} are assumed to be normally distributed with zero average and unit variance, $\vec{S}_n$ are the individual spin operators, and μ is a coupling constant. The system is invariant under global $SU(2)$ rotations generated by $\vec{J}$,

$$[H,\, J^i] = 0\,. \tag{1.3}$$

1.3.1 Hilbert Space Decomposition

This brings us to the first of the many defining questions around which this thesis is centered:

How does the Hilbert space of an isolated quantum system with a non-Abelian symmetry decompose?

This question can also be reworded as: *What is a suitable basis for the Hilbert space that respects the additional structure of a non-Abelian symmetry in our system?* To begin, let us note that given any symmtery group G there are two types of operators that immediately come to mind: (i) the generators of the symmetry $\{O_{sym}\}$, and (ii) the symmetry-resolved operators, i.e. operators $\{O_G\}$ that commute with the generators, satisfying $[O_G, O_{sym}] = 0$ for all O_{sym}. For the example at hand, $\{O_{sym}\}$ will be the observables acting on the rotational degrees of freedom, the J^i. While $\{O_G\}$ will be the observables which commute with all observables in J^i and can be called the rotationally invariant observables. Finally, the observables which are key to figuring out the decomposition of the Hilbert space are those that belong to the intersection $\{O_{sym}\} \cap \{O_G\}$. These observables are of course the Casimir operators for the group G, and the decomposition of the Hilbert space then takes the form of a direct sum over the eigenvalues of the Casimirs,

$$\mathcal{H} \;=\; \bigoplus_q \mathcal{H}^{(q)} \;=\; \bigoplus_q \big(\mathcal{H}^{(q)}_{\text{sym}} \otimes \mathcal{H}^{(q)}_G\big)\;, \tag{1.4}$$

which for our example is

$$\mathcal{H}_N \;=\; \bigoplus_j \mathcal{H}^{(j)}_N \;=\; \bigoplus_j \big(\mathcal{H}^{(j)}_{\text{sym}} \otimes \mathcal{H}^{(j)}_G\big)\;. \tag{1.5}$$

For an Abelian group, $dim(\mathcal{H}^{(q)}_{\text{sym}}) = 1$, which simplifies the decomposition $\mathcal{H} = \bigoplus_q \mathcal{H}^{(q)}_G$, making it convenient to eventually express the reduced state in a block

diagonal form.

1.3.2 Symmetry-resolved Observables and States

Now that we have the form of the Hilbert space, we can ask the question:

How do we define a symmetry-resolved state for this system?

In our example, each spin-j sector $\mathcal{H}_N^{(j)}$ contains $\big(2j+1\big) \times \dim \mathcal{H}_G^{(j)}$ mutually orthogonal states. The factor $\big(2j+1\big)$ accounts for the rotational degrees of freedom, which are spanned by the states $|j,m\rangle \in \mathcal{H}_{\text{sym}}^{(j)}$. The remaining degrees of freedom are rotationally invariant states, $|j,\chi_G\rangle \in \mathcal{H}_G^{(j)}$. Fig. 1.1 illustrates this structure. By definition, symmetry-resolved observables cannot create entanglement between the rotational and internal parts. Consequently, a symmetry-resolved state $|\psi_j\rangle$ must factorize as

$$|\psi_j\rangle = |j,\xi\rangle\,|j,\chi_G\rangle \qquad \text{with} \quad |j,\xi\rangle = \textstyle\sum_m \xi_m |j,m\rangle. \tag{1.6}$$

To see why this is relevant, consider a situation in which the parameter μ in Eq. 1.2 is large. In that case, the energy gap separating different spin-j sectors becomes quite large, making it impossible for the observables O_G (which are both rotationally invariant and symmetry-resolved) to induce high-energy transitions. Their matrix elements connecting different spin-j sectors vanish, and they also obey the selection rule $\Delta m = 0$. As a result, states that can be prepared or measured by these O_G observables necessarily take the factorized form above, ensuring that rotational and internal degrees of freedom remain unentangled.

1.3.3 Symmetry-resolved Subsystems and the Notion of Locality

The usual bipartitioning of the Hilbert space can also be done here, but that does not incorporate the presence of a symmetry in our system. Any definition of a subsystem will have to be compatible with Eq. (1.4) and should know about the symmetry of the system. So, it is crucial to ask:

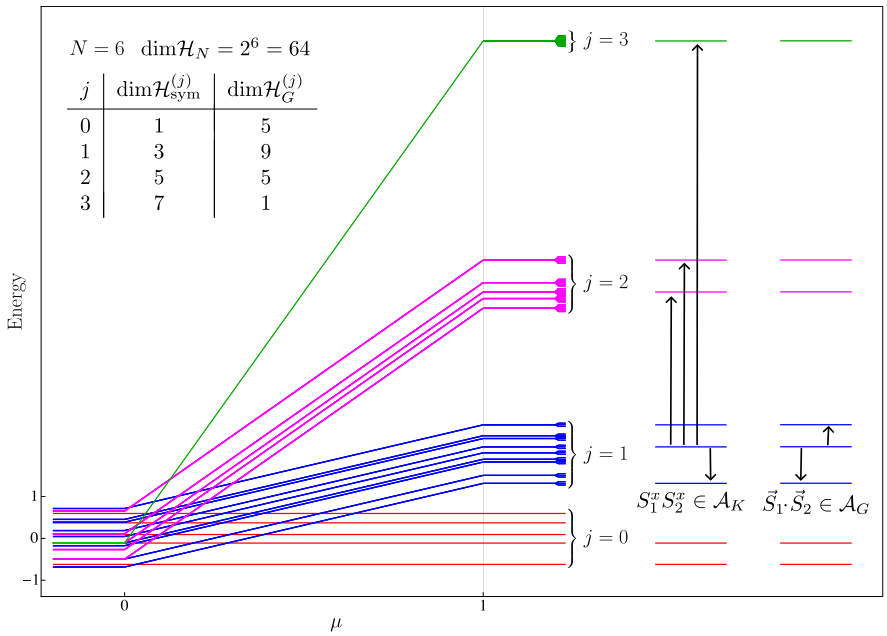

Figure 1.1. Energy spectrum of the $SU(2)$-invariant random Heisenberg Hamiltonian (1.2) with $N = 6$. On increasing the parameter μ, the spectrum splits in symmetry-resolved blocks $\mathcal{H}^{(j)}_N$ of fixed spin j, (1.5), with each block consisting of $(2j+1) \times \dim \mathcal{H}^{(j)}_G$ states as shown in the table. We show also the transitions induced by the local observable $S^x_1 S^x_2$ and by the G-invariant local observable $\vec{S}_1 \cdot \vec{S}_2$.

Can we redefine the notion of a subsystem in a manner suitable to a quantum system with a non-Abelian symmetry?

We define $\mathcal{A}_K$ as the algebra of observables defined at the kinematical level. Inside it, there is a subalgebra $\mathcal{A}_G \subset \mathcal{A}_K$ consisting of those observables that respect the symmetry group G. This means that $\mathcal{A}_G$ contains all operators that remain invariant under the symmetries of the dynamics. By contrast, $\mathcal{A}_K$ simply includes all possible observables we can construct without imposing that symmetry requirement.

A spin system such as the one described by Eq. (1.2) naturally provides a notion of locality because it is built out of individual spins $\vec{S}_n$. When we choose two subsets of spins, A and B, we can decompose the total Hilbert space as $\mathcal{H} = \mathcal{H}_A \otimes \mathcal{H}_B$. Observables O_A acting solely on the spins in A form a kinematically local subalgebra $\mathcal{A}_{KA} \subset \mathcal{A}_K$. However, these K-local operators are not required to preserve the symmetries of the dynamics. If we want operators that are both local to A

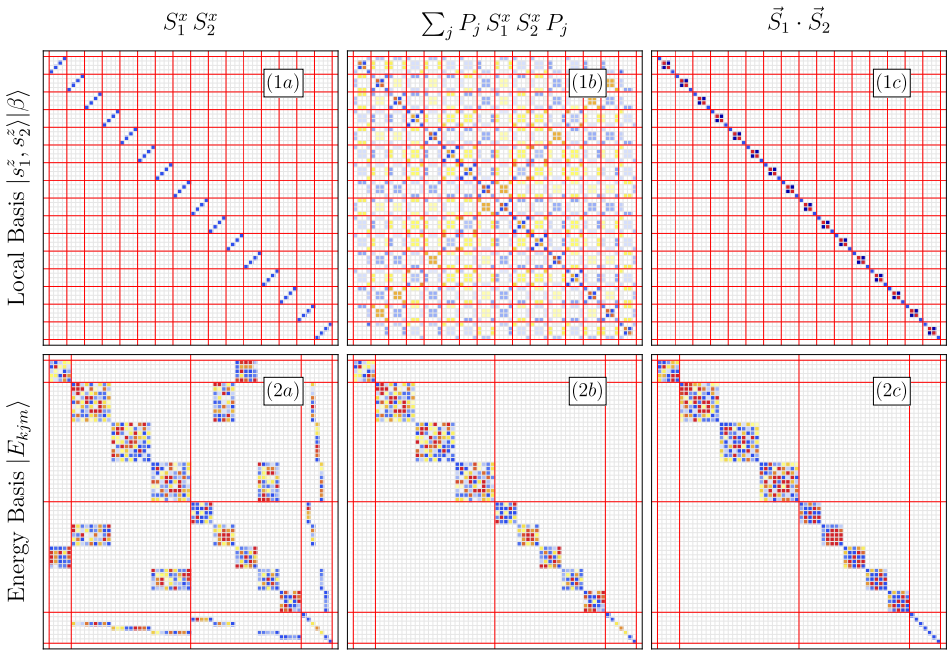

Figure 1.2. Matrix elements of the K-local observable $S_1^x S_2^x$ $(1a)$–$(2a)$, of its $SU(2)$-projected version $\sum_j P_j S_1^x S_2^x P_j$ $(1b)$–$(2b)$, and of the G-local observable $\vec{S}_1 \cdot \vec{S}_2$ $(1c)$–$(2c)$. Block-diagonal matrix elements in the spin-lattice basis $(1a)$ highlight the local or non-local nature of the observable, while the off-diagonal matrix elements in the energy basis $(2a)$ determine the possible transitions between energy levels. While the $SU(2)$-projected observable allows only $SU(2)$-invariant transitions ($\in \mathcal{A}_G$) $(2b)$, it is not a local observable ($\notin \mathcal{A}_{KA}$) $(1b)$. Hence, the $SU(2)$-projected observable is not G-local, (1.7). On the other hand, the observable $\vec{S}_1 \cdot \vec{S}_2 \in \mathcal{A}_{GA}$ is both local $(1c)$ and induces only $SU(2)$-invariant transitions $(2c)$.

and invariant under G, we must look instead at

$$\mathcal{A}_{GA} = \mathcal{A}_{KA} \cap \mathcal{A}_G \,. \tag{1.7}$$

This intersection captures observables that act only on spins in A and remain unchanged by the symmetry.

To see the difference, consider two example operators that act on spins 1 and 2. The operator $S_1^x\, S_2^x$ belongs to $\mathcal{A}_{KA}$ because it only involves spins 1 and 2, but it is not in $\mathcal{A}_{GA}$ since it breaks the rotational symmetry (it induces transitions between spin multiplets). On the other hand, $\vec{S}_1 \cdot \vec{S}_2$ is both local to spins 1 and 2 and rotationally invariant, so it belongs to $\mathcal{A}_{GA}$. This is depicted pictorially in Fig. 1.1 and through matrix elements in Fig. 1.2. Thus, this subalgebra of observables

enables us to define the notion of a subsystem compatible with the non-Abelian symmetry of the subsystem.

A symmetry-resolved state $|\psi_j\rangle$ restricted to these G-local observables is described by the density matrix ρ_{GA}. Because all operators in $\mathcal{A}_{GA}$ commute with the generators J_A^i of the symmetry within subsystem A, the density matrix ρ_{GA} also commutes with J_A^i. This commutation means ρ_{GA} is block-diagonal in the spin sectors labeled by j_A:

$$\rho_{GA} = \bigoplus_{j_A} p^{(j_A)} \rho_{GA}^{(j_A)} . \tag{1.8}$$

Such a structure also facilitates the decomposition of $\mathcal{H}_N^{(j)}$, the total Hilbert space of spin j, into a direct sum over all possible spins j_A in subsystem A:

$$\mathcal{H}_N^{(j)} = \mathcal{H}_{\text{sym}}^{(j)} \otimes \bigoplus_{j_A} \left(\mathcal{H}_{GA}^{(j_A)} \otimes \mathcal{H}_{GB}^{(j,j_A)} \right) . \tag{1.9}$$

This decomposition differs from the simpler one we would get in an Abelian symmetry scenario (such as total charge), where the labels merely add or subtract. Here, the rotational part $\mathcal{H}_{\text{sym}}^{(j)}$ cannot be factored away so simply, and the complement subsystem B depends on both j and j_A and not just on the difference $j - j_A$. If instead of the above procedure we took the usual approach of tracing out spins in B to get a reduced density matrix ρ_{KA}, we would be restricting the state to the subalgebra $\mathcal{A}_{KA}$. That choice would break the symmetry structure because ρ_{KA} does not have to commute with J_A^i. For this reason, in a non-Abelian symmetry setting, K-local observables can connect different spin sectors j_A as depicted pictorially in Fig. 1.1 and through matrix elements in Fig. 1.2.

One way to avoid these transitions and induce G-locality in K-local observables is through introducing projectors $P^{(j)}$ to forbid such transitions [68], but this comes at the price of losing strict locality as shown in Fig. 1.2. Defining a subsystem through $\mathcal{A}_{GA}$ avoids this problem because it ensures that any observable in that subsystem is both local and G-invariant. As a result, it provides a natural way to analyze parts of the system while consistently respecting the underlying symmetry.

1.3.4 Symmetry-resolved Entanglement Entropy and Typicality

How do we define the entanglement entropy for a symmetry-resolved state for isolated quantum systems with a non-Abelian symmetry?

We now have all the tools to obtain a closed form for the entanglement entropy for such a case. When we only have access to observables in the subsystem A that respect the symmetry group G, it means we can only measure operators in the subalgebra $\mathcal{A}_{GA}$. The entanglement we can observe in that situation is captured by the "accessible entanglement entropy," which comes from restricting the state to $\mathcal{A}_{GA}$. If the state of the system is a symmetry-resolved state $|\psi_j\rangle$, this accessible entropy is precisely the symmetry-resolved entanglement entropy S_{GA}. Mathematically, S_{GA} is the von Neumann entropy of the density matrix ρ_{GA}, and it decomposes into two parts. One term reflects the entropy within each block $\rho_{GA}^{(j_A)}$, weighted by its probability $p^{(j_A)}$, while the other term accounts for the classical entropy associated with the different spin sectors labeled by j_A.

$$S_{GA}(|\psi_j\rangle) = -\mathrm{tr}(\rho_{GA}\log\rho_{GA}) \;=\; -\sum_{j_A} p^{(j_A)}\,\mathrm{tr}\big(\rho_{GA}^{(j_A)}\log\rho_{GA}^{(j_A)}\big) \;-\sum_{j_A} p^{(j_A)}\log p^{(j_A)}\,. \tag{1.10}$$

It is important to emphasize that this G-invariant notion of entanglement entropy, S_{GA}, is different from the usual kinematical entanglement entropy S_{KA}. The latter, defined as $-\mathrm{tr}\big(\rho_{KA}\log\rho_{KA}\big)$, also captures the rotational degrees of freedom $|j,m\rangle$ that are not G-invariant.

Finally, after having developed methods to help us evaluate the symmetry-resolved entanglement entropy, we can ask the question

Given a random, symmetry-resolved state $|\psi_j\rangle$, what is the probability of obtaining a specific entanglement entropy, denoted by S_{GA}?

We wish to analytically compute an estimate of the probability distribution of S_{GA}, $P(S_{GA})$, through its mean and variance and then compare it to the numerical estimate of the probability distribution. If its variance scales inversely in the

subsystem size and vanishes in the thermodynamic limit, we would be able to argue that the average entanglement is also the typical entanglement. Remarkably, the exact formulas for the average $\langle S_{GA} \rangle$ and the variance $(\Delta S_{GA})^2$ derived in [69] for a general subalgebra of observables remain valid when one uses the dimensions of the Hilbert spaces appearing in the decomposition (1.9). For a system composed of $N \gg 1$ spins, we expect to see that the typical entanglement entropy $\langle S_{GA} \rangle$ completely characterizes the Page curve of subsystems [21, 69] since the variance of the probability distribution $P(S_{GA})$ is exponentially small in N.

1.4 Thesis Outline

This thesis is structured as follows:

- Chapter 2 goes through a pedagogical discussion covering the Page curve and the calculation of the typical entanglement entropy for a Haar-random state.
- In Chapter 3, we explain how to operationally define a subsystem by means of a subalgebra of observables, and we establish the fundamental expression for the typical entanglement entropy in full generality. The results presented in this chapter are based on Sec. 2 of [5].
- Then, in Chapter 4, we introduce a non-Abelian symmetry group and derive the decomposition (1.8)–(1.9) for an arbitrary group G, without imposing any locality constraints. The results presented in this chapter are based on Sec. 3 of [5].
- In Chapter 5, we address the role of locality and propose the concept of G-local observables in many-body systems, based on the definition (1.7). The results presented in this chapter are based on Sec. 4 of [5].
- We turn to many-body spin systems featuring $SU(2)$ symmetry in Chapter 6, where we obtain the exact expressions for the $SU(2)$ symmetry-resolved entanglement entropy of typical states. The results presented in this chapter are based on Sec. 5 of [5].
- In Chapter 7, we derive the large-system asymptotics of the $SU(2)$ symmetry-resolved typical entropy (see also App.A). The results presented in this

chapter are based on Sec. 6 of [5].

- In addition to this, Appendix B contains findings of a paper in progress, focused on studying the temporal behaviour of the entanglement entropy in systems governed by random matrix Hamiltonians. Starting from a factorized state, we characterize the short-time and late-time behaviors of the entanglement entropy and compute the typical entanglement entropy in time. We also extend our analysis to gaussian states in random quadratic fermionic Hamiltonians.

- Finally, Chapter 8 provides a summary of our findings and elaborates on potential research directions.

Chapter 2
Page Curves

2.1 Motivation: Black Hole Information Puzzle

Black holes have long been objects of study in general relativity. A puzzle arises when one considers black holes alongside the fundamental principles of quantum mechanics. Quantum physics with its principle of unitarity tells us that information in any isolated quantum system's initial state must be preserved. However, taking a look at black hole evaporation, first described by Hawking [23], suggests that radiation emerging from the black hole is featureless (or "thermal") and appears to carry little information of what formed the black hole in the first place. This question of whether, and how, black holes preserve information is known as the black hole information puzzle [4, 24].

One leading framework, hypothesized by Page [4], treats the black hole and its surroundings as two subsystems of a single, larger isolated quantum system. The black hole itself is described by an entropy known as the Bekenstein-Hawking entropy, which is proportional to its horizon area. Additionally, any radiation in a box around the black hole has its own thermodynamic entropy. In a typical analysis, each subsystem has a Hilbert space whose dimension depends on its entropy: a subsystem with entropy s has a Hilbert-space dimension roughly e^s. When the black hole subsystem (entropy $s_h \simeq \log n$) and the radiation subsystem (entropy $s_r \simeq \log m$) are combined into an isolated quantum system, the overall state is assumed to be pure. As a result of this construction, it is possible for the the black hole and radiation to be entangled.

In quantum physics, entropy can be understood as a measure of uncertainty of measurement outcomes: given an observable O which can result in measurement outcomes $\{o_i\}$ with probabilities $\{p_i\}$, the entropy of measurement for O is given by $-\sum_i p_i \log p_i$. Within this framework, one defines the von Neumann entanglement entropy to measure how mixed or thermal each subsystem appears when looked at individually. Specifically, if the radiation subsystem has a density matrix ρ_r, the von Neumann entropy is $S_r = -\mathrm{tr}(\rho_r \log \rho_r)$. A closely related measure, known as the information in the radiation, is $I_r = s_r - S_r \simeq \log m - S_r$. This quantity gauges the extent to which the radiation retains details of the overall state, as opposed to looking completely thermal. When I_r is small, the radiation carries little discernible information; when I_r is large, it encodes more of the black hole's microscopic state.

An especially important concept here is that of typicality, which states that, for large Hilbert spaces, a randomly chosen pure state is very nearly maximally entangled, with the difference from maximal entanglement scaling inversely with the Hilbert space dimension. Consequently, given a randomly chosen pure state, any single subsystem of such a large system usually appears thermal if its dimension is significantly smaller than that of the complement. Page conjectured the following form for the typical entanglement entropy of a subsystem [21] under the assumption $m \leq n$

$$S_r = \sum_{k=n+1}^{mn} \frac{1}{k} - \frac{m-1}{2n}, \tag{2.1}$$

which was later proven in [70–72]. Additionally, it was proven that for $1 \ll m \leq n$ this reduces to the form

$$S_r \simeq \log m - \frac{m}{2n}, \tag{2.2}$$

which tells us that the information in the smaller subsystem is

$$I_r \simeq \frac{m}{2n} \sim \frac{1}{2} \mathrm{e}^{s_r - s_h}. \tag{2.3}$$

In the regime $m > n$, when the radiation subsystem becomes the bigger subsystem, we use the fact that $S_r = S_h$ to calculate

$$I_r = \log m - \log n + I_h \simeq \log m - \log n + \frac{n}{2m}. \tag{2.4}$$

For the black hole + radiation system, if the black hole has a large entropy and the radiation entropy is initially small, using Eqs. (2.2) and (2.3) we can observe that early Hawking radiation is expected to look almost thermal and carry minimal information. However, as the black hole evaporates, it loses mass and its entropy decreases. Meanwhile, the radiation entropy grows as more quanta accumulate outside. Eventually, once the radiation becomes the larger subsystem, typicality arguments through Eq. (2.4) suggest that it can carry a significant portion of the overall quantum information. This phenomenon is depicted in Fig. 2.1.

It is this plot for the typical entanglement entropy vs. the subsystem size that has been of importance in studies of typical entanglement in condensed matter theory, and has been named the Page curve. In the next section, we look at a more technical derivation of the formula for the typical entanglement entropy whose approximate form Page conjectured in 1993.

2.2 Derivation of the Page Formula

We begin with a bipartite quantum system composed of two subsystems A and B. Subsystem A has a Hilbert-space dimension d_A, and subsystem B has a Hilbert-space dimension d_B. Consequently, the combined system resides in a Hilbert space $\mathcal{H} = \mathcal{H}_A \otimes \mathcal{H}_B$ of dimension $d = d_A \times d_B$. We consider a pure state $|\psi\rangle \in \mathcal{H}$, chosen at random according to the uniform (Haar) measure on the unit sphere in $\mathbb{C}^{d_A d_B}$. Our objective is to determine the *typical* (or average) entanglement between A and B quantified via the von Neumann entropy of the reduced density matrix of subsystem A. Although there are multiple ways in which one can derive Page's formula, we are going to be looking at one in particular. The derivation is centered around the idea that the typical entanglement entropy of such a system can be expressed in the form

$$\langle S_A \rangle = -\langle \mathrm{tr} \rho_A \log \rho_A \rangle = \lim_{r \to 1} \partial_r \langle \mathrm{tr}(\rho_A^r) \rangle. \tag{2.5}$$

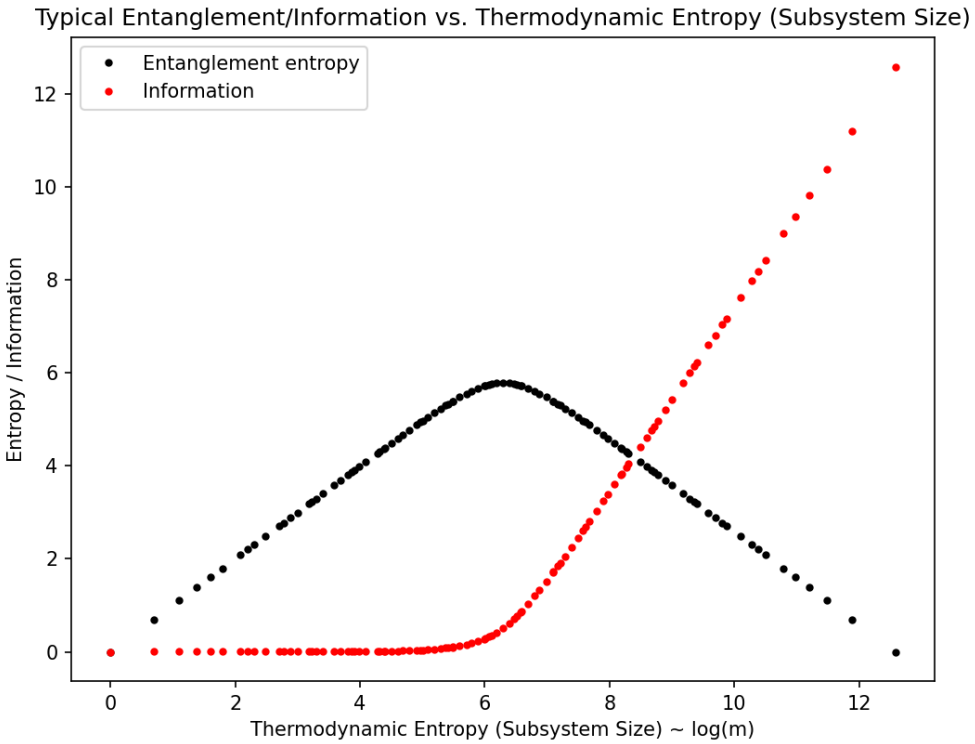

Figure 2.1. For the black hole + radiation system of dimension $mn = 291600$. If the black hole has a large entropy and the radiation entropy is initially small, using Eqs. (2.2) and (2.3) we can observe that early Hawking radiation is expected to look almost thermal and carry minimal information. However, as the black hole evaporates, it loses mass and its entropy decreases. Meanwhile, the radiation entropy grows as more quanta accumulate outside. Eventually, once the radiation becomes the larger subsystem, typicality arguments through Eq. (2.4) suggest that it can carry a significant portion of the overall quantum information.

For this reason, our goal is to evaluate the average $\langle \mathrm{tr}(\rho_A^r) \rangle$, where $\rho_A = \mathrm{tr}_B\big(|\psi\rangle\langle\psi|\big)$.

2.2.1 Defining the Measure Over Haar Random States

Starting with a fixed orthonormal basis $\{|n\rangle\}$ of $\mathcal{H}$, we write

$$|\psi\rangle \;=\; \sum_{n=1}^{d_A d_B} \psi_n \, |n\rangle, \quad \text{where} \quad \sum_{n=1}^{d_A d_B} |\psi_n|^2 \;=\; 1.$$

Because $|\psi\rangle$ is assumed to be uniformly distributed (the *Haar* or *uniform* measure on the unit sphere in $\mathbb{C}^{d_A d_B}$), the probability distribution over the complex coefficients $\{\psi_n\}$ is given schematically by

$$d\mu(\psi) \;\propto\; \delta\Big(1 - \sum_{n=1}^{d_A d_B} |\psi_n|^2\Big) \prod_{n=1}^{d_A d_B} d(\mathrm{Re}\,\psi_n)\, d(\mathrm{Im}\,\psi_n). \tag{2.6}$$

To proceed, we observe that every state in $|\psi\rangle = \sum_{i,j=1}^{d_A,d_B} c_{ij}|a_i\rangle|b_j\rangle$ where $d_A \leq d_B$, can be rewritten as $|\psi\rangle = \sum_{i=1}^{d_A} \gamma_{ij}|a_i^{'}\rangle|b_i^{'}\rangle$, where $|\gamma_i|^2 = \lambda_i$ and

$$\sum_{i=1}^{d_A} |\gamma_i|^2 = 1. \tag{2.7}$$

This set of normalized states have $2d_A d_B - 1$ free parameters, incorporating for 2 free parameters for every complex entry in the state and also for the normalization constraint $\sum_{i,j}^{d_A,d_B} |c_{ij}|^2 = 1$. Moreover, a particular sample of the c_{ij}'s fixes the γ_i's as follows

$$\gamma_k = \sum_{i,j=1}^{d_A,d_B} c_{ij}\; \langle a_k^{'}|a_i\rangle\langle b_k^{'}|b_j\rangle. \tag{2.8}$$

This along with Eq. (2.7) results in an additional $m-1$ constraints. Therefore, the number of free parameters in our space is actually $2d_A d_B - d_A$. The measure over the state $d\mu(\psi)$ can then be transformed into a measure over the eigenvalues of the reduced state $\{\lambda_i\}_{i=1}^{d_A}$ [73] as

$$d\mu(\psi) \to d\mu(\lambda_1,\ldots,\lambda_{d_A}) \propto \delta\Big(1-\sum_{i=1}^{d_A}\lambda_i\Big)\, \Delta^2(\lambda_1,\ldots,\lambda_{d_A}) \prod_{1\leq k\leq d_A} \lambda_k^{d_B-d_A} d\lambda_k, \tag{2.9}$$

where

$$\Delta^2(\lambda_1,\ldots,\lambda_{d_A}) = \prod_{n<m}^{d_A} |\lambda_n - \lambda_m|^2 \tag{2.10}$$

is the squared Vandermonde determinant. Then, we want to evaluate

$$\langle \mathrm{tr}(\rho_A^r)\rangle = \int \Big(\sum_{i=1}^{d_A} \lambda_i^r\Big) d\mu(\lambda_1,\ldots,\lambda_{d_A}) \tag{2.11}$$

Performing a change of variables $q_a = \zeta\lambda_a$ where $q_a \in [0, \infty)$ results in the integral

$$\langle \mathrm{tr}(\rho_A^r) \rangle = \frac{Z}{\Gamma(d_A d_B + r)} \int \Big(\sum_{i=1}^{d_A} q_i^r \Big) \Delta^2(q_1, \ldots, q_{d_A}) \prod_{1 \le k \le d_A} q_k^{d_B - d_A} \mathrm{e}^{-q_k} dq_k, \quad (2.12)$$

where Z includes all undermined factors including normalization constants. Noting that the integral does not distinguish between the q_i's allows us to drop the sum

$$\langle \mathrm{tr}(\rho_A^r) \rangle = \frac{Z d_A}{\Gamma(d_A d_B + r)} \int q_i^r \, \Delta^2(q_1, \ldots, q_{d_A}) \prod_{1 \le k \le d_A} q_k^{d_B - d_A} \mathrm{e}^{-q_k} dq_k. \quad (2.13)$$

2.2.2 Simplifying Using Generalized Laguerre Polynomials

Next, we use the fact that the value of a determinant does not change if the multiple of any one row is added to a different row, to rewrite the Vandermonde determinant in terms of generalized Laguerre polynomials [72]. The generalized Laguerre polynomials are defined as

$$L_k^{(d_B - d_A)}(q) \;=\; (-1)^k k! \sum_{r=0}^{k} \binom{k + d_B - d_A}{r + d_B - d_A} \frac{(-1)^r \, q^r}{r!}. \quad (2.14)$$

Then, we can write

$$\langle \mathrm{tr}(\rho_A^r) \rangle = \sum_{i_k, j_k = 0}^{d_A - 1} \frac{Z d_A \varepsilon_{i_1 i_2 \ldots i_{d_A}} \, \varepsilon_{j_1 j_2 \ldots j_{d_A}}}{\Gamma(d_A \, d_B + r)} \times \int q_1^r \prod_{k=1}^{d_A} L_{i_k}^{(d_s - d_A)}(q_k) L_{j_k}^{(d_B - d_A)}(q_k) q_k^{d_B - d_A} e^{-q_k} dq_k,$$

where ε is a fully antisymmetric tensor with d_A indices satisfying

$$\sum_{i_2, \ldots, i_{d_A}} \varepsilon_{i_1 i_2 \ldots i_{d_A}} \varepsilon_{j_1 i_2 \ldots i_{d_A}} \propto \delta_{i_1 j_1}. \quad (2.15)$$

Using this along with the orthonormality condition for Laguerre polynomials

$$\int_0^\infty L_i^{(d_B - d_A)}(q) L_j^{(d_B - d_A)}(q) q^{d_B - d_A} e^{-q} dq = \Gamma(i+1)\Gamma(d_B - d_A + i + 1)\delta_{ij}, \quad (2.16)$$

leads to a simplified esxpression for the integral

$$\langle \mathrm{tr}(\rho_A^r)\rangle = \frac{\tilde{Z}}{\Gamma(d_A d_B + r)} \sum_{i=0}^{d_A-1} X_i(r), \tag{2.17}$$

where $\tilde{Z}$ is the modified prefactor and

$$X_i(r) = \frac{1}{\Gamma(i+1)\Gamma(d_B - d_A + i + 1)} \int_0^\infty q^r \left(L_i^{(d_B-d_A)}(q)\right)^2 q^{d_B-d_A} e^{-q} dq. \tag{2.18}$$

Using the orthonormality condition we note that $X_i(0) = 1$, which when combined with Eq. (2.17) leads us to

$$\langle \mathrm{tr}(\rho_A^0)\rangle = d_A = \frac{\tilde{Z} d_A}{\Gamma(d_A d_B)}, \tag{2.19}$$

giving us $\tilde{Z} = \Gamma(d_A d_B)$. We recall that the (generalized) Laguerre polynomials $L_k^{(\alpha)}(q)$ admit the generating function

$$F(t,q) = \sum_{k=0}^{\infty} \frac{(-1)^k}{k!} t^k \, L_k^{(d_B-d_A)}(q) = \frac{1}{\big(1-t\big)^{1+d_B-d_A}} \mathrm{e}^{-\frac{t}{1-t}q}, \tag{2.20}$$

From this, one obtains

$$L_i^{(d_B-d_A)}(q) = (-1)^i \left[\frac{d^i}{dt^i} F(t,q)\right]_{t=0}. \tag{2.21}$$

Using Eqs. (2.20) and (2.21), we get

$$\begin{aligned} X_i(r) &= \frac{1}{\Gamma(i+1)\Gamma\big(d_B - d_A + i + 1\big)} \\ &\quad \times \left[\frac{d^i}{dx^i}\frac{d^i}{dy^i} \int_0^\infty q^{d_B-d_A+r} \mathrm{e}^{-q} F(x,q) F(y,q) dq\right]_{x=0,y=0} \\ &= \frac{\Gamma\big(d_B - d_A + r + 1\big)}{\Gamma(i+1)\Gamma\big(d_B - d_A + i + 1\big)} \\ &\quad \times \left[\frac{d^i}{dx^i}\frac{d^i}{dy^i} (1-x)^r (1-y)^r (1-xy)^{-d_B+d_A-r-1}\right]_{x=0,y=0} \end{aligned}$$

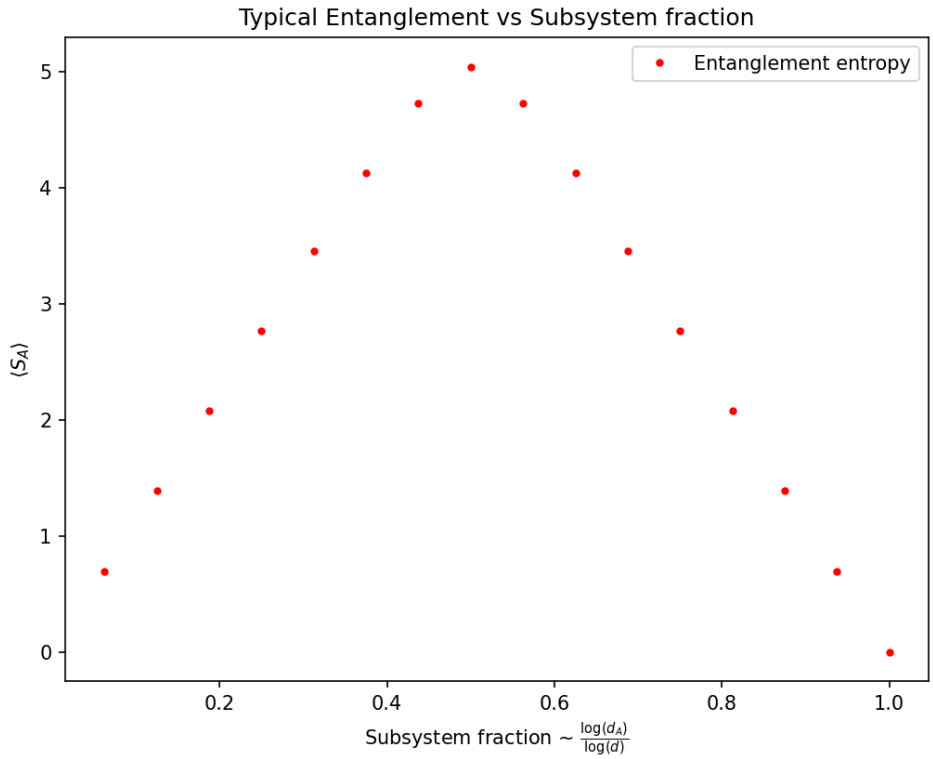

Figure 2.2. Page curve for a system with dimensions: $d = 2^{16}$. The plot shows the variation of the typical entanglement entropy $\langle S_A \rangle$ vs the subsystem fraction.

$$= \frac{\Gamma(i+1)\Gamma(r+1)^2}{\Gamma(d_B - d_A + i + 1)} \sum_{p=0}^{d_A-1} \frac{\Gamma(d_B - d_A + r + p + 1)}{\Gamma(p+1)\Gamma(i-p+1)^2\Gamma(r-i+p+1)^2}.$$

Finally, we evaluate the typical entanglement entropy as

$$\langle S_A \rangle = -\lim_{r\to 1} \partial_r \langle \mathrm{tr}(\rho_A^r) \rangle = -\lim_{r\to 1} \partial_r \Big[\frac{\Gamma(d_A d_B)}{\Gamma(d_A d_B + r)} \sum_{i=0}^{d_A-1} X_i(r) \Big], \tag{2.22}$$

which after evaluating the derivatives gives us for $d_A \leq d_B$

$$\langle S_A \rangle = \Psi\big(d_A\, d_B + 1\big) - \Psi\big(d_B + 1\big) - \frac{d_A - 1}{2d_B}; \quad (d_A \leq d_B). \tag{2.23}$$

To get the other half of the Page curve ($d_A > d_B$), we exchange d_A and d_B

$$\langle S_A \rangle = \Psi\big(d_A d_B + 1\big) - \Psi\big(d_A + 1\big) - \frac{d_B - 1}{2d_A}; \quad (d_A > d_B). \tag{2.24}$$

We can also extend this derivation to calculate $\langle S_A^2 \rangle$ and ΔS_A, as well as the average of other higher moments of S_A. A plot of $\langle S_A \rangle$ against subsystem fraction $\frac{\log(d_A)}{\log(d)}$ is shown in Fig. 2.2.

2.3 Incorporating Symmetry Constraints

So far, the discussion on typical entanglement in this chapter has been for general quantum systems. However, many physical systems have constraints sometimes in the form of symmetries of the system. In this case, it is expected that the observables and states accessible to a subsystem will change and that will have an effect on the typical entanglement of a random state in such a system. A framework for incorporating constraints through the language of algebra of observables has been presented in [69]. Here, a closed form for the average entanglement in such systems was obtained and it was shown that the variance around this average scales inversely with the Hilbert space sector dimension and vanishes in the thermodynamic limit proving that the average entanglement is indeed the typical entanglement. However, this framework does not deal with non-Abelian symmetries any quantum system might have. For this reason, we are motivated to build on the roadmap provided by this framework and extend it in a manner such that it takes into account the effect a non-Abelian symmetry might have on the observables and states accessible to a subsystem and also on the amount of entanglement in a state of such a system.

Chapter 3
Subsystems from Subalgebras and Typical Entropy

3.1 Introduction

In this chapter, we lay the foundation for a rigorous treatment of entanglement in isolated quantum systems by adopting an operational approach based on subalgebras of observables. Traditionally, the study of entanglement has relied on the tensor product structure of a composite Hilbert space; however, many physically relevant situations call for a more general perspective where the notion of a subsystem is defined through the observables that one can actually access. The motivation for this approach is twofold. First, many experimental and theoretical contexts do not naturally present a pre-defined tensor product structure; instead, we must characterize the subsystem by the specific set of measurements available. Second, the algebraic formulation provides a flexible and general framework that can be extended to incorporate additional features present in our system such as symmetries and constraints. In our setup, a subsystem is defined via a subalgebra of accessible observables. The key concepts of commutant and center of an algebra then naturally allow us to decompose the Hilbert space into sectors that are adapted to this subalgebra. This decomposition is central to our treatment as it allows us to define the restriction of any pure state to this subalgebra and thereby to construct the corresponding reduced density matrix. The entanglement entropy is then given by the von Neumann entropy of this reduced density matrix and can be expressed as the sum of the average entropy within each sector and the

Shannon entropy of the sector probabilities.

An important result of this chapter is the derivation of explicit expressions for the average entanglement entropy and its variance over the ensemble of random pure states. These expressions generalize Page's seminal result [21] to the context of subalgebra-defined subsystems. Moreover, we establish rigorous bounds on the average entropy and show that the variance vanishes in the limit of large Hilbert space dimension, thereby affirming that the average value represents the typical entanglement entropy. In subsequent chapters, this framework will serve as the basis for exploring more refined aspects of entanglement, including symmetry-resolved entanglement and its implications in locality in quantum many-body physics. The results presented in this chapter are based on Sec. 2 of [5].

3.2 Setup

We consider an isolated quantum system with Hilbert space $\mathcal{H}$ of finite dimension $D = \dim \mathcal{H} < \infty$. Pure states of the system, $|\psi\rangle \in \mathcal{H}$, can be understood as vectors in $\mathbb{C}^D$ and observables O as $D \times D$ hermitian matrices. The algebra of observables of the system,

$$\mathcal{A} = \mathcal{L}(\mathcal{H}) \simeq M_D(\mathbb{C})\,, \tag{3.1}$$

is the set $\mathcal{L}(\mathcal{H})$ of linear operators on $\mathcal{H}$ or equivalently the algebra $M_D(\mathbb{C})$ of matrices on $\mathbb{C}^D$.

In general, a Von Neumann algebra on $\mathbb{C}^D$ is an algebra of matrices that is closed under (i) hermitian conjugation, (ii) addition, (iii) multiplication, and (iv) contains all $\mathbb{C}$ multiples of the identity operator. In particular, the algebra $\mathcal{A}$ of observables of the system is a Von Neumann algebra [74, 75].[1] Here we are inter-

[1] While observables of the system are represented by hermitian matrices, linear combinations are assumed to be over $\mathbb{C}$ and therefore the Von Neumann algebra of observables contains also anti-hermitian matrices and, more importantly, unitary transformations. We note also that here we have assumed that the Hilbert space of the system is finite-dimensional, and therefore in the definition of a Von Neumann algebra reduces to the one of a matrix algebra [75], with no additional requirement about topological closure. For a discussion of the infinite-dimensional case and the classification of Von Neumann algebras of observables in quantum field theory, we refer to [76–79].

ested in Von Neumann subalgebras of $\mathcal{A}$. We say that a subalgebra is generated by the set of hermitian matrices K_i (with $i = 1, \ldots, n$) if it can be obtained by their closure under (i)–(iv), which we denote by

$$\mathbb{C}[K_i] \equiv \left\{ M \in M_D(\mathbb{C}) \,|\, M \,=\, a\,\mathbb{1} + \sum_i b_i K_i + \sum_{ij} c_{ij} K_i K_j + \ldots \right\}, \tag{3.2}$$

with coefficients $a, b_i, c_{ij} \ldots$ in $\mathbb{C}$. The notion of commutant will play a central role. The commutant of a set of matrices is defined as

$$\{K_1, \ldots, K_n\}' \equiv \{M \in M_D(\mathbb{C}) \,|\, MK_i - K_i\, M = 0\,,\ i = 1, \ldots, n\}\,. \tag{3.3}$$

There are two useful results that we will use multiple times: the first relates the double commutant of a set of matrices to the algebra they generate, $\{K_1, \ldots, K_n\}'' = \mathbb{C}[K_1, \ldots, K_n]$; the second result relates the intersection of commutants to the union of the sets of generators:

$$\mathbb{C}[K_i]' \cap \mathbb{C}[H_j]' = \mathbb{C}[K_i, H_j]'\,. \tag{3.4}$$

Note that the commutant of a Von Neumann algebra $\mathcal{A}_\mathcal{S} \subset \mathcal{A}$ is also a Von Neumann algebra $(\mathcal{A}_\mathcal{S})' \subset \mathcal{A}$, and the double commutant coincides with the algebra itself, $(\mathcal{A}_\mathcal{S})'' = \mathcal{A}_\mathcal{S}$.

3.3 Hilbert space decomposition adapted to a subalgebra of observables

Given our physical system, we define a *subsystem* $\mathcal{S}$ operationally, in terms of a set of observables $\{O_1, O_2, \ldots\}$ that we have access to or that we can probe with measuring devices available to us. These observables generate a Von Neumann algebra $\mathcal{A}_\mathcal{S}$ on $\mathcal{H}$,

$$\mathcal{A}_\mathcal{S} = \mathbb{C}\big[O_1, O_2, \ldots\big], \tag{3.5}$$

that is a subalgebra of the algebra of observables $\mathcal{A}$ of the system, $\mathcal{A}_\mathcal{S} \subseteq \mathcal{A}$. The two notions of commutant and center allow us to decompose the Hilbert space $\mathcal{H}$

in sectors adapted to the subalgebra of observables $\mathcal{A}_{\mathcal{S}}$.[2]

We start with the notion of commutant. We denote by $\overline{\mathcal{S}}$ the *complement* of the subsystem $\mathcal{S}$ and define it in terms of the subalgebra of observables that commute with $\mathcal{A}_{\mathcal{S}}$, i.e., the commutant of $\mathcal{A}_{\mathcal{S}}$ in $\mathcal{A}$,

$$\mathcal{A}_{\overline{\mathcal{S}}} = (\mathcal{A}_{\mathcal{S}})' \equiv \{M \in \mathcal{A} \mid [M, N] = 0 \ , \ \forall\, N \in \mathcal{A}_{\mathcal{S}}\} \, . \tag{3.6}$$

Next, we consider the *center* $\mathcal{Z}_{\mathcal{S}}$ of the subalgebra. Note that in general there are observables $R_1, R_2, \ldots$ that can be measured both from $\mathcal{S}$ and from $\overline{\mathcal{S}}$, i.e. the subalgebra $\mathcal{A}_{\mathcal{S}}$ can have a non-trivial center $\mathcal{Z}_{\mathcal{S}}$,

$$\mathcal{Z}_{\mathcal{S}} = \mathcal{A}_{\mathcal{S}} \cap \mathcal{A}_{\overline{\mathcal{S}}} \ = \ \mathbb{C}[R_1, R_2, \ldots] \, . \tag{3.7}$$

These structures allow us to decompose the Hilbert space $\mathcal{H}$ as a direct sum of tensor products. The construction can be understood concretely in terms of an orthonormal basis of $\mathcal{H}$ adapted to the subsystem $\mathcal{S}$. We first consider the observables $R_1, R_2, \ldots$ in the center $\mathcal{Z}_{\mathcal{S}}$. By definition, the center $\mathcal{Z}_{\mathcal{S}}$ is an Abelian algebra and, therefore, we can diagonalize these observables simultaneously. We denote by r the eigenvalues of the observables in the center $\mathcal{Z}_{\mathcal{S}}$. Then, we can select a maximal commuting set of observables in $\mathcal{A}_{\mathcal{S}}$ with simultaneous eigenvalues α, and a maximal commuting set of observables in $\mathcal{A}_{\overline{\mathcal{S}}}$ with simultaneous eigenvalues β. As a result, we obtain an orthonormal basis of $\mathcal{H}$,

$$|r, \alpha, \beta\rangle = |r, \alpha\rangle |r, \beta\rangle \, , \tag{3.8}$$

that is adapted to the subalgebra $\mathcal{A}_{\mathcal{S}}$. This basis gives a concrete meaning to the direct sum decomposition

$$\mathcal{H} = \bigoplus_r \left(\mathcal{H}_{\mathcal{S}}^{(r)} \otimes \mathcal{H}_{\overline{\mathcal{S}}}^{(r)} \right) , \tag{3.9}$$

where $|r, \alpha\rangle$ is an orthonormal basis of $\mathcal{H}_{\mathcal{S}}^{(r)}$, and $|r, \beta\rangle$ an orthonormal basis of $\mathcal{H}_{\overline{\mathcal{S}}}^{(r)}$. Note that when the center is trivial, i.e., $\mathcal{Z}_{\mathcal{S}} = \{\mathbb{1}\}$, this decomposition reduces to

[2] We refer to Ch. 11.8 in [74] for a pedagogical introduction, to [80–82] for applications to lattice systems, to [83] for applications to information transport, and to [84, 85] for applications to Hilbert space fragmentation.

the familiar tensor product structure $\mathcal{H} = \mathcal{H}_A \otimes \mathcal{H}_B$ of a composite system.

We call d_r and b_r the *dimensions* of the sectors appearing in the direct-sum decomposition associated with a subalgebra $\mathcal{A}_\mathcal{S}$,

$$d_r = \dim \mathcal{H}_\mathcal{S}^{(r)}\,, \qquad b_r = \dim \mathcal{H}_{\overline{\mathcal{S}}}^{(r)}\,, \qquad D = \dim \mathcal{H} \;=\; \textstyle\sum_r d_r b_r\,. \tag{3.10}$$

These dimensions play a central role in the expression of the typical entropy of a subsystem.

3.4 Pure states restricted to a subalgebra and entanglement entropy

Using the decomposition (3.9), observables of the subsystem $\mathcal{S}$ take the direct-sum form

$$O \in \mathcal{A}_\mathcal{S} \subseteq \mathcal{A} \qquad \Longrightarrow \qquad O = \bigoplus_r \left(O_\mathcal{S}^{(r)} \otimes \mathbb{1}_\mathcal{S}^{(r)}\right). \tag{3.11}$$

It is useful to introduce a notion of Hilbert space $\mathcal{H}_\mathcal{S}$ of the subsystem, defined as the direct sum of the subsystem sectors:

$$\mathcal{H}_\mathcal{S} \equiv \bigoplus_r \mathcal{H}_\mathcal{S}^{(r)}\,. \tag{3.12}$$

The restriction of an operator $O \in \mathcal{A}_\mathcal{S}$ to the Hilbert space of the subsystem is given by

$$O \in \mathcal{A}_\mathcal{S} \subseteq \mathcal{A} \qquad \Longrightarrow \qquad O_\mathcal{S} \equiv \bigoplus_r O_\mathcal{S}^{(r)} \;\in\; \mathcal{L}(\mathcal{H}_\mathcal{S})\,. \tag{3.13}$$

We can write this map from O to $O_\mathcal{S}$ concretely as

$$\begin{aligned} \mathrm{Tr}(\,\cdot\,\Pi_\mathcal{S}):\quad \mathcal{L}(\mathcal{H}) &\longrightarrow \mathcal{L}(\mathcal{H}_\mathcal{S}) \\ O &\longmapsto O_\mathcal{S} = \mathrm{Tr}(O\,\Pi_\mathcal{S}) \end{aligned} \tag{3.14}$$

where Tr is the trace over $\mathcal{H}$ and $\mathrm{Tr}_{\mathcal{S}}$ is the trace over $\mathcal{H}_{\mathcal{S}}$.[3] In the adapted basis $|r,\alpha,\beta\rangle \in \mathcal{H}$ and $|r,\alpha\rangle \in \mathcal{H}_{\mathcal{S}}$, the map Π_S takes the form

$$\Pi_{\mathcal{S}} = \sum_r \sum_{\alpha\alpha'} \Big(\sum_\beta |r,\alpha,\beta\rangle\langle r,\alpha',\beta| \Big) \otimes |r,\alpha'\rangle\langle r,\alpha| \,. \tag{3.15}$$

With these definitions, we can now write the restriction of a pure state $|\psi\rangle \in \mathcal{H}$ to the subsystem $\mathcal{S}$ as a density matrix $\rho_{\mathcal{S}}$,

$$\rho = |\psi\rangle\langle\psi| \quad \Longrightarrow \quad \rho_{\mathcal{S}} = \mathrm{Tr}(\rho\, \Pi_{\mathcal{S}}) \,, \tag{3.16}$$

so that the expectation value of an observable on the subsystem $\mathcal{S}$ is given by

$$O \in \mathcal{A}_{\mathcal{S}} \subseteq \mathcal{A} \qquad \Longrightarrow \qquad \langle\psi|O|\psi\rangle = \mathrm{Tr}_{\mathcal{S}}\big(O_{\mathcal{S}}\, \rho_{\mathcal{S}}\big) \,. \tag{3.17}$$

We note that the map $\rho \mapsto \rho_{\mathcal{S}}$ is completely positive and trace preserving (CPTP) [86], as can be seen by writing it in the operator sum form $\mathrm{Tr}(\rho\, \Pi_{\mathcal{S}}) = \sum_{r\beta} Y_{r\beta}^\dagger\, \rho\, Y_{r\beta}$ with Kraus operators $Y_{r\beta} = \sum_\alpha |r,\alpha,\beta\rangle\langle r,\alpha|$.

We are now ready to define the entanglement entropy S of the pure state $|\psi\rangle \in \mathcal{H}$ restricted to a subalgebra of observables $\mathcal{A}_{\mathcal{S}} \subseteq \mathcal{A} = \mathcal{L}(\mathcal{H})$: the entropy of the triple $\big(|\psi\rangle, \mathcal{A}, \mathcal{A}_{\mathcal{S}}\big)$ equals the von Neumann entropy $S_{\mathrm{vN}}(\rho_{\mathcal{S}})$ of the restricted state, i.e.,

$$S\big(|\psi\rangle, \mathcal{A}, \mathcal{A}_{\mathcal{S}}\big) = \; -\mathrm{Tr}_{\mathcal{S}}(\rho_{\mathcal{S}} \log \rho_{\mathcal{S}}) \qquad \text{with} \qquad \rho_S = \langle\psi|\Pi_{\mathcal{S}}|\psi\rangle \,. \tag{3.18}$$

It is useful to express the entanglement entropy in the basis (3.8) adapted to a subalgebra $\mathcal{A}_{\mathcal{S}}$. We introduce first the projector $P^{(r)} = \sum_{\alpha\beta} |r,\alpha,\beta\rangle\langle r,\alpha,\beta|$ to the sector r of the Hilbert space decomposition. Using this projector, we can define the probability p_r that the pure state is found to be in the sector r, together with

[3] Traces over the Hilbert spaces $\mathcal{H}$, $\mathcal{H}_{\mathcal{S}}$ and $\mathcal{H}_{\mathcal{S}}^{(r)}$ are defined as

$$\mathrm{Tr}(\,\cdot\,) = \sum_{r\alpha\beta} \langle r,\alpha,\beta|\,\cdot\,|r,\alpha,\beta\rangle \,, \qquad \mathrm{Tr}_{\mathcal{S}}(\,\cdot\,) = \sum_r \sum_\alpha \langle r,\alpha|\,\cdot\,|r,\alpha\rangle \,, \qquad \mathrm{Tr}_{\mathcal{S}}^{(r)}(\,\cdot\,) = \sum_\alpha \langle r,\alpha|\,\cdot\,|r,\alpha\rangle \,.$$

Similarly, one can define traces for $\mathcal{H}_{\overline{\mathcal{S}}}^{(r)}$ and for $\mathcal{H}_{\overline{\mathcal{S}}} = \bigoplus_r \mathcal{H}_{\overline{\mathcal{S}}}^{(r)}$ in term of the basis $|r,\beta\rangle$.

the (normalized) projected state $|\psi^{(r)}\rangle$:

$$p_r \;=\; \langle\psi|P^{(r)}|\psi\rangle \;=\; \sum_{\alpha\beta} \big|\langle r,\alpha,\beta|\psi\rangle\big|^2 , \tag{3.19}$$

$$|\psi^{(r)}\rangle \;=\; \frac{P^{(r)}|\psi\rangle}{\sqrt{\langle\psi|P^{(r)}|\psi\rangle}} = \sum_{\alpha\beta} \psi^{(r)}_{\alpha\beta}\, |r,\alpha\rangle|r,\beta\rangle\,. \tag{3.20}$$

Any pure state $|\psi\rangle \in \mathcal{H}$ can then be expressed in the basis adapted to the subalgebra of observables $\mathcal{A}_\mathcal{S}$ as

$$|\psi\rangle = \sum_r \sqrt{p_r} \sum_{\alpha\beta} \psi^{(r)}_{\alpha\beta}\, |r,\alpha\rangle|r,\beta\rangle\,. \tag{3.21}$$

The definition (3.16) of reduced density matrix takes then the direct sum form

$$\rho_\mathcal{S} = \bigoplus_r p_r\, \rho^{(r)}_\mathcal{S}\,, \tag{3.22}$$

with $\rho^{(r)}_\mathcal{S}$ simply defined as the partial trace over $\mathcal{H}^{(r)}_{\bar{\mathcal{S}}}$, i.e.,

$$\rho^{(r)}_\mathcal{S} = \mathrm{Tr}^{(r)}_{\bar{S}}\big(|\psi^{(r)}\rangle\langle\psi^{(r)}|\big) \;=\; \sum_{\alpha\alpha'} \Big(\sum_\beta \psi^{(r)}_{\alpha'\beta}\, \psi^{(r)*}_{\alpha\beta}\Big)\, |r,\alpha'\rangle\langle r,\alpha|\,. \tag{3.23}$$

Using the decomposition (3.22) and expanding

$$\mathrm{Tr}_\mathcal{S}(\rho_\mathcal{S}\log\rho_\mathcal{S}) \;=\; \sum_r \mathrm{Tr}^{(r)}_\mathcal{S}\big(p_r\,\rho^{(r)}_\mathcal{S}\log(p_r\,\rho^{(r)}_\mathcal{S})\big),$$

we can write the entanglement entropy as the sum of two terms,

$$S\big(|\psi\rangle,\mathcal{A},\mathcal{A}_\mathcal{S}\big) = -\sum_r p_r\,\mathrm{tr}\big(\rho^{(r)}_\mathcal{S}\log\rho^{(r)}_\mathcal{S}\big) \;-\sum_r p_r\log p_r\,, \tag{3.24}$$

where the first term is the average over sectors of the entanglement entropy in each sector, and the second piece is the Shannon entropy of the distribution over sectors.

We summarize some useful properties of the entanglement entropy of a subsystem defined in terms of a subalgebra:

Minimum — The entanglement entropy is non-negative and vanishes if and only if the restriction of the state to the subalgebra is pure. For this to happen, the state has to belong to a definite sector r and have a product form, i.e.,

$$S\big(|\psi\rangle, \mathcal{A}, \mathcal{A}_{\mathcal{S}}\big) = 0 \qquad \Longrightarrow \qquad \exists\, r \;:\quad |\psi\rangle = \; |r, \xi\rangle_{\mathcal{S}}\, |r, \chi\rangle_{\overline{\mathcal{S}}}\,, \tag{3.25}$$

with $|r, \xi\rangle_{\mathcal{S}} = \sum_\alpha \xi_\alpha |r, \alpha\rangle$ and $|r, \chi\rangle_{\overline{\mathcal{S}}} = \sum_\beta \chi_\beta |r, \beta\rangle$. As a special case, if we don't restrict the state to any subalgebra, then the entanglement entropy of a pure state vanishes, $S\big(|\psi\rangle, \mathcal{A}, \mathcal{A}\big) = 0$.

Maximum — We can determine the maximum entanglement entropy by varying the Lagrangian $L = -\sum_r p_r \sum_i (\lambda_{ri} \log \lambda_{ri}) \; - \; \sum_r p_r \log p_r \; + \; \mu_0 \, (1 - \sum_r p_r) + \sum_r \mu_r \, (1 - \sum_i \lambda_{ri})$, with probabilities p_r and λ_{ri}, and Lagrange multipliers μ_0 and μ_r. At the stationary point, we obtain the maximum entropy

$$S_{\max} = \log \big(\textstyle\sum_r \min(d_r, b_r) \big). \tag{3.26}$$

The maximally-entangled state can be written as

$$|I\rangle = \sum_r \sqrt{\frac{\min(d_r, b_r)}{\sum_{r'} \min(d_{r'}, b_{r'})}} \sum_{i=1}^{\min(d_r, b_r)} \frac{1}{\sqrt{\min(d_r, b_r)}} \, |r, i\rangle_{\mathcal{S}} |r, i\rangle_{\overline{\mathcal{S}}}\,. \tag{3.27}$$

Commutant Symmetry — Note that the entanglement entropy of a subsystem is symmetric under the exchange of the subsystem with its commutant, i.e.,

$$S\big(|\psi\rangle, \mathcal{A}, \mathcal{A}_{\overline{\mathcal{S}}}\big) = S\big(|\psi\rangle, \mathcal{A}, \mathcal{A}_{\mathcal{S}}\big). \tag{3.28}$$

This notion of commutant symmetry generalizes the familiar subsystem symmetry $S_A = S_B$ of the entanglement entropy of pure states in a tensor product $\mathcal{H}_A \otimes \mathcal{H}_B$.

3.5 Typical entanglement entropy: average and variance

Consider the ensemble of random pure states $|\psi\rangle \in \mathcal{H}$. Given a function of the state, $f(|\psi\rangle)$, we can define the average over the ensemble as

$$\big\langle f \big\rangle_{\mathcal{H}} = \int_{\mathcal{H}} d\mu(\psi)\; f(|\psi\rangle) \;=\; \int dU\; f(U|\psi_0\rangle)\,, \tag{3.29}$$

where $d\mu(\psi)$ is the uniform measure over the unit sphere in $\mathbb{C}^D$ or, equivalently, dU is the Haar measure over the unitary group $U(D)$ that allows us to write a random state $|\psi\rangle = U|\psi_0\rangle$ in terms of a reference state $|\psi_0\rangle$ and a random unitary U. The function f can be a linear function of $|\psi\rangle\langle\psi|$, such as the expectation value of a subsystem observable in $\mathcal{A}_{\mathcal{S}}$, or a non-linear function as the entanglement entropy $S(|\psi\rangle, \mathcal{A}, \mathcal{A}_{\mathcal{S}})$ of the state restricted to a subalgebra of observables. We note that the result of this average can be expressed purely in terms of the dimensions (3.10) of the sectors of the Hilbert space decomposition (3.9). For instance, the average density matrix of a pure state and of its restriction to a subsystem $\mathcal{S}$ is

$$\rho = |\psi\rangle\langle\psi| \implies \big\langle\rho\big\rangle_{\mathcal{H}} = \frac{1}{D}\mathbb{1}, \quad \big\langle\rho_{\mathcal{S}}\big\rangle_{\mathcal{H}} = \mathrm{Tr}_{\mathcal{S}}\Big(\big\langle\rho\big\rangle_{\mathcal{H}}\Pi_{\mathcal{S}}\Big) = \bigoplus_r \frac{d_r b_r}{D}\frac{1}{d_r}\mathbb{1}_{\mathcal{S}}^{(r)}, \tag{3.30}$$

which results in the von Neumann entropy of the average state

$$S_{\mathrm{vN}}(\langle\rho_{\mathcal{S}}\rangle_{\mathcal{H}}) = -\mathrm{Tr}_{\mathcal{S}}(\langle\rho_{\mathcal{S}}\rangle_{\mathcal{H}} \log\langle\rho_{\mathcal{S}}\rangle_{\mathcal{H}}) \;=\; \textstyle\sum_r \frac{d_r\, b_r}{D} \log\left(\frac{D}{b_r}\right). \tag{3.31}$$

While in general, the average $\big\langle f \big\rangle_{\mathcal{H}}$ alone does not characterize the typical value of a function $f(|\psi\rangle)$ for a random state, computing its moments $\big\langle f^n \big\rangle_{\mathcal{H}}$ allows us to characterize the probability distribution. We are interested in the probability $P(S)\,dS$ that a random pure state $|\psi\rangle$ has entropy S when restricted to the subalgebra $\mathcal{A}_{\mathcal{S}}$. When the dispersion around the average is small, $\Delta S \ll \langle S\rangle$, we can simply use the average entropy $\langle S\rangle$ to characterize the entropy. In this case, we say that the *typical entanglement entropy* of a random pure state is $\langle S\rangle$.

In [69], the exact formulas for the average entanglement entropy $\langle S\rangle$ and its variance $(\Delta S)^2$ for a pure random state restricted to a subalgebra of observables

corresponding to the Hilbert space decomposition (3.9) were found to be:

$$\langle S\rangle \;\equiv\; \big\langle S\big(|\psi\rangle, \mathcal{A}, \mathcal{A}_{\mathcal{S}}\big)\big\rangle_{\mathcal{H}} \;=\; \sum_r \varrho_r\, \varphi_r, \tag{3.32}$$

$$(\Delta S)^2 \;\equiv\; \langle S^2\rangle - \langle S\rangle^2 \;=\; \frac{1}{D+1}\Big(\sum_r \varrho_r\,\big(\varphi_r^2 + \chi_r\big) \;-\; \big(\sum_r \varrho_r\,\varphi_r\big)^2\Big), \tag{3.33}$$

with the quantities ϱ_r, φ_r, χ_r expressed in terms of the dimensions d_r, b_r, D (3.10) given by

$$\varrho_r = \frac{d_r\, b_r}{D}\,, \tag{3.34}$$

$$\varphi_r = \begin{cases} \Psi(D+1) - \Psi(b_r+1) - \dfrac{d_r - 1}{2\, b_r} & d_r \le b_r\,, \\[2ex] b_r \;\longleftrightarrow\; d_r & d_r > b_r\,, \end{cases} \tag{3.35}$$

$$\chi_r = \begin{cases} (d_r + b_r)\Psi'(b_r+1) - (D+1)\Psi'(D+1) - \dfrac{(d_r-1)(d_r+2b_r-1)}{4b_r^2} & d_r \le b_r, \\[2ex] b_r \;\longleftrightarrow\; d_r & d_r > b_r\,, \end{cases} \tag{3.36}$$

where $\Gamma(x)$ is the gamma function, $\Psi(x) = \Gamma'(x)/\Gamma(x)$ is the digamma function and $\Psi'(x)$ its derivative. This formula in terms of the dimensions (3.10) generalizes a seminal result of Page [21] that applies to the special case of an a priori factorization of the Hilbert space into subsystems.

It is useful to determine bounds on the average entropy and its variance that do not rely on any special choice of system and subsystem or on any asymptotic limit. We use the following inequalities for the digamma function and its derivative:

$$\log(x) + \tfrac{1}{2x+1} \;<\; \Psi(x+1) \;<\; \log(x) + \tfrac{1}{2x}\,, \tag{3.37}$$

$$\tfrac{1}{x} - \tfrac{1}{2x^2+1} \;<\; \Psi'(x+1) \;<\; \tfrac{1}{x} - \tfrac{1}{2x^2}\,. \tag{3.38}$$

We start with the average $\langle S\rangle$. For any choice of non-trivial subsystem and for all r we have $b_r < D = \sum_{r'} d_{r'} b_{r'}$. Using (3.37) we can then put a tight bound on

φ_r:

$$\log\min\left(\tfrac{D}{b_r},\tfrac{D}{d_r}\right)-\tfrac{1}{2}\min\left(\tfrac{d_r}{b_r},\tfrac{b_r}{d_r}\right)\;\leq\;\varphi_r\;\leq\;\log\min\left(\tfrac{D}{b_r},\tfrac{D}{d_r}\right). \tag{3.39}$$

It follows that the average entropy is bounded from above and from below by

$$\sum_r \tfrac{d_r b_r}{D}\left(\log\min\left(\tfrac{D}{b_r},\tfrac{D}{d_r}\right)-\tfrac{1}{2}\min\left(\tfrac{d_r}{b_r},\tfrac{b_r}{d_r}\right)\right)\;\leq\;\langle S\rangle\;\leq\;\sum_r \tfrac{d_r b_r}{D}\log\min\left(\tfrac{D}{b_r},\tfrac{D}{d_r}\right). \tag{3.40}$$

We note that, as $\min\left(\frac{d_r}{b_r},\frac{b_r}{d_r}\right)\leq 1$, we have also the exact inequality

$$\left|\;\langle S\rangle-\textstyle\sum_r \frac{d_r b_r}{D}\log\min\left(\frac{D}{b_r},\frac{D}{d_r}\right)\;\right|\leq\tfrac{1}{2}\,, \tag{3.41}$$

which is useful for extracting the asymptotics of the average entropy in the limit of large dimension D, up to terms of order one. We note also that, because of the min, the upper bound is tighter than the entropy of the average (3.31), consistently with the inequality $\langle S_{\rm vN}(\rho_{\mathcal{S}})\rangle\leq S_{\rm vN}(\langle\rho_{\mathcal{S}}\rangle)$. Clearly, the average entropy is also smaller than the maximum entropy (3.26).[4]

We consider then the variance $(\Delta S)^2$. Here we use two (rather loose, but useful) inequalities for the functions φ_r and χ_r,

$$0\leq\varphi_r\leq\log D\,,\qquad 0\leq\chi_r\leq 2\,. \tag{3.42}$$

It is immediate then to show that the variance of the entanglement entropy is bounded from above by a decreasing function of the dimension D,

$$(\Delta S)^2\leq\frac{(\log D)^2+2}{D}\,. \tag{3.43}$$

This bound shows that, independently of the details of the system and of the subsystem, the variance of the entropy vanishes in the large dimension of the Hilbert space limit, i.e., $\Delta S\to 0$ as $D\to\infty$. Therefore, if the average $\langle S\rangle$ is finite and non-vanishing in this limit, then its value represents the typical entanglement entropy of a random pure state restricted to the subsystem.

[4] In fact $\sum_r \frac{d_r b_r}{D}\log\min\left(\frac{D}{b_r},\frac{D}{d_r}\right)\leq\log\left(\sum_r\min(d_r,b_r)\right)$ because log is concave and $\langle\log\cdot\rangle\leq\log\langle\cdot\rangle$.

Chapter 4
Non-Abelian Symmetry-resolved States and Entropy

4.1 Introduction

Symmetry plays a central role in modern physics, shaping the dynamics and structure of physical systems from elementary particles to complex many-body systems. In this chapter, we develop a comprehensive framework to analyze entanglement in systems that exhibit nontrivial symmetry properties, focusing particularly on the case where the symmetry group G leaves the Hamiltonian invariant. This invariance implies that the Hilbert space $\mathcal{H}$ carries a (reducible) unitary representation of G. We call the physical observables, including the Hamiltonian, that commute with the action of G as G-invariant observables. In this context, it becomes natural to restrict attention to G-invariant observables and, correspondingly, to define *symmetry-resolved states* as those pure states that remain pure when confined to the subalgebra of G-invariant observables. While the entanglement properties of systems with an Abelian symmetry (such as $U(1)$) are well understood, non-Abelian symmetry groups, in particular semisimple Lie groups, i.e., continuous groups that do not have any Abelian invariant subgroup [87–89], like $SU(2)$ or $SU(3)$, introduce novel features. In these cases, the non-commuting nature of the generators leads to a richer structure in the Hilbert space and a more intricate interplay between symmetry and entanglement. For this reason, the conventional methods of defining subsystems and the entanglement entropy are meaningless in this setting.

To address these challenges, we note that for semisimple Lie groups, the presence of nontrivial Casimir operators—which are constructed from the generators and remain invariant under G—allows us to label irreducible representations. As a consequence, the Hilbert space admits a symmetry-resolved decomposition with sectors corresponding to the eigenvalues of the Casimir operators. After establishing the Hilbert space decomposition, we introduce the notion of a symmetry-resolved subsystem using a subalgebra of accessible observables. Furthermore, we derive explicit expressions for the symmetry-resolved entanglement entropy. Using the adapted basis from the symmetry-resolved decomposition, we express a generic state as a direct sum over sectors and show that the entanglement entropy decomposes into two contributions: the average of the entropies in each sector and a Shannon entropy associated with the distribution of the sectors. Finally, we obtain bounds on the entropy in terms of the dimensions of the subspaces, generalizing Page's result to the symmetry-resolved setting. The results presented in this chapter are based on Sec. 3 of [5].

4.2 Symmetry-resolved decomposition of the Hilbert space

A compact Lie group G is defined by the Lie algebra of its generators T^a with real structure constants $f^{ab}{}_c$,

$$[T^a, T^b] = \mathrm{i}\, f^{ab}{}_c\, T^c\,. \tag{4.1}$$

We say that the finite-dimensional Hilbert space $\mathcal{H}$ carries a unitary representation of the group G if the generators T^a are realized as $D \times D$ Hermitian matrices that satisfy the commutation relations (4.1), with $D = \dim \mathcal{H}$. A group element with real parameters α_a acts on the Hilbert space as the unitary transformation U given by

$$U = \mathrm{e}^{\,\mathrm{i}\,\alpha_a T^a}\,. \tag{4.2}$$

This representation of the group is, in general, reducible. It is useful to introduce the Cartan-Killing metric $\eta^{ab} = \mathrm{tr}(\tau^a \tau^b)$ where τ^a are the generators in the adjoint representation, $[\tau^a]^b{}_c = -\mathrm{i}\, f^{ab}{}_c$. Here we restrict attention to the case of real

compact semisimple Lie groups, for which the metric η^{ab} is positive definite[1]. We use this metric and its inverse η_{ab}, with $\eta^{ac}\,\eta_{cb} = \delta^a{}_b$, to raise and lower indices.

The symmetry generators T^a generate a subalgebra $\mathcal{A}_{\rm sym}$ of the algebra of observables $\mathcal{A} = \mathcal{L}(\mathcal{H})$ of the system,

$$\mathcal{A}_{\rm sym} = \mathbb{C}[T^a]\,. \tag{4.3}$$

The commutant of this subalgebra defines the algebra of G-invariant observables,

$$\mathcal{A}_G \equiv (\mathcal{A}_{\rm sym})' \;=\; \{M \in \mathcal{A}\,|\,[M, T^a] = 0\}\,. \tag{4.4}$$

Observables in $\mathcal{A}_G$ commute with the generators T^a and therefore satisfy the G-invariance condition

$$U(T^a)\,O\,U(T^a)^{-1} \;=\; O\,. \tag{4.5}$$

The rank of a semisimple Lie group G is the dimension $\mathrm{rank}(G)$ of any one of the Cartan subalgebras of its Lie algebra. The number of linearly independent Casimir operators Q_k is exactly given by $\mathrm{rank}(G)$ [90, 91]. The Casimir operators are obtained by listing all the completely-symmetric G-invariant tensors $\eta_{a_1\cdots a_p}$ of order p, and then contracting them with the generators:

$$Q_k \;=\; \eta_{a_1\cdots a_{p(k)}}\,T^{a_1}\cdots T^{a_{p(k)}}\,, \qquad\qquad k = 1, \ldots, \mathrm{rank}(G)\,. \tag{4.6}$$

These operators generalize the familiar quadratic Casimir operator $Q_1 = \eta_{ab}\,T^aT^b$ defined in terms of the Cartan-Killing metric. They belong to the G-invariant subalgebra $\mathcal{A}_G$ as they are invariants, and they belong to the algebra $\mathcal{A}_{\rm sym}$ as they are expressed in terms of the generators. Therefore, they belong to the center $\mathcal{Z}_{\rm sym}$ of the algebra. In fact, for semisimple Lie groups (that is, Lie groups that have no Abelian subgroup), a much stronger result holds [90, 91]: these R linearly independent Casimir operators generate the center,

$$\mathcal{Z}_{\rm sym} \;=\; \mathcal{A}_{\rm sym} \cap \mathcal{A}_G = \mathbb{C}[Q_k]\,, \tag{4.7}$$

[1]Note that in this case, by rescaling the generators, the metric η^{ab} can be brought to the Euclidean form δ^{ab}. Here, we use the standard tensorial notation, where we keep track of upper and lower indices, and repeated indices are contracted. As usual, the symbols $^{(\cdots)}$ and $^{[\cdots]}$ stand for complete symmetrization or anti-symmetrization of the tensor.

and characterize completely the irreducible representations of the group.

Using the results of Sec. 3.3, and denoting collectively q the eigenvalues of the Casimir operators, we obtain a symmetry-resolved decomposition of the Hilbert space:

$$\mathcal{H} = \bigoplus_q \left(\mathcal{H}_{\text{sym}}^{(q)} \otimes \mathcal{H}_G^{(q)} \right) , \tag{4.8}$$

where $\mathcal{H}_{\text{sym}}^{(q)}$ carries the irreducible representation (q) of the symmetry generarators, and $\mathcal{H}_G^{(q)}$ is the space of G-invariant degrees of freedom of the system defined as

$$\mathcal{H}_G^{(q)} = \text{Inv}_G(\mathcal{H}_{\text{sym}}^{(\bar{q})} \otimes \mathcal{H}) \ , \tag{4.9}$$

where Inv_G denotes the G-invariant subspace in the tensor product and $(\bar{q})$ is the conjugate representation [88, 89].

The symmetry-resolved decomposition (4.8) is a decomposition of the Hilbert space $\mathcal{H}$ into a direct sum of irreducible representations labeled by the quantum numbers q that label the eigenvalues of the Casimir operators. Furthermore, each irreducible representation is a tensor product of the sym factor $\mathcal{H}_{\text{sym}}^{(q)}$ that transforms under an irreducible representation of the group, and the G-invariant Hilbert space $\mathcal{H}_G^{(q)}$ of internal degrees of freedom defined by (4.9). A generic state $|\psi\rangle$ in $\mathcal{H}$ can be expanded on the orthonormal basis adapted to this decomposition:

$$|\psi\rangle = \sum_q \sqrt{p_q} \sum_m \sum_i \psi_{m\,i}^{(q)} \, |q, m\rangle_{\text{sym}} \, |q, i\rangle_G \, , \tag{4.10}$$

where m in the basis $|q, m\rangle_{\text{sym}}$ denotes collectively the eigenvalues of the Cartan generators of the group G, and i in the basis $|q, i\rangle_G$ labels the internal G-invariant degrees of freedom of the system.

We give three examples of the symmetry-resolved Hilbert space for semisimple Lie groups:

$\boldsymbol{G = SU(2)}$ — This is the simplest non-trivial case illustrated in Chapter 1. The generators are the spin operators $\vec{J} = (J^i)$ with $i = 1, 2, 3$, the structure constants are $\epsilon^{ij}{}_k$, the Cartan-Killing metric δ_{ij}. The rank of the group is one, and therefore, the decomposition is in terms of a single Casimir operator, the quadratic Casimir $Q = \delta_{ik} \, J^i J^k = \vec{J}^2$. As usual, the eigenvalues of the Casimir operator are written

as $j(j+1)$ with $j = 0, \frac{1}{2}, 1, \ldots$ half-integer, and the eigenvalues of the Cartan subalgebra operator J^z are $m = -j, \ldots, +j$. The Hilbert space decomposes as $\mathcal{H} = \bigoplus_j \left(\mathcal{H}^{(j)}_{\text{sym}} \otimes \mathcal{H}^{(j)}_G\right)$, with $\mathcal{H}^{(j)}_{\text{sym}}$ of dimension $\dim \mathcal{H}^{(j)}_{\text{sym}} = 2j+1$ and orthonormal basis $|j, m\rangle_{\text{sym}}$. In Chapter 6 we discuss a concrete example of symmetry-resolved spin system where the G-invariant Hilbert space of internal degrees of freedom $\mathcal{H}^{(j)}_G$ is the space of $SU(2)$ intertwiners of a spin system, which can also be interpreted geometrically as quantum polyhedra [92, 93].

$\boldsymbol{G = SU(3)}$ — Starting from the 3×3 Gell-Mann matrices λ^a (with $a = 1, \ldots, 8$) and using the textbook normalization $\lambda^a/2$ of the generators in the fundamental representation [88, 89], we can express the Cartan-Killing metric as $\eta^{ab} = \frac{1}{4}\text{tr}(\lambda^a \lambda^b) = \frac{1}{2}\delta^{ab}$, the structure constants as $f^{abc} = -\frac{\mathrm{i}}{4}\,\text{tr}(\lambda^{[a}\lambda^b\lambda^{c]})$ (which is completely antisymmetric when all indices are raised), and the completely symmetric tensor $d^{abc} = \frac{1}{2}\text{tr}(\lambda^{(a}\lambda^b\lambda^{c)})$. The rank of the group is 2, and therefore, there are two linearly independent Casimir operators Q_1 and Q_2. The quadratic Casimir operator $Q_1 = \frac{1}{2}\eta_{ab}T^aT^b$ has eigenvalues $\frac{1}{3}(q^2+p^2+qp+3q+3p)$. The cubic Casimir operator $Q_2 = \frac{1}{8}d_{abc}\,T^aT^bT^c$ has eigenvalues $\frac{1}{18}(q-p)(q+2p+3)(p+2q+3)$ sometimes called the anomaly coefficient. The quantum numbers $q, p = 0, 1, 2, \ldots$ label the irreducible representations and the decomposition as a direct sum over the center is $\mathcal{H} = \bigoplus_{q,p} \left(\mathcal{H}^{(q,p)}_{\text{sym}} \otimes \mathcal{H}^{(q,p)}_G\right)$. The dimension of the sym factor is $\dim \mathcal{H}^{(q,p)}_{\text{sym}} = \frac{1}{2}(q+1)(p+1)(q+p+2)$.

$\boldsymbol{G = SO(4)}$ — The algebra of the group is the same as the algebra of $SU(2)_L \times SU(2)_R$ with generators given by the spin operators $\vec{J}_L$ and $\vec{J}_R$ [87]. The group has rank 2, and the two linearly independent Casimir operators can be taken as $Q_L = \vec{J}_L^2$ and $Q_R = \vec{J}_R^2$. The half-integer quantum numbers j_L and j_R label the irreducible representations, and the symmetry-resolved decomposition of the Hilbert space is $\mathcal{H} = \bigoplus_{j_L, j_R} \left(\mathcal{H}^{(j_L,j_R)}_{\text{sym}} \otimes \mathcal{H}^{(j_L,j_R)}_G\right)$. The dimension of the sym factor is $\dim \mathcal{H}^{(j_L,j_R)}_{\text{sym}} = (2j_L+1)(2j_R+1)$.

In general, for the classical compact matrix groups $A_n = SU(n+1)$, $B_n = SO(2n+1)$ and $C_n = Sp(2n)$ of rank n, the list of the n linearly independent Casimir operators is given by $Q_k = \eta_{a_1 \ldots a_k} T^{a_1} \cdots T^{a_k}$ with the invariant tensor $\eta_{a_1 \ldots a_k} = \text{tr}(\tau^{(a_1} \cdots \tau^{a_k)})$ defined using where τ^a in the fundamental representation [91]. If one took τ^a in the adjoint representation instead, one could not

distinguish the representation (q,p) from its conjugate (p,q) in $SU(3)$, for instance. In the case $D_n = SO(2n)$, one can construct the invariant tensors from the spinor representation or, equivalently, one can take the $(n-1)$ Casimir operators of even order, Q_{2k} with $k = 1, \ldots, n-1$, together with the order-n Casimir invariant $\tilde{Q} = \epsilon_{\mu_1\nu_1\ldots\mu_n\nu_n} J^{\mu_1\nu_1} \cdots J^{\mu_n\nu_n}$, where $J^{\mu\nu}$ are the generators. The Casimir operator $\tilde{Q}$ allows us to distinguish the two mirror representations of $SO(2n)$. In the case of $SO(4)$, this construction reduces to the two quadratic invariants $Q = J_{\mu\nu}J^{\mu\nu} = 4\,(\vec{J}_L^{\,2} + \vec{J}_R^{\,2})$ and $\tilde{Q} = \epsilon_{\mu\nu\rho\sigma}J^{\mu\nu}J^{\rho\sigma} = 8\,(\vec{J}_L^{\,2} - \vec{J}_R^{\,2})$. A similar construction applies to the exceptional Lie groups G_2, F_4, E_6, E_7, E_8, with the invariant tensors $\eta_{a_1\ldots a_k}$ built from the generators in an irreducible representation that is non-degenerate.

Finally, let us comment on the Abelian case using the compact Lie group $U(1)$ or many copies of it:

$\boldsymbol{G = U(1) \times \cdots \times U(1)}$ — We note that the symmetry-resolved decomposition (4.8) becomes trivial. In fact, in this case the structure constants $f^{ab}{}_c$ vanish because the generators T^a commute, and therefore their algebra coincides with the center, $\mathcal{A}_{\text{sym}} = \mathcal{Z}_{\text{sym}} = \mathbb{C}[T^a]$. As a result, we have a decomposition of the form $\mathcal{H} = \bigoplus_m \mathcal{H}_G^{(m)}$ where the eigenvalues of the commuting generators T^a (sometimes called charges or particle numbers) are collectively denoted as m. The sym factor in the decomposition is trivial, $\dim \mathcal{H}_{\text{sym}}^{(m)} = 1$, and can be reabsorbed into a phase in each sector $\mathcal{H}_G^{(m)}$.

4.3 Symmetry-resolved states and subsystems

The symmetry-resolved decomposition of the Hilbert space (4.8) allows us to write G-invariant observables as

$$O \in \mathcal{A}_G \qquad \Longrightarrow \qquad O = \bigoplus_q \left(\mathbb{1}_{\text{sym}}^{(q)} \otimes O_G^{(q)}\right). \tag{4.11}$$

Given a pure state $|\psi\rangle \in \mathcal{H}$, we can write the restriction of the state to the G-invariant observables as $\rho_G = \langle\psi|\Pi_G|\psi\rangle$, where the map Π_G is defined concretely by (3.15). A *symmetry-resolved state* is defined as a pure state that remains pure when restricted to the G-invariant subalgebra of observables $\mathcal{A}_G$. As shown in

Chapter 3, Eq. (3.25), this implies that it belongs to an irreducible representation q and has the product form:

$$|\psi\rangle \quad \textit{symmetry-resolved state in } \mathcal{H} \qquad \Longleftrightarrow \qquad \exists\, q \;:\quad |\psi\rangle = |q,\xi\rangle_{\rm sym}\, |q,\chi\rangle_G\,. \tag{4.12}$$

In other words, symmetry-resolved states have no entanglement between internal G-invariant degrees of freedom and *sym* degrees of freedom that change under transformations of the group G.

A *symmetry-resolved subsystem* is defined by a set O_1, O_2, ... of G-invariant observables that we have access to. The algebra $\mathcal{A}_{G\mathcal{S}}$ that they generate is

$$\mathcal{A}_{G\mathcal{S}} = \mathbb{C}[O_l] \;\subseteq \mathcal{A}_G \qquad \text{with} \qquad O_l \in \mathcal{A}_G\,, \qquad l = 1,\ldots,L\,. \tag{4.13}$$

We are interested in the restriction of a state $|\psi\rangle$ to this subalgebra, $\rho_{G\mathcal{S}} = \langle\psi|\Pi_{G\mathcal{S}}|\psi\rangle$. To build the map $\Pi_{G\mathcal{S}}$, we follow the steps discussed in Chapter 3. First, we define the rest of the system using the commutant algebra,

$$\mathcal{A}_{\overline{G\mathcal{S}}} \equiv (\mathcal{A}_{G\mathcal{S}})' \;=\; \{M \in \mathcal{A}\,|\,[M,O_l] = 0\,,\;\; \forall\, O_l \in \mathcal{A}_{G\mathcal{S}}\}\,. \tag{4.14}$$

Note that $\mathcal{A}_{\overline{G\mathcal{S}}}$ also contains observables that are not G-invariant. The center of the subalgebra is generated by a set of commuting G-invariant observables R_i in the intersection of the two,

$$\mathcal{Z}_{G\mathcal{S}} = \mathcal{A}_{G\mathcal{S}} \cap \mathcal{A}_{\overline{G\mathcal{S}}} = \mathbb{C}[R_i]\,. \tag{4.15}$$

By diagonalizing first the commuting observables R_i and calling collectively their eigenvalues r, we obtain the direct sum decomposition

$$\mathcal{H} = \bigoplus_r \left(\mathcal{H}^{(r)}_{G\mathcal{S}} \otimes \mathcal{H}^{(r)}_{\overline{G\mathcal{S}}}\right). \tag{4.16}$$

This decomposition allows us to define the map $\Pi_{G\mathcal{S}}$. As we are interested in the restriction of a symmetry-resolved state to a symmetry-resolved subsystem, it is useful to have a decomposition of the Hilbert space and an orthonormal basis that is adapted to both decompositions (4.8) and (4.16). We show that this is possible in general with a concrete construction.

We introduce a decomposition adapted to symmetry-resolved states and symmetry-resolved subsystems. Let us consider the algebra $\mathcal{A}_{\mathrm{sym}G\mathcal{S}}$ generated by the symmetry generators T^a and by the G-invariant observables O_l that generate the subsystem,

$$\mathcal{A}_{\mathrm{sym}G\mathcal{S}} = \mathbb{C}[T^a, O_l]\,. \tag{4.17}$$

The commutant of this algebra is[2]

$$\mathcal{A}_{G\,\overline{\mathcal{S}}} \equiv (\mathcal{A}_{\mathrm{sym}G\mathcal{S}})' \;=\; \mathbb{C}[T^a, O_l]' \;=\; \mathbb{C}[T^a]' \cap \mathbb{C}[O_l]' \tag{4.18}$$

$$= (\mathcal{A}_{\mathrm{sym}})' \cap (\mathcal{A}_{G\mathcal{S}})' \;=\; \mathcal{A}_G \cap \mathcal{A}_{\overline{G\mathcal{S}}} \tag{4.19}$$

Note that, because of the presence of the symmetry generators T^a in $\mathcal{A}_{\mathrm{sym}G\mathcal{S}}$, the algebra $\mathcal{A}_{G\,\overline{\mathcal{S}}}$ contains only the G-invariant observables in $\mathcal{A}_{\overline{G\mathcal{S}}}$. We can now define the center

$$\mathcal{Z}_{\mathrm{sym}G\mathcal{S}} = \mathcal{A}_{\mathrm{sym}G\mathcal{S}} \cap \mathcal{A}_{G\,\overline{\mathcal{S}}} \;=\; \mathbb{C}[Q_k, R_i]\,. \tag{4.20}$$

Note that the center of the algebra $\mathcal{A}_{\mathrm{sym}G\mathcal{S}}$ is generated by the elements of the center R_i of the symmetry-resolved subsystem and by the Casimir operators Q_k of the group G. The fact that the two commutes, $[R_i, Q_k] = 0$, follows immediately from the fact that R_i are G-invariant observables, i.e., $[R_i, T^a] = 0$, and the Casimir operators (4.6) are functions of the symmetry generator. By diagonalizing simultaneously the commuting set $\{Q_k, R_i\}$ with eigenvalues denoted collectively by q and r, we obtain the decomposition

$$\mathcal{H} = \bigoplus_q \left(\mathcal{H}^{(q)}_{\mathrm{sym}} \;\otimes\; \bigoplus_r \left(\mathcal{H}^{(r)}_{G\mathcal{S}} \otimes \mathcal{H}^{(q,r)}_{G\,\overline{\mathcal{S}}} \right) \right). \tag{4.21}$$

The decomposition comes with an orthonormal basis adapted simultaneously to symmetry-resolved states and to the symmetry-resolved subsystems,

$$|q, r, \alpha, \beta\rangle \;=\; |q, m\rangle_{\mathrm{sym}}\, |r, \alpha\rangle_{G\mathcal{S}}\, |q, r, \beta\rangle_{G\,\overline{\mathcal{S}}}\,. \tag{4.22}$$

Note that the basis elements $|r, \alpha\rangle_{G\mathcal{S}}$ of the symmetry-resolved system depend on the eigenvalues r of R_i but not on the eigenvalues q of the Casimirs Q_k. This feature can also be understood by considering the two decompositions $\mathcal{H}^{(q)}_G =$

[2] In the first line we used the relation (3.4) that applies to any set of observables H_i and K_j.

$\bigoplus_r \left(\mathcal{H}^{(r)}_{G\mathcal{S}} \otimes \mathcal{H}^{(q,r)}_{G\overline{\mathcal{S}}}\right)$ and $\mathcal{H}^{(r)}_{\overline{G\mathcal{S}}} = \bigoplus_q \left(\mathcal{H}^{(q)}_{\rm sym} \otimes \mathcal{H}^{(q,r)}_{G\overline{\mathcal{S}}}\right)$, that relate the formulas (4.8), (4.16) and (4.21).

4.4 Symmetry-resolved entanglement entropy

The entanglement entropy of a symmetry-resolved state $|\psi\rangle$ restricted to a symmetry-resolved subsystem can be defined and computed using the tools introduced above. The symmetry-resolved state can be first written in the basis adapted to the subsystem:

$$|\psi\rangle \;=\; \Big(\sum_m \xi_m \,|q,m\rangle_{\rm sym}\Big)\,\Big(\sum_r \sqrt{p_r}\sum_{\alpha,\beta}\chi^{(r)}_{\alpha\beta}\,|r,\alpha\rangle_{G\mathcal{S}}\,|q,r,\beta\rangle_{G\overline{\mathcal{S}}}\Big)\,, \tag{4.23}$$

with p_r, the probability of finding the state in the sector is r. The state belongs to a definite sector q, it does not have entanglement between internal G-invariant degrees of freedom and sym degrees of freedom, and, in general, can have entanglement between the G-invariant degrees of freedom in the subsystem and its complement. The restriction to the subsystem can be written as

$$\rho_{G\mathcal{S}} = \langle\psi|\Pi_{G\mathcal{S}}|\psi\rangle \;=\; \bigoplus_r p_r\,\rho^{(r)}_{G\mathcal{S}} \qquad \text{with} \qquad (\rho^{(r)}_{G\mathcal{S}})_{\alpha\alpha'} = \sum_\beta \chi^{(r)}_{\alpha\beta}\chi^{(r)*}_{\alpha'\beta}\,. \tag{4.24}$$

The entanglement entropy $S(|\psi\rangle,\mathcal{A},\mathcal{A}_{G\mathcal{S}})$ can then be computed using (3.18), (3.24). Bounds on the entanglement entropy can be written in terms of the dimensions of the sectors:

$$d_r = \dim\mathcal{H}^{(r)}_{G\mathcal{S}}\,, \qquad b_{qr} = \dim\mathcal{H}^{(q,r)}_{G\overline{\mathcal{S}}}\,, \qquad D_q = \dim\mathcal{H}^{(q)}_G \;=\; \textstyle\sum_r d_r b_{qr}\,. \tag{4.25}$$

In particular a symmetry-resolved state $|\psi^{(q)}\rangle$ in the sector q has entanglement entropy bounded from above by

$$0 \;\le\; S(|\psi^{(q)}\rangle,\mathcal{A},\mathcal{A}_{G\mathcal{S}}) \;\le\; \log\Big(\sum_r \min(d_r,b_{qr})\Big)\,. \tag{4.26}$$

Note that here, the sector $\mathcal{H}^{(q)}_{\rm sym}$ is simply an ancilla, and the entropy is independent of ξ_m.

A random symmetry-resolved state with fixed q can be defined starting from a reference state of the symmetry-resolved form $|q,\xi\rangle_{\rm sym}\,|q,\chi\rangle_G$, and acting on it with a random unitary of the form $\bigoplus_q(U^{(q)}_{\rm sym}\otimes U^{(q)}_G)$, where $U^{(q)}_{\rm sym}$ and $U^{(q)}_G$ are Haar-measure distributed on $\mathcal{H}^{(q)}_{\rm sym}$ and $\mathcal{H}^{(q)}_G$ respectively. The average entanglement entropy and its variance are then given by the expressions (3.32) and (3.33), with the dimensions d_r and b_{qr} given above.

Chapter 5
Locality, Many-body Systems and G-local Entanglement

5.1 Introduction

In certain quantum systems, the inherent notion of locality, stemming from the spatial arrangement of particles or sites, provides a natural way of selecting a subset to define subsystems. This chapter explores how the presence of a global symmetry group G further refines this picture. In many-body systems, the standard tensor-product structure based solely on spatial locality (often referred to as the K-local decomposition) does not capture the full physical content when global symmetries are present. While the K-local subalgebra of observables is associated with a spatial region A, such observables do not necessarily respect the symmetry of the system. Extending the work in Chaper 4, we introduce a G-local subalgebra which comprises those observables that are both local (acting solely on region A) and invariant under the action of G. Unlike the K-local case, the G-local observables (illustrated in Chapter 1 in Figs. (1.1) and (1.2)) are not, in general, mutually commuting with those on the complementary region, a fact that leads to subtle differences in the entanglement structure.

In this chapter we develop a formalism to decompose the symmetry-resolved Hilbert space further into subsystems defined by the G-local algebra. In particular, by introducing Casimir operators associated with the subgroup acting on region A, we obtain an additional decomposition intp sectors labeled by the eigenvalues of the

subsystem Casimir operators. This refined decomposition enables us to define a symmetry-resolved entanglement entropy that quantifies the entanglement of a state when restricted to the G-local observables in region A. The chapter presents exact formulas for the average symmetry-resolved entanglement entropy and its decomposition into configurational and number entropy contributions. For random symmetry-resolved states, these formulas are expressed in terms of the dimensions of the various sectors. In the Abelian case, illustrated with $G = U(1)$, the analysis simplifies considerably, and we recover known results, including the equivalence between G-local and K-local entropies and the expected equipartition behavior under specific limits. This chapter sets the stage for the analysis of typical entanglement for non-Abelian symmetry groups where the two notions are expected to differ, highlighting the nontrivial interplay between symmetry and locality. The results presented in this chapter are based on Sec. 4 of [5].

5.2 Setup

In a lattice many-body system, there is a built-in notion of locality associated with the N bodies, or particles, at the sites of the lattice. We assume that the Hilbert space at each site n is a copy of a finite-dimensional Hilbert space $\mathcal{H}_d \simeq \mathbb{C}^d$ that carries a unitary (reducible) representation of a compact Lie group G. Therefore, the kinematical Hilbert space $\mathcal{H}_N$ of the system is the tensor product of the Hilbert spaces at sites [67,94]:

$$\mathcal{H}_N = \underbrace{\mathcal{H}_d \otimes \cdots \otimes \mathcal{H}_d}_{N} \,. \tag{5.1}$$

Calling T_n^a the d-dimensional (reducible) representation of the generators of the group G at each site n, we have that the generator of global transformation for the group G acting on $\mathcal{H}_N$ is simply given by the sum

$$T^a = \sum_{n=1}^{N} T_n^a \,. \tag{5.2}$$

We can then use the results of Chapter 4, and in particular (4.8)–(4.9), to decompose the Hilbert space in symmetry-resolved sectors

$$\mathcal{H}_N = \bigoplus\nolimits_q \mathcal{H}_N^{(q)} \;=\; \bigoplus\nolimits_q \left(\mathcal{H}_{\text{sym}}^{(q)} \otimes \mathcal{H}_G^{(q)}\right) \tag{5.3}$$

where the quantum number q labels the irreducible representations of the group G, i.e., the eigenvalues of the Casimir operators for a semisimple Lie group. The representation space $\mathcal{H}^{(q)}_{\rm sym}$ is the one already described in Sec. 4.2 and the invariant space is

$$\mathcal{H}^{(q)}_G = {\rm Inv}_G\big(\mathcal{H}^{(\bar{q})}_{\rm sym} \otimes \underbrace{\mathcal{H}_d \otimes \cdots \otimes \mathcal{H}_d}_{N}\big)\,, \tag{5.4}$$

where $\bar{q}$ is the conjugate representation.

5.3 K-local decomposition of the Hilbert space

Let us consider a subset $n \in A$ of the nodes of the many-body lattice, for instance, the ones defining a local region A of the lattice and excluding its complement B [94]. This subsystem corresponds to the standard tensor-product decomposition

$$\mathcal{H}_N = \mathcal{H}_A \otimes \mathcal{H}_B\ , \qquad \text{with} \qquad \mathcal{H}_A = \bigotimes_{n\in A} \mathcal{H}_d\,, \qquad \mathcal{H}_B = \bigotimes_{n\in B} \mathcal{H}_d\ . \tag{5.5}$$

This decomposition is associated with a K-local subalgebra of observables. Let us define first the kinematical algebra of observables $\mathcal{A}_K = \mathcal{L}(\mathcal{H}_N)$. The K-local subalgebra in A is

$$\mathcal{A}_{KA} = \{O \in \mathcal{A}_K \mid O = O_A \otimes \mathbb{1}_B \ \text{ with } \ O_A \in \mathcal{L}(\mathcal{H}_A)\}\,. \tag{5.6}$$

Clearly we have that the K-local subalgebra in B coincides with the commutant of A, i.e., $\mathcal{A}_{KB} = (\mathcal{A}_{KA})'$, and that the center is trivial $\mathcal{A}_{KA} \cap \mathcal{A}_{KB} = \mathbb{1}$.

We note that the operator (5.2) that generates global unitary transformations for the group G takes the form

$$T^a \ = \ T^a_A \otimes \mathbb{1}_B \ + \ \mathbb{1}_A \otimes T^a_B\,, \tag{5.7}$$

which is additive over the subsystems A and B. The operator T^a_A given by

$$T^a_A \otimes \mathbb{1}_B \ = \sum_{n\in A} T^a_n \ \in \mathcal{A}_{KA}\,, \tag{5.8}$$

and generates unitary transformations for the group G in A.[1]

5.4 G-local decomposition and symmetry-resolution

G-invariant observables O_G of the many-body system belong to the algebra $\mathcal{A}_G$ defined in (4.4). G-local observables in the subsystem A are observables that are both G-invariant and belong to the subsystem A. They are, therefore, elements of the intersection of the two algebras,

$$\mathcal{A}_{GA} = \mathcal{A}_{KA} \cap \mathcal{A}_G \,. \tag{5.9}$$

We can similarly define G-local observables in B,

$$\mathcal{A}_{GB} = \mathcal{A}_{KB} \cap \mathcal{A}_G \,. \tag{5.10}$$

Note that in general, for a non-Abelian group, the two subalgebras are not the commutant of each other, $\mathcal{A}_{GB} \neq (\mathcal{A}_{GA})'$. In fact, using $\mathcal{A}_G = (\mathcal{A}_{\rm sym})'$ and the intersection formula (3.4), we find

$$(\mathcal{A}_{GA})' = (\mathcal{A}_{KA} \cap \mathcal{A}_G)' = \big((\mathcal{A}_{KB})' \cap (\mathcal{A}_{\rm sym})'\big)' = \mathbb{C}[\mathbb{1}_A \otimes O_B,\, T^a_A \otimes \mathbb{1}_B] \,. \tag{5.11}$$

We can now determine the center of the subalgebra,

$$\mathcal{Z}_{GA} = \mathcal{A}_{GA} \cap (\mathcal{A}_{GA})' = \mathbb{C}\big[Q^{(1)}_A, \ldots, Q^{(\mathrm{rank}(G))}_A\big] \,, \tag{5.12}$$

which is generated by the Casimir operators in the subsystem A,

$$Q^{(k)}_A \;=\; \eta_{a_1 \cdots a_{p(k)}}\, T^{a_1}_A \cdots T^{a_{p(k)}}_A \,, \qquad\qquad k = 1, \ldots, \mathrm{rank}(G) \,, \tag{5.13}$$

with the symmetric tensors $\eta_{a_1 \cdots a_{p(k)}}$ defined in (4.6). Denoting collectively q_A the eigenvalues of the subsystem Casimir operators in A, and using the results of Sec. 4.3, we obtain a decomposition of the Hilbert space sector $\mathcal{H}^{(q)}_N$ in G-local

[1] Note that we are using the same notation for the generator acting on the Hilbert space of a single site $T^a_n \in \mathcal{L}(\mathcal{H}_d)$ and for the generator acting on a single site of the many-body Hilbert space, $T^a_n \equiv \mathbb{1}_d \otimes \cdots \otimes T^a_n \otimes \cdots \otimes \mathbb{1}_d \in \mathcal{L}(\mathcal{H}_d \otimes \cdots \otimes \mathcal{H}_d)$.

subsystems:

$$\mathcal{H}_N^{(q)} \;=\; \mathcal{H}_{\text{sym}}^{(q)} \otimes \bigoplus_{q_A} \left(\mathcal{H}_{GA}^{(q_A)} \otimes \mathcal{H}_{GB}^{(q,\,q_A)} \right), \tag{5.14}$$

where the factors are defined as

$$\mathcal{H}_{GA}^{(q_A)} = \text{Inv}_G(\mathcal{H}_{\text{sym}}^{(\bar{q}_A)} \otimes \mathcal{H}_A) \;, \qquad \mathcal{H}_{GB}^{(q,\,q_A)} = \text{Inv}_G(\mathcal{H}_{\text{sym}}^{(\bar{q})} \otimes \mathcal{H}_{\text{sym}}^{(q_A)} \otimes \mathcal{H}_B) \;. \tag{5.15}$$

This decomposition provides us with an orthonormal basis of $\mathcal{H}_N^{(q)}$ adapted to the subalgebra $\mathcal{A}_{GA}$. It is then immediate to compute the entanglement entropy S_{GA} of a state $|\psi\rangle$ restricted to the G-local subalgebra in A,

$$S_{GA} = S(|\psi\rangle, \mathcal{A}, \mathcal{A}_{GA}) \,. \tag{5.16}$$

It is interesting to compare the properties of the G-local entanglement entropy S_{GA} to the ones of the familiar K-local entanglement entropy S_{KA},

$$S_{KA} = S(|\psi\rangle, \mathcal{A}, \mathcal{A}_{KA}) \,. \tag{5.17}$$

In general, the two entropies do not coincide because the G-local subalgebra can be understood as a coarse-graining of the K-local one [74], i.e., $\mathcal{A}_{GA} \subset \mathcal{A}_{KA}$. They both probe local properties of the many-body system and can be understood as functions of the number of bodies N_A in the subsystem A. However, there is a crucial difference between the two. Commutant symmetry (3.28) implies that $S_{KA}(|\psi\rangle) = S_{KB}(|\psi\rangle)$, but in general $S_{GA}(|\psi\rangle) \neq S_{GB}(|\psi\rangle)$ because $\mathcal{A}_{GB} \neq (\mathcal{A}_{GA})'$.

Bringing together the results of Chapter 3, Chapter 4, and the decomposition (5.14), we obtain the exact formulas for the typical G-local symmetry-resolved entanglement entropy that apply to a compact Lie group G. For a random symmetry-resolved state $|\psi^{(q)}\rangle$ with total charge q, the total symmetry-resolved entanglement entropy has average value

$$\langle S_{GA} \rangle_q \;=\; \sum_{q_A|\; d_{q_A} \leq b_{qq_A}} \frac{d_{q_A} b_{qq_A}}{D} \left(\Psi(D+1) - \Psi(b_{qq_A}+1) - \frac{d_{q_A}-1}{2\, b_{qq_A}} \right) \tag{5.18}$$

$$+ \sum_{q_A|\; d_{q_A} > b_{qq_A}} \frac{d_{q_A} b_{qq_A}}{D} \left(\Psi(D+1) - \Psi(d_{q_A}+1) - \frac{b_{qq_A}-1}{2\, d_{q_A}} \right), \tag{5.19}$$

where the dimensions of the sectors are defined as

$$d_{q_A} = \mathcal{H}_{GA}^{(q_A)}\,, \qquad b_{qq_A} = \dim \mathcal{H}_{GB}^{(q,\,q_A)}\,, \qquad D = \dim \mathcal{H}_{GA}^{(q_A)} \;=\; \textstyle\sum_{q_A} d_{q_A} b_{qq_A}\,. \tag{5.20}$$

Note that the formula takes into account the fact that, in the sum over subsystem charges q_A, the dimensions of the subsystem sectors can satisfy either $d_{q_A} \leq b_{qq_A}$ or $d_{q_A} > b_{qq_A}$.

The symmetry-resolved entanglement entropy $S_{GA}(|\psi_j\rangle)$ can be understood as the sum of two terms, $S_{GA}^{(\mathrm{conf})}$ and $S_{GA}^{(\mathrm{num})}$. One first defines the symmetry-resolved entanglement entropy at fixed system *and* subsystem charges $S_{GA}^{(j_A)}$ as the von Neumann entropy of the density matrix $\rho_{GA}^{(j_A)}$ in each sector j_A. Then the configurational entropy $S_{GA}^{(\mathrm{conf})}$ is given by its average over the probability $p^{(j_A)}$ of finding the state in the sector j_A, and the number entropy $S_{GA}^{(\mathrm{num})}$ is the Shannon entropy of the probability $p^{(j_A)}$. The table below summarizes the definitions commonly used in the literature:

Total symmetry-resolved entanglement entropy	$S_{GA}(\|\psi_j\rangle)$
Symmetry-resolved entanglement entropy at fixed system & subsystem charges	$S_{GA}^{(j_A)} = -\mathrm{tr}\big(\rho_{GA}^{(j_A)} \log \rho_{GA}^{(j_A)}\big)$
Configurational entropy	$S_{GA}^{(\mathrm{conf})} = \sum_{j_A} p^{(j_A)}\, S_{GA}^{(j_A)}$
Number entropy (Shannon)	$S_{GA}^{(\mathrm{num})} = -\sum_{j_A} p^{(j_A)} \log p^{(j_A)}$

(5.21)

The average symmetry-resolved entanglement entropy at fixed subsystem charge, $\langle S_{GA}^{(q_A)} \rangle_q$, i.e., the entanglement entropy of a random symmetry-resolved state $|\psi^{(q)}\rangle$ projected to the sector with subsystem charge q_A, is given by the standard Page formula [21, 69]

$$\langle S_{GA}^{(q_A)} \rangle_q = \begin{cases} \Psi(d_{q_A} b_{qq_A} + 1) - \Psi(b_{qq_A} + 1) - \dfrac{d_{q_A} - 1}{2\, b_{qq_A}} & d_{q_A} \leq b_{qq_A}\,, \\[2ex] b_{qq_A} \;\longleftrightarrow\; d_{q_A} & d_{q_A} > b_{qq_A}\,. \end{cases} \tag{5.22}$$

The average over the subsystem sectors q_A, weighted with the probability

$$\varrho_{q_A} = \frac{d_{q_A} b_{qq_A}}{D} \tag{5.23}$$

of the state $|\psi^{(q)}\rangle$ being found in each sector, is given by the configurational entropy

$$\langle S_{GA}^{(\mathrm{conf})}\rangle_q = \sum_{q_A} \varrho_{q_A} \langle S_{GA}^{(q_A)}\rangle_q \,. \tag{5.24}$$

The average Shannon entropy of the probability distribution (5.23) defines the number entropy

$$\langle S_{GA}^{(\mathrm{num})}\rangle_q = \sum_{q_A} \varrho_{q_A} \left(\Psi(D+1) - \Psi(d_{q_A} b_{qq_A} + 1)\right) \tag{5.25}$$

Finally, the total symmetry-resolved entanglement entropy can be written as the sum

$$\langle S_{GA}\rangle_q = \langle S_{GA}^{(\mathrm{conf})}\rangle_q + \langle S_{GA}^{(\mathrm{num})}\rangle_q \,. \tag{5.26}$$

5.5 $U(1)$ symmetry-resolved entanglement

In the case of an Abelian symmetry group there are significant simplifications that we illustrate here with the example of $G = U(1)$ and charge conservation [13–20].

We consider a lattice many-body system with nodes carrying a copy of the two-dimensional Hilbert space $\mathcal{H}_2 = \mathbb{C}^2$ of a spin-1/2 particle, and transforming under a reducible representation of the group $U(1)$, i.e.,

$$\mathcal{H}_N = \underbrace{\mathcal{H}_2 \otimes \cdots \otimes \mathcal{H}_2}_{N} \qquad \text{with} \qquad \mathcal{H}_2 = \bigoplus_{m'=\pm 1/2} \mathcal{H}_2^{(m')} = \mathrm{span}(|1/2,\, \pm 1/2\rangle) \,. \tag{5.27}$$

The generator of the $U(1)$ symmetry at each site is the spin operator $S_n^z = \sigma^z/2$, and the generator of global $U(1)$ transformations is

$$J^z = \sum_{n=1}^{N} S_n^z \,, \tag{5.28}$$

which generates global rotations that preserve the direction of the axis z. The Hilbert space of the system decomposes as a direct sum over irreducible representations of the group $U(1)$ labeled by the quantum number m, the eigenvalue of J^z

or the total charge,

$$\mathcal{H}_N \;=\; \bigoplus_{m=-N/2}^{+N/2} \left(\mathcal{H}_{\rm sym}^{(m)} \otimes \mathcal{H}_G^{(m)}\right) \;=\; \bigoplus_{m=-N/2}^{+N/2} \mathcal{H}_G^{(m)} \tag{5.29}$$

We note that, as the group is Abelian, the sym factor $\mathcal{H}_{\rm sym}^{(m)}$ is trivial, it has dimension $\dim \mathcal{H}_{\rm sym}^{(m)} = 1$ and the pure phase $\mathrm{e}^{\mathrm{i}m\theta}$ associated to each irreducible representation m can be reabsorbed in the $U(1)$-invariant part of the state in $\mathcal{H}_G^{(m)}$. Moreover, as for $U(1)$ the conjugate representation is simply $\overline{m} = -m$, the invariant Hilbert space is given by

$$\mathcal{H}_G^{(m)} = \mathrm{Inv}_G\big(\mathcal{H}_{\rm sym}^{(-m)} \otimes \mathcal{H}_N\big) = \bigoplus_{\substack{m_1,\dots,m_N=\pm 1/2 \\ m_1+\cdots+m_N=m}} \mathcal{H}_2^{(m_1)} \otimes \cdots \otimes \mathcal{H}_2^{(m_N)}\,. \tag{5.30}$$

To define a G-local subsystem with N_A bodies, we define the generator of $U(1)$ transformations in A,

$$J_A^z = \sum_{n\in A} S_n^z\,, \tag{5.31}$$

with eigenvalues m_A. The decomposition in G-local subsystems is then given by

$$\mathcal{H}_G^{(m)} = \bigoplus_{m_A} \left(\mathcal{H}_{GA}^{(m_A)} \otimes \mathcal{H}_{GB}^{(m,m_A)}\right) \;=\; \bigoplus_{\substack{m_A,m_B \\ m_A+m_B=m}} \left(\mathcal{H}_{GA}^{(m_A)} \otimes \mathcal{H}_{GB}^{(m_B)}\right), \tag{5.32}$$

where we used the relation $\mathcal{H}_{\rm sym}^{(m_A)} \otimes \mathcal{H}_{\rm sym}^{(m_B)} = \mathcal{H}_{\rm sym}^{(m_A+m_B)}$ that holds only in the Abelian case, together with the definitions

$$\mathcal{H}_{GA}^{(m_A)} \equiv \mathrm{Inv}_G(\mathcal{H}_{\rm sym}^{(-m_A)} \otimes \mathcal{H}_A)\,, \tag{5.33}$$

$$\mathcal{H}_{GB}^{(m,m_A)} \equiv \mathrm{Inv}_G(\mathcal{H}_{\rm sym}^{(-m)} \otimes \mathcal{H}_{\rm sym}^{(m_A)} \otimes \mathcal{H}_B) \;=\; \mathrm{Inv}_G(\mathcal{H}_{\rm sym}^{(-m+m_A)} \otimes \mathcal{H}_B) \;=\; \mathcal{H}_{GB}^{(m-m_A)}\,. \tag{5.34}$$

Note that, in the Abelian case, for a symmetry-resolved state $|\psi^{(m)}\rangle \in \mathcal{H}_G^{(m)}$, the G-local and the K-local entropy coincide,

$$G = U(1) \quad\Longrightarrow\quad S_{GA}(|\psi^{(m)}\rangle) = S_{KA}(|\psi^{(m)}\rangle)\,, \tag{5.35}$$

and the commutant symmetry (3.28) implies the subsystem symmetry

$$G = U(1) \quad \Longrightarrow \quad S_{GB}(|\psi^{(m)}\rangle) = S_{GA}(|\psi^{(m)}\rangle)\,. \tag{5.36}$$

Applying the general formulas (5.18)–(5.26) to the Abelian Lie group $G = U(1)$, we see that the total symmetry-resolved entanglement entropy in the sector of charge m has the average value

$$\langle S_{GA}\rangle_m = \sum_{m_A|\; d_{m_A} \le b_{m\,m_A}} \frac{d_{m_A} b_{m\,m_A}}{D} \left(\Psi(D+1) - \Psi(b_{m\,m_A}+1) - \frac{d_{m_A}-1}{2\,b_{m\,m_A}} \right) \tag{5.37}$$

$$+ \sum_{m_A|\; d_{m_A} > b_{m\,m_A}} \frac{d_{m_A} b_{m\,m_A}}{D} \left(\Psi(D+1) - \Psi(d_{m_A}+1) - \frac{b_{m\,m_A}-1}{2\,d_{m_A}} \right), \tag{5.38}$$

where the dimensions of the sectors are given by

$$D_m = \dim \mathcal{H}_G^{(m)} = \binom{N}{\frac{N}{2}+m} \tag{5.39}$$

$$d_{m_A} = \dim \mathcal{H}_{GA}^{(m_A)} = \binom{N_A}{\frac{N_A}{2}+m_A} \tag{5.40}$$

$$b_{m\,m_A} = \dim \mathcal{H}_{GB}^{(m,m_A)} = \binom{N-N_A}{\frac{N-N_A}{2}+m-m_A} \tag{5.41}$$

Note that the formula takes into account the fact that, in the sum over subsystem charges q_A, the dimensions of the subsystem sectors can satisfy either $d_{m_A} \le b_{m\,m_A}$ or $d_{m_A} > b_{m\,m_A}$.

We can also decompose the total symmetry-resolved entanglement entropy into different components. The average symmetry-resolved entanglement entropy at fixed subsystem charge, $\langle S_{GA}^{(m_A)}\rangle_m$, i.e., the entanglement entropy of a random symmetry-resolved state $|\psi^{(m)}\rangle$ projected to the sector with subsystem charge m_A,

is given by the standard Page formula [21,69]

$$\langle S_{GA}^{(m_A)}\rangle_m = \begin{cases} \Psi(d_{m_A} b_{m\,m_A}+1) - \Psi(b_{m\,m_A}+1) - \dfrac{d_{m_A}-1}{2\,b_{m\,m_A}} & d_{m_A} \leq b_{m\,m_A}\,, \\ \\ b_{m\,m_A} \;\longleftrightarrow\; d_{m_A} & d_{m_A} > b_{m\,m_A}\,. \end{cases} \tag{5.42}$$

The average over the subsystem sectors m_A, weighted with the probability

$$\varrho_{m_A} = \frac{d_{m_A} b_{m\,m_A}}{D} \tag{5.43}$$

of the state $|\psi^{(m)}\rangle$ being found in each sector, is given by the configurational entropy

$$\langle S_{GA}^{(\mathrm{conf})}\rangle_m = \sum_{m_A} \varrho_{m_A} \langle S_{GA}^{(m_A)}\rangle_m\,. \tag{5.44}$$

The average Shannon entropy of the probability distribution (5.23) defines the number entropy

$$\langle S_{GA}^{(\mathrm{num})}\rangle_m = \sum_{m_A} \varrho_{m_A} \Big(\Psi(D+1) - \Psi(d_{m_A} b_{m\,m_A}+1) \Big) \tag{5.45}$$

Finally, the total symmetry-resolved entanglement entropy can be written as the sum

$$\langle S_{GA}\rangle_m = \langle S_{GA}^{(\mathrm{conf})}\rangle_m + \langle S_{GA}^{(\mathrm{num})}\rangle_m\,. \tag{5.46}$$

To compare to the literature on the thermodynamic limit [13–16] and on equipartition of entanglement [27], we introduce intensive quantities and study the behavior of subsystem entropy in the limit $N \to \infty$ at fixed intensive properties. Specifically, we define the subsystem fraction f, the system $U(1)$ charge density s, and the subsystem charge density t as follows:

$$f = \frac{N_A}{N}, \qquad s = \frac{2m}{N}, \qquad t = \frac{2m_A}{N_A}\,, \tag{5.47}$$

and we restrict here to $f < 1/2$. At the leading order in N, the symmetry-resolved entanglement entropy at fixed system and subsystem charge reduces to

$$\langle S_{GA}^{(m_A)}\rangle_m = \log d_{m_A} + O(1) \;=\; fN\beta(t) - \frac{1}{2}\log N + O(1)\;, \tag{5.48}$$

where we used the property (3.37) that allows us to write the digamma function $\Psi(x)$ as a logarithm at the leading order, and we have defined the function $\beta(t)$ as:

$$\beta(t) = -\frac{1-t}{2}\log\left(\frac{1-t}{2}\right) - \frac{1+t}{2}\log\left(\frac{1+t}{2}\right) \ . \tag{5.49}$$

This result corresponds exactly to the one found in [14].[2] We then compute the configurational entropy, number entropy, and total symmetry-resolved entropy in the thermodynamic limit. In this limit, the probability ϱ_{m_A} (5.43) is approximated by a discrete Gaussian probability with mean $\bar{m}_A = Nf\frac{s}{2}$ and variance $\sigma_A^2 = N\frac{f(1-f)}{4}$. In terms of intensive quantities, this translates into a continuous probability density function $\varrho(t)$ with mean $\bar{t} = s$ and variance $\sigma_t^2 = \frac{1-f}{fN}$. We evaluate the configurational entropy at leading order in N using saddle-point techniques. This is equivalent to computing the symmetry-resolved entanglement entropy at fixed system and subsystem charge (5.48) at the mean $t = \bar{t} = s$:

$$\langle S_{GA}^{(\mathrm{conf})}\rangle_m = fN\beta(s) - \frac{1}{2}\log N + O(1) \ . \tag{5.50}$$

The computation of the number entropy is straightforward. The Shannon entropy of a discrete Gaussian probability is simply given by $\frac{1}{2}\log(2\pi\sigma_A^2) + \frac{1}{2}$ where σ_A is the variance. Hence, the number entropy is:

$$\langle S_{GA}^{(\mathrm{num})}\rangle_m = \frac{1}{2}\log(N\frac{\pi f(1-f)}{2}) + \frac{1}{2} + O(1) \ = \ \frac{1}{2}\log N + O(1) \ . \tag{5.51}$$

We note that when we sum the configurational entropy and the number entropy to obtain the total symmetry-resolved entanglement entropy, the logarithmic contributions cancel, resulting in the formula

$$\langle S_{GA}\rangle_m = fN\beta(s) + O(1) \ , \tag{5.52}$$

with no logarithmic corrections.

Finally, we comment on the equipartition (or lack of equipartition) of entanglement entropy in the thermodynamic limit, as discussed in [27] and [14]. By equipartition of entanglement, one means that the entropy $\langle S_{GA}^{(m_A)}\rangle_m$ is indepen-

[2] A note about conventions. In [14], the $U(1)$ charges are defined as positive quantities. To compare the formulas, one can use the relations $M \equiv m + N/2$ and $Q = m_A + N_A/2$.

dent of m_A in some limit. As we found that $\langle S_{GA}^{(m_A)} \rangle_m \approx fN\beta(t)$ with $t = 2m_A/N_A$, we conclude that there is no equipartition of entanglement entropy, as the leading order in N depends explicitly on the subsystem charge m_A, as already found in [14]. Furthermore, following the argument in [14], we emphasize the importance of the order of limits. If m_A is fixed before taking the limit $N \to \infty$, using the expansion $\beta(t) = \log 2 - \frac{1}{2}t^2 + O(t^4)$, we obtain instead $\langle S_{GA}^{(m_A)} \rangle_m \approx fN \log 2$. This result matches that of [27], where the leading order is independent of m_A and the equipartition of entanglement entropy is restored.

Chapter 6
$SU(2)$ symmetry-resolved entanglement in a spin system

6.1 Introduction

In certain quantum systems like the lattice models composed of spin-$\frac{1}{2}$ particles, the natural tensor product structure of the Hilbert space provides a standard framework to study entanglement via the division of the system into spatially localized regions. However, when the system is endowed with a non-Abelian symmetry—in our case, the group $G = SU(2)$—this conventional approach must be refined. The presence of a global non-Abelian symmetry (group G) imposes additional constraints on the system, reduces the number of accessible observables respecting the symmetry, and naturally leads to a symmetry-resolved decomposition of the Hilbert space as seen in Chapter 4. This chapter is devoted to developing the theoretical tools needed to analyze entanglement in such symmetry-resolved sectors and to distinguish between two notions of locality: the standard K-local observables and the more restrictive G-local observables, which are invariant under the symmetry group. While the standard K-local subalgebra is generated by observables acting on a spatial region A (and leads to the familiar tensor-product decomposition, it does not respect the symmetry constraints imposed by G. In contrast, as seen in Chapter 5, the G-local subalgebra is defined as the intersection of the K-local subalgebra with the algebra of G-invariant observables. This refinement is essential because we are interested in quantifying the entanglement of symmetry-resolved states which are prepared and measured by G-invariant observables. The resulting

G-local entanglement entropy, computed by restricting a symmetry-resolved state to the G-local subalgebra, can differ significantly from the conventional K-local entropy.

This chapter systematically develops the framework to compute the G-local entanglement entropy for our spin system with a $SU(2)$ symmetry. We first review the symmetry-resolved decomposition of the Hilbert space and construct the corresponding G-invariant subalgebra along with its center. We obtain explicit formulas for the dimensions of the internal spaces, and we illustrate how symmetry-resolved states can be written in a factorized form for the particular system at hand. We then construct G-local subsystems and compute the symmetry-resolved entanglement entropy. Several examples with small numbers of spins are presented to highlight the differences between K-local and G-local entanglement. In particular, we show that for some states the G-local entropy vanishes even though the K-local entropy is nonzero, reflecting the loss of information when only rotationally invariant operators are accessible. Finally, by combining these ideas with statistical techniques developed in earlier chapters, we derive exact formulas for the average and variance of the G-local entanglement entropy for random symmetry-resolved states. These results, which are expressed in terms of the dimensions of the various sectors, allow us to characterize the Page curve in symmetry-resolved systems. The analysis reveals features unique to a non-Abelian symmetry, including an asymmetry of entanglement under the exchange of subsystems. The results presented in this chapter are based on Sec. 5 of [5].

6.2 Setup

We consider a system consisting of N spin-$\frac{1}{2}$ particles. Each particle has Hilbert space $\mathcal{H}^{(1/2)} \simeq \mathbb{C}^2$, and the Hilbert space of the system comes with a built-in tensor product structure,

$$\mathcal{H}_N = \underbrace{\mathcal{H}^{(1/2)} \otimes \cdots \otimes \mathcal{H}^{(1/2)}}_{N} . \tag{6.1}$$

The spin operators $\vec{S}_n = (S_n^x, S_n^y, S_n^z)$ generate $SU(2)$ rotations of each particle, satisfy the algebra

$$[S_n^i\,, S_{n'}^j] = \mathrm{i}\,\delta_{nn'}\,\epsilon^{ij}{}_k\,S_n^k\,, \qquad\qquad n, n' = 1, \ldots, N, \tag{6.2}$$

and can be represented in terms of Pauli matrices $\vec{\sigma}$ as $\vec{S}_n = \mathbb{1}_2 \otimes \ldots \otimes \frac{\vec{\sigma}}{2} \otimes \ldots \otimes \mathbb{1}_2$. We also introduce the total spin operator $\vec{J}$,

$$\vec{J} = \sum_{n=1}^{N} \vec{S}_n\,, \tag{6.3}$$

which generates $SU(2)$ rotations of the full system, i.e., $[J^i, S_n^j] = \mathrm{i}\,\epsilon^{ij}{}_k\,S_n^k$. As usual, we write the eigenvalues of $\vec{J}^2$ as $j(j+1)$. There is a minimum and a maximum spin of the system, which depends on the number N of particles:

$$N \text{ even} \quad \Longrightarrow \quad j_{\min} = 0\,, \;\; j_{\max} = \tfrac{N}{2}\,, \;\; j \text{ integer}, \tag{6.4}$$

$$N \text{ odd} \quad \Longrightarrow \quad j_{\min} = \tfrac{1}{2}\,, \;\; j_{\max} = \tfrac{N}{2}\,, \;\; j \text{ half-integer}. \tag{6.5}$$

6.3 Symmetry-resolved decomposition of the Hilbert space

We start with the algebra of observables of the system, which we call the *kinematical* algebra $\mathcal{A}_K$ to distinguish it from the group-invariant algebra $\mathcal{A}_G$ discussed later. The kinematical algebra of observables of the system is generated by the spin operators S_n^i,

$$\mathcal{A}_K = \mathcal{L}(\mathcal{H}_N) = \mathbb{C}\big[S_n^i\big]\,, \qquad \text{with} \qquad n = 1, \ldots, N, \tag{6.6}$$

where $\mathcal{L}(\mathcal{H}_N) \simeq M_{2^N}(\mathbb{C})$ is the set of linear operators on $\mathcal{H}_N$, and $\mathbb{C}\big[S_n^i\big]$ denotes the algebra generated by S_n^i as defined in (3.2). The subalgebra generated by the $SU(2)$ *symmetry generators* J^i is

$$\mathcal{A}_{\text{sym}} = \mathbb{C}\big[J^i\big]\,. \tag{6.7}$$

We can introduce then the commutant $(\mathcal{A}_{\rm sym})'$, which defines the algebra $\mathcal{A}_G$ of group-invariant observables,

$$\mathcal{A}_G \equiv (\mathcal{A}_{\rm sym})' = \{ M \in \mathcal{A}_K \,|\, [M, J^i] = 0 \} \;=\; \mathbb{C}[\vec{S}_n \cdot \vec{S}_{n'}] \,. \tag{6.8}$$

This is the algebra of observables that commute with the symmetry generators J^i or, equivalently, that are invariant under rotations:

$$O \in \mathcal{A}_G \qquad \Longleftrightarrow \qquad U\,O\,U^{-1} = O \qquad \text{with} \qquad U = \mathrm{e}^{\mathrm{i}\alpha_i J^i} \,. \tag{6.9}$$

The center of the subalgebra is generated by the Casimir operator $\vec{J}^2$,

$$\mathcal{Z}_{\rm sym} = \mathcal{A}_{\rm sym} \cap \mathcal{A}_G \;=\; \mathbb{C}[\vec{J}^2] \,. \tag{6.10}$$

The symmetry-resolved decomposition of the Hilbert space is then given by a direct sum over the eigenvalues of the elements in the center,

$$\mathcal{H}_N \;=\; \bigoplus_{j=j_{\rm min}}^{j_{\rm max}} \left(\mathcal{H}^{(j)}_{\rm sym} \otimes \mathcal{H}^{(j)}_G \right) \,, \tag{6.11}$$

that is a sum over the irreducible representations j, with each j-sector consisting of a tensor product of the Hilbert spaces for *rotational symmetry* degrees of freedom and for *internal* (rotationally invariant) degrees of freedom. The rotational-symmetry degrees of freedom span a Hilbert space of dimension $\dim \mathcal{H}^{(j)}_{\rm sym} = 2j+1$, with an orthonormal basis given by the spin-j states

$$|j, m\rangle \;\in\; \mathcal{H}^{(j)}_{\rm sym} \,, \tag{6.12}$$

where $m = -j, \ldots, +j$ are the eigenvalues of J^z. The internal degrees of freedom can be understood as the $SU(2)$-invariant tensors in the tensor product of N spin-$\frac{1}{2}$ representations and one spin-j representation, which form the intertwiner space

$$\mathcal{H}^{(j)}_G = \mathrm{Inv}_G\big(\mathcal{H}^{(j)} \otimes \underbrace{\mathcal{H}^{(1/2)} \otimes \cdots \otimes \mathcal{H}^{(1/2)}}_{N} \big) \,. \tag{6.13}$$

Note that we have used Eq. (5.4) with the conjugate representation $\overline{j} = j$ for the group $SU(2)$. An orthonormal basis of this space is given by the recoupling

basis [95],

$$|j, k_1, \ldots, k_{N-2}\rangle \;=\; \in \; \mathcal{H}_G^{(j)} \,. \tag{6.14}$$

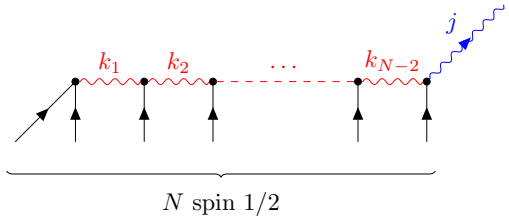

The quantum numbers $k_1, \ldots, k_{N-2}$ label the eigenvalues $k_r(k_r+1)$ of the recoupling operators $\vec{K}_r^2$. These operators form a maximal set of commuting observables defined in terms of the operators

$$\vec{K}_r = \sum_{n=1}^{r} \vec{S}_n \,, \qquad\qquad r = 1, \ldots, N-2 \tag{6.15}$$

which are the generator of $SU(2)$ rotations of the first r spins.

The dimension of the Hilbert space $\mathcal{H}_G^{(j)}$ of the internal degrees of freedom can be computed using the general formula for the dimension of $SU(2)$ intertwiner space between the representations $j_1, \ldots, j_L$, (see App. 6.5 for a detailed derivation):

$$D_j \equiv \dim \mathcal{H}_G^{(j)} = \frac{2j+1}{j+\frac{N}{2}+1} \binom{N}{\frac{N}{2}+j} \,, \tag{6.16}$$

where $\binom{n}{k} = \frac{n!}{k!(n-k)!}$ is the binomial coefficient. The sum of the dimensions of symmetry-resolved sectors matches the dimension 2^N of the Hilbert space of N spin-$\frac{1}{2}$ particles, i.e., $\dim \mathcal{H}_N = \sum_j (2j+1) D_j = 2^N$.

Symmetry-resolved states are states of N spin-$\frac{1}{2}$ particles that transform in a spin-j representation of the total spin and have no entanglement between its rotational and its internal degrees of freedom, i.e., states of the form:

$$|\psi\rangle = |j, \xi\rangle_{\text{sym}} \, |j, \chi\rangle_G \;\in\; \mathcal{H}_N \,, \tag{6.17}$$

with

$$|j, \xi\rangle_{\text{sym}} = \sum_m \xi_m \, |j, m\rangle \in \mathcal{H}_{\text{sym}}^{(j)} \,, \tag{6.18}$$

$$|j,\chi\rangle_G = \sum_{k_1,\ldots,k_{N-2}} c_{k_1,\ldots,k_{N-2}}\, |j,k_1,\ldots,k_{N-2}\rangle \in \mathcal{H}_G^{(j)}\,, \tag{6.19}$$

i.e.,

$$|\psi\rangle \;=\; \sum_{m,\,k_1,\ldots,k_{N-2}} \xi_m\, c_{k_1,\ldots,k_{N-2}}\, |j,m\rangle\, |j,k_1,\ldots,k_{N-2}\rangle\,. \tag{6.20}$$

6.4 Symmetry-resolved subsystems: K-local vs G-local observables

A system of N-particles often comes with a built-in notion of locality. For instance, the particles might be distributed at the nodes of a lattice, therefore inducing a notion of first-neighbors and regions. Local observables of the system can then be expressed in terms of the spin operators $\vec{S}_n$ of a subset of spins belonging to the region. The kinematical algebra of observables $\mathcal{A}_K$ is generated by the complete set of spin operators (6.6), while the subalgebra of observables in a region A is generated by the N_A spin operators in the region,

$$\mathcal{A}_{KA} = \mathbb{C}\big[S_a^i\big]\;, \qquad \text{with} \qquad a = 1,\ldots,N_A. \tag{6.21}$$

We call $\mathcal{A}_{KA}$ the *K-local* subalgebra of observables for the region A. Note that this subalgebra induces the standard decomposition of the Hilbert space as a tensor product $\mathcal{H}_N = \mathcal{H}_A \otimes \mathcal{H}_B$ over the region A and its complement B. In fact one finds that the commutant of $\mathcal{A}_{KA}$ is generated by the observables in the complementary region B, with $N_A + N_B = N$ and

$$\mathcal{A}_{KB} \equiv (\mathcal{A}_{KA})' = \mathbb{C}\big[S_b^i\big]\;, \qquad \text{with} \qquad b = N_A+1,\ldots,N_A+N_B. \tag{6.22}$$

Moreover, note that the center of the subalgebra is trivial, $\mathcal{A}_{KA} \cap \mathcal{A}_{KB} = \mathbb{1}$, which results in the familiar tensor product structure with no direct sum.

Observables that are invariant under the group $G = SU(2)$ form the algebra $\mathcal{A}_G$, (6.8). To identify a local subalgebra of G-invariant observables we take the intersection with $\mathcal{A}_{KA}$,

$$\mathcal{A}_{GA} \equiv \mathcal{A}_G \cap \mathcal{A}_{KA} \;=\; \mathbb{C}\big[\vec{S}_a \cdot \vec{S}_{a'}\big]\;, \qquad \text{with} \qquad a,a' = 1,\ldots,N_A. \tag{6.23}$$

We call $\mathcal{A}_{GA}$ the *G-local* subalgebra of observables for the region A. Note that this subalgebra is generated by the scalar products $\vec{S}_a \cdot \vec{S}_{a'}$ of spins in A. The commutant of $\mathcal{A}_{GA}$ in $\mathcal{A}_K$ is

$$\mathcal{A}_{\overline{GA}} \equiv (\mathcal{A}_{GA})' = (\mathcal{A}_G \cap \mathcal{A}_{KA})' = \big((\mathcal{A}_{\rm sym})' \cap (\mathcal{A}_{KB})'\big)' \tag{6.24}$$

$$= \big(\mathbb{C}[J^i]' \cap \mathbb{C}[S_b^i]'\big)' = \mathbb{C}\big[J^i, S_b^i\big] = \mathbb{C}\big[J^i, L^i, S_b^i\big]\,, \tag{6.25}$$

where we have used the intersection formula (3.4). Note that $\mathcal{A}_{\overline{GA}}$ is not a subalgebra of $\mathcal{A}_{KB}$ as it contains also the total symmetry generator J^i. Note also that $\mathcal{A}_{\overline{GA}}$ is not the same as $\mathcal{A}_{GB}$. As we have highlighted in the last equality above, it is useful also to introduce the operator L^i that measures the total spin of the particles in A,

$$\vec{L} = \sum_{a=1}^{N_A} \vec{S}_a\,, \tag{6.26}$$

and generates rotations of the spins in A. Note that $[\vec{L}^2, J^i] = 0$ because J^i generates global rotations and $\vec{L}^2$ is rotationally invariant. Therefore, the center of the subalgebra is non-trivial

$$\mathcal{Z}_{GA} = \mathcal{A}_{GA} \cap \mathcal{A}_{\overline{GA}} = \mathbb{C}[\vec{L}^2]\,, \tag{6.27}$$

and is generated by the Casimir operator $\vec{L}^2$ of A. We denote its eigenvalues $\ell(\ell+1)$ with

$$N_A \text{ even} \quad \Longrightarrow \quad \ell_{\rm min} = 0\,, \;\; \ell_{\rm max} = \tfrac{N_A}{2}\,, \;\; \ell \text{ integer}, \tag{6.28}$$

$$N_A \text{ odd} \quad \Longrightarrow \quad \ell_{\rm min} = \tfrac{1}{2}\,, \;\; \ell_{\rm max} = \tfrac{N_A}{2}\,, \;\; \ell \text{ half-integer}. \tag{6.29}$$

Using the results of Chapter 4 on subsystems from subalgebras, we find the decomposition

$$\mathcal{H}_N = \bigoplus_{\ell=\ell_{\rm min}}^{\ell_{\rm max}} \Big(\mathcal{H}_{GA}^{(\ell)} \otimes \mathcal{H}_{\overline{GA}}^{(\ell)}\Big)\,. \tag{6.30}$$

This decomposition is useful for computing the reduction of a generic pure state of the system to the $G-$local subalgebra. We are interested in the reduction of a special class of states—symmetry-resolved states—and it is useful to introduce a

decomposition adapted to them.

We prepare a symmetry-resolved state $|\psi\rangle = |j,\xi\rangle_{\rm sym}\,|j,\chi\rangle_G$ and we are interested in measurements of G-local observables in A. In order to build a basis adapted to both the decomposition associated with $\mathcal{A}_{\rm sym} = \mathbb{C}[J^i]$ and $\mathcal{A}_{GA} = \mathbb{C}[\vec{S}_a \cdot \vec{S}_{a'}]$, we consider the algebra generated by the union of the generating sets,

$$\mathcal{A}_{{\rm sym}GA} = \mathbb{C}[J^i, \vec{S}_a \cdot \vec{S}_{a'}]\,. \tag{6.31}$$

Note that, using (3.4), this algebra can also be written in terms of the intersection of commutants,

$$\mathcal{A}_{{\rm sym}GA} = \big((\mathcal{A}_{\rm sym})' \cap (\mathcal{A}_{GA})'\big)'\,. \tag{6.32}$$

To build the decomposition, we need its commutant and center. The commutant of $\mathcal{A}_{{\rm sym}GA}$ in $\mathcal{A}_K$ is

$$(\mathcal{A}_{{\rm sym}GA})' = (\mathcal{A}_{\rm sym})' \cap (\mathcal{A}_{GA})' = \mathcal{A}_G \cap \mathcal{A}_{\overline{GA}} \tag{6.33}$$

$$= \mathbb{C}\big[\vec{S}_n \cdot \vec{S}_{n'}\big] \cap \mathbb{C}\big[J^i, L^i, S^i_b\big] = \mathbb{C}[\vec{J}^2, \vec{L}^2, \vec{S}_b \cdot \vec{S}_{b'}]\,. \tag{6.34}$$

The center of $\mathcal{A}_{{\rm sym}GA}$ is then non-trivial,

$$\mathcal{Z}_{{\rm sym}GA} = \mathcal{A}_{{\rm sym}GA} \cap (\mathcal{A}_{{\rm sym}GA})' = \mathbb{C}[\vec{J}^2, \vec{L}^2]\,. \tag{6.35}$$

Note that the observables $\vec{J}^2$ and $\vec{L}^2$ commute,[1] which is always the case for the center as it is an Abelian algebra by definition. Simultaneously diagonalizing the observables $\vec{J}^2$ and $\vec{L}^2$, we find the decomposition of the Hilbert space as a sum over j and ℓ

$$\mathcal{H}_N = \bigoplus_{j=j_{\rm min}}^{j_{\rm max}} \bigoplus_{\ell=\ell_{\rm min}}^{\ell_{\rm max}} \left(\mathcal{H}^{(j)}_{\rm sym} \otimes \mathcal{H}^{(\ell)}_{GA} \otimes \mathcal{H}^{(j,\ell)}_{GB}\right)\,, \tag{6.36}$$

which can be reorganized as

$$\mathcal{H}_N = \bigoplus_{j=j_{\rm min}}^{j_{\rm max}} \mathcal{H}^{(j)}_N \qquad \text{with} \qquad \mathcal{H}^{(j)}_N = \mathcal{H}^{(j)}_{\rm sym} \otimes \bigoplus_{\ell=\ell_{\rm min}}^{\ell_{\rm max}} \left(\mathcal{H}^{(\ell)}_{GA} \otimes \mathcal{H}^{(j,\ell)}_{GB}\right)\,, \tag{6.37}$$

[1] The fact that the commutator $[\vec{J}^2, \vec{L}^2] = 0$ vanishes can be quickly shown by noticing that $[J^i, \vec{L}^2] = 0$ as J^i generates rotations of the full system and $\vec{L}^2$ is a scalar.

which provides a derivation of the expression (1.9) in the introduction. The Hilbert spaces appearing in (6.37) are defined by

$$\mathcal{H}^{(\ell)}_{GA} = \mathrm{Inv}_G\big(\,\mathcal{H}^{(\ell)} \otimes \underbrace{\mathcal{H}^{(1/2)} \otimes \cdots \otimes \mathcal{H}^{(1/2)}}_{N_A}\,\big)\ , \tag{6.38}$$

$$\mathcal{H}^{(j,\ell)}_{GB} = \mathrm{Inv}_G\big(\,\mathcal{H}^{(j)} \otimes \mathcal{H}^{(\ell)} \otimes \underbrace{\mathcal{H}^{(1/2)} \otimes \cdots \otimes \mathcal{H}^{(1/2)}}_{N_B}\,\big)\ . \tag{6.39}$$

Their dimensions can be computed using the general formula for the dimension of $SU(2)$ intertwiner space (see App. 6.5 for a detailed derivation):

$$d_\ell \equiv \dim \mathcal{H}^{(\ell)}_{GA} \ = \ \frac{2\ell+1}{\frac{N_A}{2}+\ell+1}\binom{N_A}{\frac{N_A}{2}+\ell}\,, \tag{6.40}$$

$$b_{j\ell} \equiv \dim \mathcal{H}^{(j,\ell)}_{GB} \ = \ \binom{N-N_A}{\frac{N-N_A}{2}+j-\ell} - \frac{\frac{N-N_A}{2}-j-\ell}{\frac{N-N_A}{2}+j+\ell+1}\binom{N-N_A}{\frac{N-N_A}{2}+j+\ell}\,. \tag{6.41}$$

These formulas are derived in the next section.

6.5 Dimensions of $SU(2)$ intertwiner spaces

In this section we give a derivation of the dimension of the Hilbert spaces $\mathcal{H}^{(\ell)}_{GA}$, $\mathcal{H}^{(j,\ell)}_{GB}$, and $\mathcal{H}^{(j)}_{G}$ based on the calculation of the dimension of the $SU(2)$ invariant spaces

$$\nu(j_1,\ldots,j_L) = \dim \mathrm{Inv}_G(\mathcal{H}^{(j_1)} \otimes \cdots \otimes \mathcal{H}^{(j_L)})\ . \tag{6.42}$$

These invariant spaces, also known as intertwiners, are well studied in loop quantum gravity [96, 97], where they are the fundamental building blocks for describing quantum geometries [92, 93]. Using techniques typical of intertwiner calculations [95], we write the projector to intertwiner space

$$P\ :\ \mathcal{H}^{(j_1)} \otimes \cdots \otimes \mathcal{H}^{(j_L)} \ \longrightarrow\ \mathrm{Inv}_G(\mathcal{H}^{(j_1)} \otimes \cdots \otimes \mathcal{H}^{(j_L)}) \tag{6.43}$$

via group averaging

$$P = \int_{SU(2)} D^{(j_1)}(g) \otimes \cdots \otimes D^{(j_L)}(g)\, \mathrm{d}g\,, \tag{6.44}$$

where $D^{(j)}(g)^m{}_{m'}$ are Wigner matrices for the representation with spin j and $\mathrm{d}g$ is the Haar measure for the group $SU(2)$. The dimension of the $SU(2)$–invariant space can then be computed as the trace of the identity in this space or, equivalently, the trace of the projector $\mathrm{Tr}P$, i.e., ν is given by the integral

$$\nu(j_1, \ldots, j_L) = \int_{SU(2)} \chi^{(j_1)}(g) \cdots \chi^{(j_L)}(g)\, \mathrm{d}g\,, \tag{6.45}$$

where $\chi^{(j)}(g) = \mathrm{Tr}D^{(j)}(g)$ is the character of the representation with spin j. We compute the integral using the class-angle parametrization $g = h\, \mathrm{e}^{\mathrm{i}\theta\sigma_z} h^{-1}$ of a group element, which results in the character $\chi^{(j)}(g) = \frac{\sin(2j+1)\theta}{\sin\theta}$ expressed as a function of the class angle θ. The Haar measure for class functions $\psi(g) = f(\theta)$ reduces to $\int \mathrm{d}g = \frac{2}{\pi}\int_0^{2\pi} (\sin\theta)^2\, \mathrm{d}\theta$.

This paper uses the dimension ν with N spin-1/2 and one spin-j. After a few manipulations with elementary trigonometric identities, we find

$$\nu(\tfrac{1}{2}, \ldots, \tfrac{1}{2}, j) = \frac{2^N}{\pi} \int_0^{2\pi} (\sin\theta)\, (\cos\theta)^N\, (\sin{(2j+1)\,\theta})\, \mathrm{d}\theta\,. \tag{6.46}$$

Using the residue theorem, we evaluate the integral (6.46) as a contour integral on the unit circle of the complex plane. The only contribution to the integral comes from the pole in the origin

$$\nu(\tfrac{1}{2}, \ldots, \tfrac{1}{2}, j) = -\tfrac{1}{2}\mathrm{Res}_{z=0} \left(\tfrac{1}{z} \left(\tfrac{1}{z} - z \right) \left(\tfrac{1}{z^{2j+1}} - z^{2j+1} \right) \left(\tfrac{1}{z} + z \right)^N \right)\,. \tag{6.47}$$

We expand the binomial $\left(\frac{1}{z} + z\right)^N = \sum_{k=0}^N \binom{N}{k} z^{2k-N}$ and read the residue from the coefficient of $\frac{1}{z}$. If $N + 2j$ is odd, the integral vanishes. If $N + 2j$ is even, we find

$$\nu(\tfrac{1}{2}, \ldots, \tfrac{1}{2}, j) = \frac{2j+1}{\frac{N}{2} + j + 1} \binom{N}{\frac{N}{2} + j}\,. \tag{6.48}$$

This is the expression also found, for instance, in [98, 99] and derived via combinatorial methods.

Using the intertwiner methods discussed above, we can now compute the dimension ν with $N - N_A$ spin-1/2, one spin-j, and one spin-ℓ which appears in the formula for the non-Abelian symmetry-resolved entanglement entropy. We find

$$\nu(\tfrac{1}{2},\ldots,\tfrac{1}{2},j,\ell) = \frac{2^{N-N_A+1}}{\pi}\int_0^{2\pi}(\cos\theta)^{N-N_A}\big(\sin(2j+1)\theta\big)\big(\sin(2\ell+1)\theta\big)\,\mathrm{d}\theta \tag{6.49}$$

$$= \binom{N-N_A}{\frac{N-N_A}{2}+j-\ell} - \frac{\frac{N-N_A}{2}-j-\ell}{\frac{N-N_A}{2}+j+\ell+1}\binom{N-N_A}{\frac{N-N_A}{2}+j+\ell}\,. \tag{6.50}$$

We note that this formula reduces to the expression (6.48) for $\ell = 0$ or $j = 0$.

To summarize, we have

$$D_j = \dim\mathcal{H}_G^{(j)} = \nu(\tfrac{1}{2},\ldots,\tfrac{1}{2},j)\,, \tag{6.51}$$

$$d_\ell = \dim\mathcal{H}_{GA}^{(\ell)} = \nu(\tfrac{1}{2},\ldots,\tfrac{1}{2},\ell)\,, \tag{6.52}$$

$$b_{j\ell} = \dim\mathcal{H}_{GB}^{(j,\ell)} = \nu(\tfrac{1}{2},\ldots,\tfrac{1}{2},j,\ell)\,. \tag{6.53}$$

6.6 Symmetry-resolved State

If we compare the decomposition (6.11) with (6.37), we obtain the decomposition of the Hilbert space of G-invariant degrees of freedom at fixed total angular momentum,

$$\mathcal{H}_G^{(j)} = \bigoplus_{\ell=\ell_{\min}}^{\ell_{\max}} \big(\mathcal{H}_{GA}^{(\ell)}\otimes\mathcal{H}_{GB}^{(j,\ell)}\big)\,, \tag{6.54}$$

with the adapted orthonormal basis [95]

$|\ell,k_a\rangle|j,\ell,h_b\rangle =$ 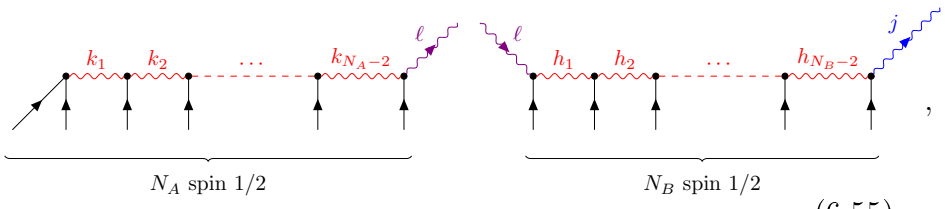

, (6.55)

which coincides with (6.14), $|j, k_r\rangle$ with k_r equal to k_a for $r = 1, \ldots, N_A - 2$, equal to ℓ for $r = N_A - 1$, and equal to h_b for $r = N_A, \ldots, N_A + N_B - 2$. From this decomposition, we also derive the relation between the dimensions d_ℓ, $b_{j\ell}$ and D_j,

$$D_j \;=\; \textstyle\sum_\ell d_\ell \, b_{j\ell} \, . \tag{6.56}$$

We can now compute the density matrix ρ_{GA} of a symmetry-resolved state $|\psi\rangle$ reduced to $\mathcal{A}_{GA}$. Following the general construction described in Chapter 4, the generic symmetry-resolved state in this basis is:

$$|\psi\rangle \;= |j, \xi\rangle \sum_\ell \sqrt{p_\ell} \sum_{k_a, h_b} \chi^{(\ell)}_{k_a, h_b} \, |\ell, k_a\rangle |j, \ell, h_b\rangle \; . \tag{6.57}$$

The density matrix of the symmetry-resolved state reduced to $\mathcal{A}_{GA}$ is

$$\rho_{GA} = \bigoplus_\ell p_\ell \, \rho_\ell, \tag{6.58}$$

where

$$\rho_\ell = \sum_{k_a, k'_a} \sum_{h_b} \chi^{(\ell)}_{k_a, h_b} \chi^{(\ell)*}_{k'_a, h_b} \, |\ell, k_a\rangle \langle \ell, k'_a| \; . \tag{6.59}$$

This is the expression used in the next section to compute the G-local entanglement entropy S_{GA}.

We conclude this section with a few observations. By direct comparison of the decomposition (6.30) and (6.36), we see that the decomposition of the complement of the GA-Hilbert space is not the GB-Hilbert space as

$$\mathcal{H}^{(\ell)}_{\overline{GA}} = \textstyle\bigoplus_j \left(\mathcal{H}^{(j)}_{\rm sym} \otimes \mathcal{H}^{(j,\ell)}_{GB} \right) . \tag{6.60}$$

Moreover, differently from what happens in the Abelian case discussed in Sec. 5.5, we note that here states in $\mathcal{H}^{(j,\ell)}_{GB}$ are eigenstates of the total angular momentum $\vec{J}^2$ and of the angular momentum of A, i.e., $\vec{L}^{\,2}$, but they are not in an eigenstate of the angular momentum of B, i.e., $\vec{J}^{\,2}_B = (\sum_b \vec{S}_b)^2$, unless $\vec{J}^{\,2} = 0$ in which case $\vec{J}^{\,2}_B = \vec{L}^{\,2}$.

6.7 G-local entanglement entropy of symmetry-resolved states

Given a symmetry-resolved state, i.e., a state of the form (6.57), we can compute its density matrix reduced to the G-local subalgebra of observables $\mathcal{A}_{GA}$ using the techniques of the previous section. The G-local entanglement entropy is then given by the general formula (3.18),

$$S_{GA} \equiv S\big(|\psi\rangle, \mathcal{A}_G, \mathcal{A}_{GA}\big) = -\mathrm{tr}(\rho_{GA} \log \rho_{GA}) \tag{6.61}$$

$$= -\sum_\ell p_\ell \,\mathrm{tr}(\rho_\ell \log \rho_\ell) \; - \sum_\ell p_\ell \log p_\ell \,, \tag{6.62}$$

where ρ_ℓ is the reduced density matrix in the sector ℓ and p_ℓ the probability of the sector, as defined in (6.58). We give a few examples to illustrate how S_{GA} is computed and its differences from S_{KA}:

$\boldsymbol{N = 2,\, j = 0}$ — This is the singled state $|s\rangle$ of two spin-1/2 particles,

$$|s\rangle = \frac{|\uparrow\downarrow\rangle - |\downarrow\uparrow\rangle}{\sqrt{2}} \tag{6.63}$$

As K-local subsystem with $N_A = 1$, we can take the first particle with the algebra of observables $\mathcal{A}_{KA} = \mathbb{C}[\vec{S}_1]$. As usual [86], the associated entanglement entropy is $S_{KA}(|s\rangle) = \log 2$. On the other hand, if we consider the algebra of G-local observables of the first particle we find that it is trivial as there is no rotational invariant observable besides $\vec{S}_1^{\,2} = \frac{1}{2}(\frac{1}{2}+1)\mathbb{1}$, i.e., $\mathcal{A}_{GA} = \{\mathbb{1}\}$ and $S_{GA}(|s\rangle) = 0$.

$\boldsymbol{N = 4,\, j = 0}$ — The recoupling of $N = 4$ spin-1/2 particles into a scalar ($j = 0$) defines a two-dimensional Hilbert space spanned by the two orthogonal states

$$|\psi_0\rangle = |s\rangle_A \, |s\rangle_B \,, \tag{6.64}$$

$$|\psi_1\rangle = \sum_{m=0,\pm1} \tfrac{(-1)^{1-m}}{\sqrt{3}} \, |t_{+m}\rangle_A \, |t_{-m}\rangle_B \,, \tag{6.65}$$

where we have denoted $A = (1,2)$ and $B = (3,4)$ the coupling of the four particles.

The K-local and the G-local entanglement entropies of the subsystem A are

$$\begin{aligned} S_{KA}(|\psi_0\rangle) &= 0\,, \qquad S_{GA}(|\psi_0\rangle) = 0\,, \\ S_{KA}(|\psi_1\rangle) &= \log 3\,, \quad S_{GA}(|\psi_1\rangle) = 0\,. \end{aligned} \tag{6.66}$$

Note that the K-local entropy measures the entanglement in the magnetic degrees of freedom m, which results in the $\log 3$ above. On the other hand, the G-local entanglement entropy for each of the two states vanishes as they are eigenstates of $(\vec{S}_1 + \vec{S}_2)^2$, which is the only non-trivial observable in $\mathcal{A}_{GA} = \mathbb{C}[\vec{S}_1 \cdot \vec{S}_2]$. In fact, using the basis (6.55), we see that $|\psi_1\rangle$ is factorized. To show a non-trivial G-local entropy, we consider the superposition

$$|\psi\rangle = \sqrt{1-p}\,|\psi_0\rangle \,+\, \sqrt{p}\,\mathrm{e}^{\mathrm{i}\phi}\,|\psi_1\rangle \tag{6.67}$$

for which we can easily compute the reduced density matrices

$$\rho_{KA} = (1-p)\,|s\rangle\langle s| + \,p \sum_{m=0,\pm 1} \tfrac{1}{3}\,|t_m\rangle\langle t_m|\,, \tag{6.68}$$

$$\rho_{GA} = (1-p)\,|0\rangle\langle 0| + \,p\,|1\rangle\langle 1|\,, \tag{6.69}$$

where the states $|0\rangle$ and $|1\rangle$ are the eigenstates with $\ell = 0, 1$ of the G-local observable $\vec{L}^{\,2} = (\vec{S}_1 + \vec{S}_2)^2$. It follows that the entanglement entropies for the K-local and the G-local subalgebras are

$$S_{KA}(|\psi\rangle) = -(1-p)\log(1-p) - p\log(p/3)\,, \tag{6.70}$$

$$S_{GA}(|\psi\rangle) = -(1-p)\log(1-p) - p\log p\,. \tag{6.71}$$

In this simple case, the G-local entanglement entropy is purely due to the Shannon entropy of the sector, i.e., the last term in (6.62), because the subalgebra coincides with the center, $\mathcal{A}_{GA} = \mathcal{A}_{GB} = \mathcal{Z}$.

$\boldsymbol{N = 4,\, j = 1,\, m = +1}$ — The recoupling of $N = 4$ spin-1/2 particles into a vector ($j = 1$) defines the Hilbert space $\mathcal{H}_4^{(1)} = \mathcal{H}_{\mathrm{sym}}^{(1)} \otimes \mathcal{H}_G^{(1)}$ of dimension 3×3.

We consider a $(m = +1)$ symmetry-resolved state

$$|\psi\rangle = \sqrt{1-p}\,|\eta_1\rangle \,+\, \sqrt{p}\,\mathrm{e}^{\mathrm{i}\phi}\,|\eta_2\rangle \tag{6.72}$$

given by the superposition of the two orthogonal basis states with $m = +1$

$$|\eta_1\rangle = |s\rangle_A\,|t_+\rangle_B\,, \qquad |\eta_2\rangle = \tfrac{1}{\sqrt{2}}\,\big(|t_+\rangle_A\,|t_0\rangle_B - |t_0\rangle_A\,|t_+\rangle_B\big)\,, \tag{6.73}$$

where $|s\rangle$ and $|t_m\rangle$ are the singlet state and the triplet state (with the magnetic number $m = 0, \pm 1$) obtained by coupling two spin-1/2 particles. The K-local density matrix for the two spins in A, defined as usual as $\rho_{KA} = \mathrm{Tr}_B|\psi\rangle\langle\psi|$, is

$$\rho_{KA} = (1-p)|s\rangle\langle s| + \tfrac{p}{2}\,\big(|t_+\rangle\langle t_+| + |t_0\rangle\langle t_0|\big) - \sqrt{\tfrac{p(1-p)}{2}}\big(\mathrm{e}^{-\mathrm{i}\phi}|s\rangle\langle t_0| + \mathrm{e}^{+\mathrm{i}\phi}|t_0\rangle\langle s|\big)\,. \tag{6.74}$$

The non-vanishing eigenvalues of ρ_{KA} are $\{\frac{p}{2}, 1-\frac{p}{2}\}$. Therefore, K-local entanglement entropy is

$$S_{KA}(|\psi\rangle) = -\tfrac{p}{2}\log\tfrac{p}{2} \;-(1-\tfrac{p}{2})\log(1-\tfrac{p}{2})\,. \tag{6.75}$$

On the other hand, if we have only access to the rotational invariant observable of the particles in subsystem $A = (1,2)$, that is only the observable $\vec{S}_1 \cdot \vec{S}_2$, then the accessible entropy is given by the probability of outcomes $\{p, 1-p\}$,

$$S_{GA}(|\psi\rangle) = \;-p\log p \;-(1-p)\log(1-p)\,. \tag{6.76}$$

We note that, for $\frac{2}{3} \le p \le 1$, we have that the G-local entropy is smaller than the K-local entropy, $S_{GA}(|\psi\rangle) \le S_{KA}(|\psi\rangle)$, while for $0 \le p \le \frac{2}{3}$ the G-local entropy is larger $S_{GA}(|\psi\rangle) \ge S_{KA}(|\psi\rangle)$. We note also another difference compared to the Abelian case (1.1) where the reduced density matrix is shown to be black diagonal. From (6.74), we see that the density matrix ρ_{KA} is not block diagonal as it has non-vanishing matrix elements $|s\rangle\langle t_0|$ that connect blocks with different ℓ. This is a generic feature of $SU(2)$-symmetry-resolved states.

$\boldsymbol{N = 6,\, j = 1,\, m = +1}$ — The Hilbert space $\mathcal{H}_6^{(1)} = \mathcal{H}_{\mathrm{sym}}^{(1)} \otimes \mathcal{H}_G^{(1)}$ has dimension 3×9. We consider the subsystem of the first $N_A = 3$ particles. The G-local entanglement entropy is associated to the restriction of the state to the subalge-

bra $\mathcal{A}_{GA} = \mathbb{C}[\vec{S}_1 \cdot \vec{S}_2,\, \vec{S}_1 \cdot \vec{S}_3,\, \vec{S}_2 \cdot \vec{S}_3]$ which now is a non-commutative algebra and therefore allows intertwiner entanglement, i.e., the first term in (6.62). The associated Hilbert space decomposition is

$$\mathcal{H}_G^{(1)} = \bigoplus_{\ell=\frac{1}{2},\frac{3}{2}} \left(\mathcal{H}_{GA}^{(\ell)} \otimes \mathcal{H}_{GB}^{(1,\ell)}\right). \tag{6.77}$$

We consider the two orthogonal states $|\psi_1\rangle$ and $|\psi_2\rangle$ with $j = 1$, $m = +1$ obtained from the coupling of the angular momentum of six spin-1/2 particles as described by the diagrams below [95]:

$|\psi_1\rangle =$ 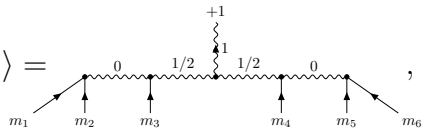

, $|\psi_2\rangle =$ 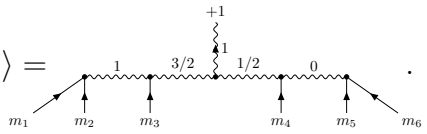

. (6.78)

These two states are simultaneous eigenstates of the observables $(\vec{S}_1 + \vec{S}_2)^2$ and $(\vec{S}_1 + \vec{S}_2 + \vec{S}_3)^2$. As a result, when restricted to G-invariant observables of the first three spins, they have vanishing G-local entropy $S_{GA}(|\psi_1\rangle) = 0$ and $S_{GA}(|\psi_2\rangle) = 0$. On the other hand, because of the entanglement in the rotational degrees of freedom, we have that the K-local entropies are $S_{KA}(|\psi_1\rangle) = 0$ and non-vanishing $S_{KA}(|\psi_2\rangle) \neq 0$. Next, we consider the symmetry-resolved state with $m = +1$ described in Fig. 6.1(b),

$$|\psi\rangle = \tfrac{1}{\sqrt{2}}(|\psi_1\rangle + |\psi_2\rangle)\,, \tag{6.79}$$

given by the superposition of the two orthonormal $|\psi_1\rangle$ and $|\psi_2\rangle$ introduced in (6.78). As shown in Fig. 6.1(b) for $p = 1/2$, the G-local entropy of this state is $S_{GA}(|\psi\rangle) = \log 2$ while the K-local entropy is $S_{KA}(|\psi\rangle) = -\frac{3}{8}\log\frac{3}{8} - \frac{5}{8}\log\frac{5}{8}$. This example allows us to comment on the symmetry under the exchange of A with B. Clearly $S_{KA}(|\psi\rangle) = S_{KB}(|\psi\rangle)$. On the other hand, we note that the restriction to the subalgebra $\mathcal{A}_{GB} = \mathbb{C}[\vec{S}_4 \cdot \vec{S}_5,\, \vec{S}_4 \cdot \vec{S}_6,\, \vec{S}_5 \cdot \vec{S}_6]$ is associated with Hilbert space decomposition

$$\mathcal{H}_G^{(1)} = \bigoplus_{j_B=\frac{1}{2},\frac{3}{2}} \left(\mathcal{H}_{GB}^{(j_B)} \otimes \mathcal{H}_{GA}^{(1,j_B)}\right), \tag{6.80}$$

and $S_{GB}(|\psi\rangle) = 0$ because $|\psi\rangle$ is an eigenstate of $(\vec{S}_5 + \vec{S}_6)^2 = 0$ and $(\vec{S}_4 + \vec{S}_5 + \vec{S}_6)^2 = \frac{1}{2}(\frac{1}{2}+1)$. This example shows concretely that, in the non-Abelian case, the commutant symmetry (3.28) allows an asymmetry under subsystem exchange in

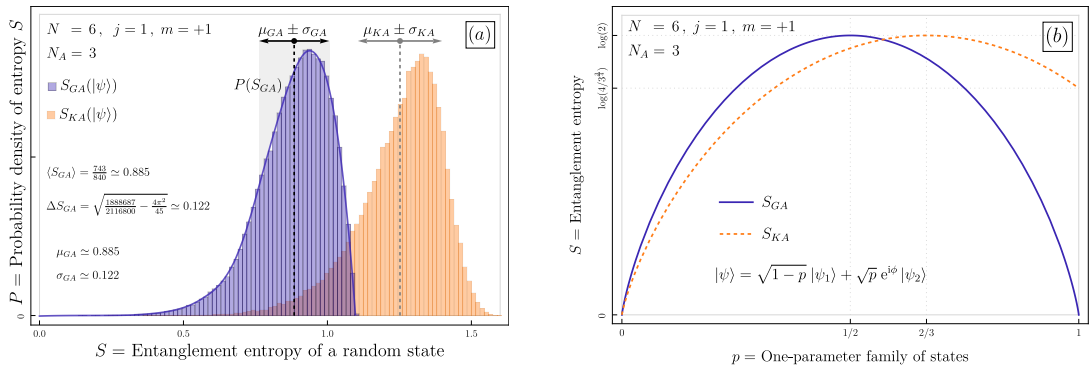

Figure 6.1. For a system of $N = 6$ spins with total spin $j = 1$, magnetization $m = +1$ and subsystem size $N_A = 3$, we show: (a) the probability distribution of the G-local (purple) and the K-local (yellow) entanglement entropies S_{GA} and S_{KA} of a sample of random symmetry-resolved states, including a comparison of the numerical values (μ_{GA}, σ_{GA}) and the exact values $(\langle S_{GA}\rangle, \Delta S_{GA})$ of the average and variance of $P(S_{GA})$; (b) the entanglement entropy of a superposition of the two states (6.78), which highlights the non-trivial relation between S_{GA} and S_{KA}; at $p = 0$: $S_{GA} = S_{KA} = 0$, at $p = \frac{1}{2}$: $S_{GA} > S_{KA}$, and at $p = 1$: $S_{KA} > S_{GA} = 0$.

the G-local entanglement entropy, $S_{GB}(|\psi\rangle) \neq S_{GA}(|\psi\rangle)$.

6.8 Typical G-local entanglement entropy: exact formulas

We combine the results of Sec. 3.5 on the typical entanglement entropy of a subsystem defined in terms of a subalgebra of observables, together with the results of Sec. 4.4 on symmetry-resolved entanglement entropy, to derive the exact formulas for the typical G-local entanglement entropy for the group $G = SU(2)$.

The average entanglement entropy for a random symmetry-resolved state in $\mathcal{H}_N^{(j)} = \mathcal{H}_{\text{sym}}^{(j)} \otimes \mathcal{H}_G^{(j)}$, restricted to a G-local subsystem of N_A spin-1/2 particles is given by the formula (3.32), specialized to the $SU(2)$ case:

$$\langle S_{GA}\rangle_j = \sum_{\ell=\ell_{\min}}^{\ell_{\max}} \varrho_\ell \, \varphi_\ell \,, \tag{6.81}$$

where ϱ_ℓ and φ_ℓ are given in terms of the dimensions d_ℓ, $b_{j\ell}$, D_j defined in (6.16),

(6.40), (6.41). The first quantity is

$$\varrho_\ell = \frac{d_\ell\, b_{j\ell}}{D_j}\,, \tag{6.82}$$

and the second is

$$\varphi_\ell \;=\; \Psi(D_j+1)-\Psi(\max(d_\ell,b_{j\ell})+1)-\min\left(\tfrac{d_\ell-1}{2b_{j\ell}},\tfrac{b_{j\ell}-1}{2d_\ell}\right). \tag{6.83}$$

The variance $(\Delta S_{GA})^2 = \langle S_{GA}^2\rangle_j - \langle S_{GA}\rangle_j^2$ can be written as

$$(\Delta S_{GA})^2 = \frac{1}{D+1}\Big(\sum_{\ell=\ell_{\min}}^{\ell_{\max}} \varrho_\ell\left(\varphi_\ell^2+\chi_\ell\right) \;-\; \Big(\sum_{\ell=\ell_{\min}}^{\ell_{\max}} \varrho_\ell\;\varphi_\ell\Big)^2\Big), \tag{6.84}$$

where ϱ_ℓ and φ_ℓ are given above and χ_ℓ is defined as

$$\chi_\ell \;= (d_\ell + b_{j\ell})\,\Psi'(\max(d_\ell,b_{j\ell})+1) - (D_j+1)\,\Psi'(D_j+1)+ \tag{6.85}$$

$$- \frac{(\min(d_\ell,b_{j\ell})-1)(d_\ell+b_{j\ell}+\max(d_\ell,b_{j\ell})-1)}{4\,\max(d_\ell^2,b_{j\ell}^2)}\,. \tag{6.86}$$

The formulas for average (6.81) and the variance (6.84) of the symmetry-resolved entanglement entropy of a random state are exact and can be computed from the expressions of the dimensions of the Hilbert spaces d_ℓ, $b_{j\ell}$, and D_j.

In Fig. 6.1(a), we show the average and variance compared to the statistical distribution of a sample of symmetry-resolved random states with $N = 6$, $j = 1$, $m = +1$ restricted to $N_A = 3$. For this sample of random states, we report the histograms for the probability distributions $P(S_{GA})$ and $P(S_{KA})$, which are shown to be distinct, Fig. 6.1(a). The statistical average μ_{GA} and variance σ_{GA}^2 match numerically the exact formulas $\langle S_{GA}\rangle$ and $(\Delta S_{GA})^2$ that we derive in this paper for the G-local entanglement entropy. The K-local entanglement entropy with $SU(2)$ symmetry is studied in [99] where asymptotic formulas at large N are derived for $\langle S_{KA}\rangle$ and $(\Delta S_{KA})^2$ using a combination of analytical and numerical methods. To date, there is no analytical result for the average K-local entanglement entropy $\langle S_{KA}\rangle$ at finite N. We note that, because of the contribution of the rotational degrees of freedom $|j,m\rangle$, we have that typically, the kinematical entanglement entropy S_{KA} is larger than the symmetry-resolved entanglement entropy S_{GA} of a

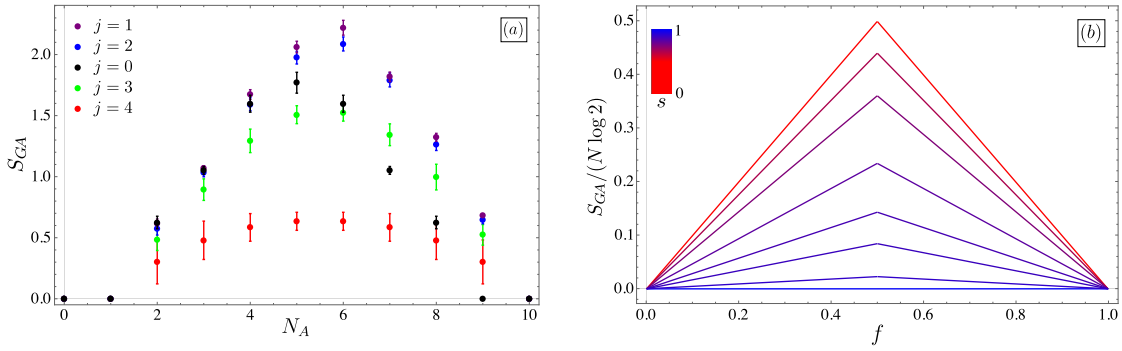

Figure 6.2. (a) Page curve for the $SU(2)$ symmetry-resolved entanglement entropy in a system consisting of $N = 10$ spins. The average entanglement entropy $\langle S_{GA}\rangle_j$ and its dispersion $(\Delta S_{GA})_j$ are computed using the exact formulas (6.81)–(6.84) and reported as a function of the number of spins N_A in the subsystem. The Page curve with $j = 1$ has the largest peak entropy. The curves with $j = 2$, $j = 0$, $j = 3$ and $j = 4$ follow. The maximum spin $j = 5$ has $S_{GA} = 0$. The ordering of the curves reflects the dimension of the Hilbert spaces D_j. For $N_A = 1$, the G-local subsystem is trivial, $d_\ell = 1$, and the entropy $S_{GA} = 0$ vanishes. The Page curve is generally not symmetric under the exchange $N_A \leftrightarrow N - N_A$, except in the special case $j = 0$ where this exchange symmetry is present. (b) Leading order of the symmetry-resolved entanglement entropy in the thermodynamic limit. At this order, the entanglement entropy is symmetric under exchange $f \leftrightarrow 1 - f$. We plot the Page curve for spin densities $s = 0$, $s = 0.4$, $s = 0.6$, $s = 0.8$, $s = 0.9$, $s = 0.95$, $s = 0.99$, and $s = 1$, which corresponds to curves from the top to the bottom.

random state. However, the relation between the two is non-trivial as shown in Fig. 6.1(b) where we consider a specific (non-random) family of states for which S_{GA} is instead larger than S_{KA}. Moreover, in the superposition $(|\psi_1\rangle + |\psi_2\rangle)/\sqrt{2}$ we have that S_{GA} is larger than S_{KA}, which shows that the relation between the two is non-trivial.

In Fig. 6.2(a), we show the exact average and variance for $N = 10$ and different values of j as a function of the subsystem size N_A, i.e., the Page curve [21,69] for a symmetry-resolved system. Note the asymmetry under exchange $N_A \to N - N_A$, due to the asymmetry in the dimensions d_ℓ and $b_{j\ell}$ in (6.40)–(6.41), which is a generic feature of non-Abelian symmetry-resolved entanglement (see Sec. 5.4).

As discussed in (5.22)–(5.26), one can also decompose the total symmetry-resolved entanglement entropy $\langle S_{GA}\rangle_j$ in a configurational $\langle S_{GA}^{(\mathrm{conf})}\rangle_j$ and a number contribution $\langle S_{GA}^{(\mathrm{num})}\rangle_j$.

Chapter 7
Large N asymptotics of the $SU(2)$ typical entropy

7.1 Introduction

Building upon the work in Chapter 6, in this chapter, we focus on the symmetry-resolved entanglement entropy in a lattice of spin-$\frac{1}{2}$ particles, with special emphasis on its behavior in the thermodynamic limit. To extract the asymptotic behavior, we introduce intensive quantities that enable us to systematically analyze the scaling of entanglement as the number of particles N grows to infinity. Using these asymptotic techniques, we derive explicit expressions for the dimensions of the symmetry-resolved Hilbert spaces and their complements. These expressions allow us to convert the sums over subsystem spins into integrals over probability distributions which we use to extract asymptotic formulas for the average entanglement entropy and its variance. We find that the variance around the average entanglement entropy is exponentially suppressed in N, which implies that the average entropy becomes typical in the thermodynamic limit. In addition, we compare the asymptotics of the G-local and K-local entropies for the extremal cases of fixed spin density, maximum spin ($j = j_{\max}$) and minimum spin ($j = j_{\min}$). For $j = j_{\max}$, the symmetry-resolved state is essentially factorized, leading to zero G-local entanglement entropy, while for $j = j_{\min}$ nontrivial entanglement arises via a $O(\log N)$ and $O(1)$ contributions. These results help us explicitly observe the differences between the K-local and G-local notions of entanglement. We summarize these comparisons in a tabular form to underscore how symmetry and locality affect the

scaling behavior of entanglement. The results presented in this chapter are based on Sec. 6 of [5].

7.2 Fixed spin density

The symmetry-resolved entanglement entropy (6.81) depends on the system size N, the total spin j, and the subsystem size N_A. Moreover, the expression contains a sum over the subsystem spin ℓ. We introduce intensive quantities representing the subsystem fraction f, the system spin density s, and the subsystem spin density t:

$$f = \frac{N_A}{N}, \qquad s = \frac{2j}{N}, \qquad t = \frac{2\ell}{N_A} \ . \tag{7.1}$$

The thermodynamic limit is defined as the limit $N \to \infty$ while keeping the intensive quantities f and s fixed. We compute the average entropy (6.81) and its variance (6.84) in this limit up to terms of order one, $O(1)$.

First, we derive the asymptotic expressions of the dimensions d_ℓ, $b_{j\ell}$, and D_j in the thermodynamic limit. We use the asymptotic expansion of the binomial coefficients for $n \to \infty$ with λ fixed,

$$\binom{n}{\frac{n}{2}(1+\lambda)} = \sqrt{\frac{2\,|\beta''(\lambda)|}{\pi n}}\, \mathrm{e}^{n\beta(\lambda)} \left(1 - \frac{1}{12n}\frac{3+\lambda^2}{1-\lambda^2} + O(n^{-2})\right) \tag{7.2}$$

where the function $\beta(s)$ is defined by

$$\beta(s) = -\frac{1-s}{2}\log\left(\frac{1-s}{2}\right) - \frac{1+s}{2}\log\left(\frac{1+s}{2}\right) \ , \tag{7.3}$$

and its derivatives are

$$\beta'(s) = -\frac{1}{2}\log\left(\frac{1+s}{1-s}\right) \ , \qquad \beta''(s) = -\frac{1}{1-s^2} \ . \tag{7.4}$$

The approximation (7.2) holds for $\lambda = O(1)$ and is useful for deriving the large-N asymptotics of the dimensions at fixed $0 < s < 1$. This approximation is invalid in the extremal cases $j = j_{\min}$ and $j = j_{\max}$ defined in (6.4), and we will deal with them separately in the next section. The asymptotic form of the dimensions in

terms of intensive quantities are

$$D_j = \frac{2s}{1+s}\sqrt{\frac{2\,|\beta''(s)|}{\pi N}}\;\mathrm{e}^{N\beta(s)}\left(1+\frac{1}{12N}\frac{12-s(9-s)(3-s)}{s(1-s^2)}+O(N^{-2})\right), \quad (7.5)$$

$$d_\ell = \frac{2t}{1+t}\sqrt{\frac{2\,|\beta''(t)|}{\pi f N}}\;\mathrm{e}^{fN\beta(t)}\left(1+\frac{1}{12fN}\frac{12-t(9-t)(3-t)}{t(1-t^2)}+O(N^{-2})\right), \quad (7.6)$$

$$b_{j\ell} = \sqrt{\frac{2\,|\beta''(\frac{s-tf}{1-f})|}{\pi N\,(1-f)}}\;\mathrm{e}^{(1-f)N\beta(\frac{s-tf}{1-f})}\left(1-\frac{1}{12(1-f)N}\frac{3+\left(\frac{s-tf}{1-f}\right)^2}{1-\left(\frac{s-tf}{1-f}\right)^2}+O(N^{-2})\right). \quad (7.7)$$

Note that, in the asymptotic formula for $b_{j\ell}$, the second term in the exact expression (6.41) is exponentially small, and therefore it does not contribute to the asymptotics for $0 < s < 1$ and large N. On the other hand, this approximation is invalid for $s = 0$, that is, when $j = j_{\min}$ which is not compatible with the scaling assumed in (7.1), and will be treated separately in the next section. In the thermodynamic limit, the sum over the spin ℓ becomes an integral over the spin density $\sum_\ell \to \int_0^1 f\frac{N}{2}\mathrm{d}t$ and the probability distribution (6.82) is given by a continuous probability distribution

$$\varrho(t)\mathrm{d}t = \frac{d_\ell b_{j\ell}}{D_j} f\frac{N}{2}\mathrm{d}t = \varrho_0(t)\Big(1+\frac{\varrho_1(t)}{N}+O(N^{-2})\Big)\,\mathrm{e}^{N\left(f\beta(t)+(1-f)\beta\left(\frac{s-ft}{1-f}\right)-\beta(s)\right)}\mathrm{d}t\ , \quad (7.8)$$

where

$$\varrho_0(t) = f\frac{N}{2}\sqrt{\frac{2}{\pi f(1-f)N}}\;\frac{(s+1)t}{s(t+1)}\;\sqrt{\frac{|\beta''(t)|\;|\beta''\left(\frac{s-ft}{1-f}\right)|}{|\beta''(s)|}}\ , \quad (7.9)$$

$$\varrho_1(t) = \frac{1}{12f}\frac{12-t(9-t)(3-t)}{t(1-t^2)} - \frac{1}{12(1-f)}\frac{3+\left(\frac{s-tf}{1-f}\right)^2}{1-\left(\frac{s-tf}{1-f}\right)^2} - \frac{1}{12}\frac{12-s(9-s)(3-s)}{s(1-s^2)}\ . \quad (7.10)$$

The limit of function φ_ℓ (6.83) is given by the lower bound (3.39),

$$\varphi(t) = \log\min\left(\tfrac{D_j}{b_{j\ell}},\tfrac{D_j}{d_\ell}\right) - \tfrac{1}{2}\min\left(\tfrac{d_\ell}{b_{j\ell}},\tfrac{b_{j\ell}}{d_j}\right), \quad (7.11)$$

and the average entanglement entropy at fixed s is given by the integral

$$\langle S_{GA}\rangle_s = \int_0^1 \varrho(t)\varphi(t)\,\mathrm{d}t\,. \tag{7.12}$$

We evaluate the integral over t using the Laplace approximation for large N (see App. A). The integral is concentrated at the critical point $t = s$ defined as the maximum of the exponent of (7.8). If $f < \frac{1}{2}$, at the critical point the dimension $b_{j\ell}$ is exponentially larger than d_j. Therefore, we can ignore the second term in (7.11) as it is exponentially small. Similarly, at the critical point, the min in the logarithm in (7.11) selects the ratio $D_j/b_{j\ell}$, which allows us to write

$$\varphi(t) = N\left(\beta(s) - (1-f)\,\beta\left(\tfrac{s-ft}{1-f}\right)\right) + \tfrac{1}{2}\log\left(\frac{\beta''(s)}{\beta''\left(\frac{s-ft}{1-f}\right)}\right) + \log\left(\tfrac{2s\sqrt{1-f}}{1+s}\right) + O(N^{-1})\,. \tag{7.13}$$

At half-system size, $f = 1/2$, extra care is necessary because of a discontinuity in the integral. The dimensions satisfy the inequalities $b_{j\ell} > d_\ell$ for $t < s$, but $b_{j\ell} < d_\ell$ for $t > s$. The logarithm in (7.11) is discontinuous at the critical point $t = s$, and we have to resort to a Laplace approximation that allows for discontinuities (see App. A). There are additional contributions at order $O(\sqrt{N})$ and at order $O(1)$. Note that, at $f = 1/2$, the second term in (7.11) is not exponentially small, but detailed analysis shows that it is of order $O(1/\sqrt{N})$ and therefore does not contribute to the thermodynamic limit. Summarizing, the average entanglement entropy for $f \le 1/2$ is:

$$\begin{aligned}\langle S_{GA}\rangle_s = {}& \beta(s)fN - \frac{|\beta'(s)|}{\sqrt{2\pi|\beta''(s)|}}\sqrt{N}\,\delta_{f,\frac{1}{2}} + \tfrac{f+\log(1-f)}{2} + \left(1 - \tfrac{1}{2}\delta_{f,\frac{1}{2}}\right)\log\left(\tfrac{2s}{1+s}\right) \\ & - \left(1 - f - \tfrac{1}{2}\delta_{f,\frac{1}{2}}\right)\tfrac{1-s}{2s}\log\left(\tfrac{1+s}{1-s}\right) + O(N^{-\frac{1}{2}}) \qquad \text{for} \quad f \le \tfrac{1}{2}\,,\end{aligned} \tag{7.14}$$

and for $f > 1/2$

$$\langle S_{GA}\rangle_s = \beta(s)(1-f)N + \tfrac{(1-f)+\log f}{2} + (1-f)\tfrac{1-s}{2s}\log\left(\tfrac{1+s}{1-s}\right) + O(N^{-\frac{1}{2}}) \qquad \text{for} \quad f > \tfrac{1}{2}\,. \tag{7.15}$$

Note that the leading order $O(N)$ and the subleading order $O(\sqrt{N})$ are symmetric under exchange of the subsystem with its complement. However, the order $O(1)$

term is not symmetric, $f \not\leftrightarrow (1-f)$. The leading order and its dependence on the spin density s via the function $\beta(s)$ (7.3) is displayed in Fig. 6.2(b).

Using the same technique, we find that the variance is:

$$(\Delta S_{GA})^2_s = \sqrt{\tfrac{\pi}{2}}\big(f(1-f) - \tfrac{1}{2\pi}\delta_{f,\frac{1}{2}}\big)\tfrac{(1-s)^{3/2}(s+1)^{5/2}}{8s}\big(\log\tfrac{1+s}{1-s}\big)^2 N^{\frac{3}{2}} e^{-N\beta(s)}\big(1+O(N^{-1})\big). \tag{7.16}$$

We note that the variance is exponentially small in N. Moreover, at the order considered, the variance is invariant under the symmetry $f \leftrightarrow (1-f)$.

7.3 Extremal cases: $j_{\max}$ and $j_{\min}$

In the extremal case of maximum spin, $j = j_{\max} = N/2$, the Hilbert space $\mathcal{H}_G^{(j_{\max})}$ contains only one state and the dimension (6.16) is $D_{j_{\max}} = 1$. Moreover, the composition of angular momenta constrains the spin of the subsystem A to be maximal, i.e., $\ell = \ell_{\max}$, and the dimensions (6.40) and (6.41) of the factors are $d_{\ell_{\max}} = 1$, $b_{j_{\max}\ell_{\max}} = 1$. Therefore, the unique symmetry-resolved state with $j = j_{\max}$ is factorized, as the exact formula of the average and variance of the entanglement entropy confirm:

$$\langle S_{GA}\rangle_{j_{\max}} = 0\ , \qquad (\Delta S_{GA})^2_{j_{\max}} = 0\ . \tag{7.17}$$

The other extremal case, $j = j_{\min}$, is non trivial. Let us assume that N is even so that $j_{\min} = 0$. In this case, the relevant asymptotic formula for the binomial coefficient is

$$\binom{n}{\frac{n}{2}+x} = \sqrt{\frac{2}{n\pi}}\,\mathrm{e}^{n\log 2}\,\mathrm{e}^{-\frac{2x^2}{n}}\,\big(1+O(n^{-1})\big)\ , \tag{7.18}$$

that is valid for $x = O(\sqrt{n})$ and $n \to \infty$.[1] In the sum (6.81), we first assume $\ell = O(\sqrt{N})$, motivated by the fact that it corresponds to the subsystem with the largest dimension. We then check this hypothesis a posteriori. In this limit, the dimensions of the Hilbert spaces are

$$D_0 = \sqrt{\frac{8}{\pi}}\frac{1}{N^{3/2}}\,\mathrm{e}^{N\log 2}\,\big(1+O(N^{-1})\big)\,, \tag{7.19}$$

[1] Note that here we cannot use (7.2) where $\lambda = O(1)$

$$d_\ell = \sqrt{\frac{2}{\pi}} \frac{4\ell}{(fN)^{3/2}} \, \mathrm{e}^{fN \log 2} \, \mathrm{e}^{-2\frac{\ell^2}{fN}} \left(1 + O(N^{-1})\right). \tag{7.20}$$

Note that, for $j = 0$, the dimensions $b_{0\ell}$ and d_ℓ are mapped into each other by sending $f \leftrightarrow 1 - f$. This is an exact property of (6.40) and (6.41) which in the asymptotic limit results into the expression

$$b_{0\ell} = \sqrt{\frac{2}{\pi}} \frac{4\ell}{((1-f)N)^{3/2}} \, \mathrm{e}^{(1-f)N \log 2} \, \mathrm{e}^{-2\frac{\ell^2}{(1-f)N}} \left(1 + O(N^{-1})\right). \tag{7.21}$$

It is useful to introduce the rescaled variable

$$u = \sqrt{\tfrac{2}{f(1-f)N}} \, \ell \,, \tag{7.22}$$

which simplifies the calculation of the integral. The probability distribution (6.82) in the thermodynamic limit becomes the continuous distribution

$$\varrho(u) \, \mathrm{d}u = \frac{4}{\sqrt{\pi}} u^2 \, \mathrm{e}^{-u^2} \left(1 + O(N^{-1})\right) \mathrm{d}u \,. \tag{7.23}$$

The sum over the spin ℓ becomes an integral over the positive real line in the thermodynamic limit. It is worth noticing that (7.23) is independent of the system's parameters N and f at the leading order and is normalized at all orders. The calculation of the average entropy is straightforward. If $f < \frac{1}{2}$, the dimension $b_{0\ell}$ is exponentially larger than d_ℓ, therefore (7.11) is just given by the logarithmic term. If $f = \frac{1}{2}$, then $b_{0\ell} = d_\ell$ and the second term in (7.11) contributes a $-\frac{1}{2}$ correction. Therefore,

$$\varphi(u) = fN \log 2 - \frac{1}{2} \log N - \frac{1}{2} \log f - \frac{1}{2} \log 2 + \log(1-f) + u^2 f - \log u - \tfrac{1}{2} \delta_{f,\frac{1}{2}} + O(N^{-1}) \,. \tag{7.24}$$

We obtain the average entanglement entropy by performing the integral

$$\langle S_{GA} \rangle_0 = \int_0^\infty \varrho(u) \varphi(u) \, \mathrm{d}u \,, \tag{7.25}$$

keeping all terms up to $O(1)$. Summarizing, the average entanglement entropy for

$f \leq \frac{1}{2}$ is

$$\langle S_{GA}\rangle_0 = \; fN\log 2 - \tfrac{1}{2}\log N \; - \tfrac{1}{2}\log f \; + \log(1-f) \\ + (\tfrac{1}{2}-f)\log 2 + \tfrac{3}{2}f - 1 - \tfrac{\gamma_E}{2} - \tfrac{1}{2}\delta_{f,\frac{1}{2}} + O(N^{-1}) \; . \tag{7.26}$$

The average entropy for $f > 1/2$ can be obtained via the exact symmetry $f \leftrightarrow (1-f)$ that applies to the case of $j = 0$. The calculation for the variance (6.84) is similar, and we find

$$(\Delta S_{GA})_0^2 = \tfrac{\sqrt{2\pi}}{4}\Big(f(\tfrac{3}{2}f-1) + \tfrac{\pi^2}{8} - 1 + \tfrac{1}{4}\delta_{f,\frac{1}{2}}\Big) N^{\frac{3}{2}} \; \mathrm{e}^{-N\log 2}\,(1+O(N^{-1}))\;, \tag{7.27}$$

for $f \leq 1/2$, and the formula for $f > 1/2$ can again be obtained via the exact symmetry $f \leftrightarrow (1-f)$ that applies to the case of $j = 0$.

Furthermore, we comment on the equipartition (or lack of equipartition) of entanglement entropy in the thermodynamic limit for the non-Abelian symmetry $SU(2)$, generalizing the discussion in [27] and [14] for the $U(1)$ case. By equipartition of entanglement, one means that the entropy $\langle S_{GA}^{(\ell)}\rangle_j$ is independent of ℓ in some limit. For generic spin j (Sec. 7.2), we found in (7.13) that at the leading order at fixed subsystem charge ℓ, the entanglement entropy is $\langle S_{GA}^{(\ell)}\rangle_j \approx N\left(\beta(s) - (1-f)\,\beta\big(\frac{s-ft}{1-f}\big)\right)$ with $s = 2j/N$ and $t = 2\ell/N_A$. Therefore, we conclude that there is no equipartition of entanglement entropy, as the leading order in N depends explicitly on the subsystem charge ℓ. This result extends the observation of [14] of lack of equipartition in the thermodynamic limit to the non-Abelian case. Furthermore, following the argument in [14], we emphasize the importance of the order of limits. If ℓ is fixed before taking the limit $N \to \infty$, using the expansion $\beta\big(\frac{s-ft}{1-f}\big) = \beta(\frac{s}{1-f}) - \beta'(\frac{s}{1-f})\frac{ft}{1-f} + O(t^2)$, we obtain instead $\langle S_{GA}^{(\ell)}\rangle_j \approx N\left(\beta(s) - (1-f)\,\beta\big(\frac{s}{1-f}\big)\right)$. This result matches the behavior found [27] for the $U(1)$ case, with the leading order independent of ℓ and the equipartition of entanglement entropy restored.

Interestingly, in the $j = 0$ case, using (7.22) and (7.24), we find that at the leading order the entanglement entropy at fixed subsystem charge ℓ is $\langle S_{GA}^{(\ell)}\rangle_0 \approx fN\log 2$. As this quantity is independent of the subsystem charge, we conclude that in this case, there is equipartition of entanglement for all ℓ.

7.4 Comparison of G-local and K-local asymptotics

The asymptotics of the average K-local entanglement entropy was studied in [99]. The system considered is the same as the one described here in Sec. 6.3, with the additional assumption of vanishing magnetization, $m = 0$, to select symmetry-resolved states. Using a combination of analytical and numerical methods, asymptotic formulas for the thermodynamic limit $N \to \infty$ at fixed f and s were studied. We compare these results for the ones obtained here in Sec. 7.2–7.3 for the G-local entanglement entropy of the same symmetry-resolved states.

For maximal spin $j_{\max} = N/2$, i.e., for the case $s = 1$, the Hilbert space takes the form

$$\mathcal{H}_N^{(j_{\max})} = \mathcal{H}_{\text{sym}}^{(j_{\max})} \otimes \mathcal{H}_{GA}^{(\ell_{\max})} \otimes \mathcal{H}_{GB}^{(j_{\max},\ell_{\max})}, \tag{7.28}$$

i.e., in the decomposition (6.37) there is a single allowed value of ℓ, and the dimensions are $\dim \mathcal{H}_{GA}^{(\ell_{\max})} = 1$, $\dim \mathcal{H}_{GB}^{(j_{\max},\ell_{\max})} = 1$, and $\dim \mathcal{H}_{\text{sym}}^{(j_{\max})} = N + 1$. As a result, the average G-local entropy necessarily vanishes (7.17) because any symmetry-resolved state in this sector has zero entanglement between G-local degrees of freedom. On the other hand, the K-local entanglement entropy also measures the entanglement in magnetic degrees of freedom m_A at fixed $m = m_A + m_B$ in $\mathcal{H}_{\text{sym}}^{(j_{\max})}$, which are not G-local. This K-local entanglement results in an average entropy that scales as $\frac{1}{2}\log N$. The comparison of the two different scalings found in [99] and in Sec. 7.3 is shown in the table:

Table 7.1. Comparison of large N asymptotics: S_{GA} vs S_{KA} for $j = j_{max}$

$j = j_{\max}$	N	$\sqrt{N}\,\delta_{f,\frac{1}{2}}$	$\log N$	1	$\delta_{f,\frac{1}{2}}$
$\langle S_{GA}\rangle_{j_{\max}}$	0	0	0	0	0
$\langle S_{KA}\rangle_{j_{\max},m=0}$	0	0	$\frac{1}{2}$	$\frac{1}{2}\log\frac{\pi e f(1-f)}{2}$	0

For minimum spin, $j = 0$ (assuming N even), i.e., for the case $s = 0$, the leading order $O(N)$ of the K-local and G-local average entropies coincide. There is again a difference at order $O(\log N)$ and at order $O(1)$ (first computed in [100]

for the K-local entropy). A comparison of the contributions found in [99] and in Sec. 7.3 is shown in Table 7.2

Table 7.2. Comparison of large N asymptotics: S_{GA} vs S_{KA} for $j = 0$

$j=0$	N	$\sqrt{N}\,\delta_{f,\frac{1}{2}}$	$\log N$	1	$\delta_{f,\frac{1}{2}}$
$\langle S_{GA}\rangle_0$	$f\log 2$	0	$-\frac{1}{2}$	$a_{GA}(f)$	$-\frac{1}{2}$
$\langle S_{KA}\rangle_0$	$f\log 2$	0	0	$a_{KA}(f)$	$-\frac{1}{2}$

where

$$a_{KA}(f) = \begin{cases} \frac{3}{2}f + \frac{3}{2}\log(1-f) & f \leq 1/2\,, \\ f \longleftrightarrow (1-f) & f > 1/2\,, \end{cases} \tag{7.29}$$

$$a_{GA}(f) = \begin{cases} \frac{3}{2}f + \log(1-f) - \frac{1}{2}\log f + (\frac{1}{2}-f)\log(2) - 1 - \frac{\gamma_E}{2} & f \leq 1/2\,, \\ f \longleftrightarrow (1-f) & f > 1/2\,. \end{cases} \tag{7.30}$$

We note the symmetry $f \leftrightarrow (1-f)$, which is an exact symmetry for $j = 0$.

For spin j of order $O(N)$, i.e., fixed spin density $s = 2j/N$ with $0 < s < 1$, the asymptotics of the K-local average entropy studied in [99] and the G-local average entropy derived in Sec. 7.2 agree at order $O(N)$ and $O(\sqrt{N})$. A difference again arises at order $O(\log N)$ and $O(1)$, as summarized in Table 7.3

Table 7.3. Comparison of large N asymptotics: S_{GA} vs S_{KA} for $0 < s = \frac{2j}{N} < 1$

$0<s<1$	N	$\sqrt{N}\,\delta_{f,\frac{1}{2}}$	$\log N$	1	$\delta_{f,\frac{1}{2}}$
$\langle S_{GA}\rangle_s$	$\beta(s)\,f$	$-\frac{\lvert\beta'(s)\rvert}{\sqrt{2\pi\,\lvert\beta''(s)\rvert}}$	0	$b_{GA}(f,s)$	$c_{GA}(s)$
$\langle S_{KA}\rangle_{s,\,m=0}$	$\beta(s)\,f$	$-\frac{\lvert\beta'(s)\rvert}{\sqrt{2\pi\,\lvert\beta''(s)\rvert}}$	$\frac{1}{2}$	$b_{KA}(f,s)$	0

where $\beta(s)$, $\beta'(s)$, $\beta''(s)$ are given by (7.3)–(7.4), and

$$b_{KA}(f,s) = \begin{cases} \frac{f+\log(1-f)}{2} - \frac{1-2f(1-s)}{2s}\log\left(\frac{1+s}{1-s}\right) + \log\frac{2s^{3/2}}{\sqrt{1-s^2}} + \frac{1}{2}\log\frac{\pi e f(1-f)}{2} & f \leq 1/2\,, \\ f \longleftrightarrow (1-f) & f > 1/2\,, \end{cases} \tag{7.31}$$

$$b_{GA}(f,s) = \begin{cases} \frac{f+\log(1-f)}{2} - (1-f)\frac{1-s}{2s}\log\left(\frac{1+s}{1-s}\right) + \log\left(\frac{2s}{1+s}\right) & f \leq 1/2\,, \\ \frac{(1-f)+\log f}{2} + (1-f)\frac{1-s}{2s}\log\left(\frac{1+s}{1-s}\right) & f > 1/2\,, \end{cases} \tag{7.32}$$

$$c_{GA}(f,s) = \tfrac{1}{2}\tfrac{1-s}{2s}\log\left(\tfrac{1+s}{1-s}\right) - \tfrac{1}{2}\log\left(\tfrac{2s}{1+s}\right)\ . \tag{7.33}$$

We note that the asymmetry of the G-local average entropy under subsystem exchange, $f \longleftrightarrow (1-f)$, discussed in Sec. 6.8 and Sec. 7.2 arises only at order $O(1)$, as shown explicitly in (7.32).

Additionally, we observe that in all the cases considered here, we find that the average K-local entropy studied in [99] and the average G-local entropy derived here satisfy:

$$\langle S_{KA}\rangle - \langle S_{GA}\rangle = \tfrac{1}{2}\log N + O(1)\,. \tag{7.34}$$

The difference can be attributed to the entanglement in the magnetic degrees of freedom probed by K-local observables, as discussed in Table 7.1.

Chapter 8
Conclusion & Outlook

8.1 Summary

This thesis presents a rigorous mathematical formulation for symmetry-resolved entanglement in systems possessing a non-Abelian symmetry. The results presented are entirely general and do not rely on the specifics of any Hamiltonian; they depend solely on the structure of the Hilbert space and the representation of the symmetry group G.

In Chapters 3 and 4, we began developing our framework based on an operational definition of a subsystem, characterized through a subalgebra of observables (Chapter 3). In the presence of non-Abelian symmetry, the G-invariant, symmetry-resolved observables define states (see Eq. (4.23)) that are both preparable and measurable, leading to the Hilbert space decomposition in Eq. (4.21), that generalized the standard direct-sum decomposition over Abelian charges and the tensor product structure associated with independent subsystems. Moreover, in analyses of symmetry-resolved entanglement [25–27] for an Abelian symmetry, the block-diagonal structure of the reduced density matrix under $U(1)$ symmetry has played a crucial role. In the non-Abelian symmetry case, the block-diagonal structure given by (4.24) emerged once we identified the generalized symmetry-resolved subsystems as in (4.21). Using this, we then obtained exact formulas for the average and variance of the entanglement entropy distribution for random pure states with a non-Abelian symmetry group G, as expressed in (3.32)–(3.33)–(4.25).

In Chapter 5, we began by noting that our framework is entirely general and does not presuppose any inherent notion of locality or a specific Hamiltonian. When a locality criterion was introduced, we distinguished between K-local (Eq. (5.6)) and G-local observables (Eq. (5.9)): while the kinematical observables of a many-body system are naturally local, they are typically not invariant under the action of G; in contrast, invariant observables tend to be non-local. Observables that are both local and G-invariant—termed G-local—often represent the only accessible operators defining a symmetry-resolved subsystem. In this context, symmetry-resolved entanglement entropy was defined as the entropy S_{GA} of the symmetry-resolved state, restricted to a symmetry-resolved subsystem. We then showed that, in the case of an Abelian symmetry, $G = U(1)$, our framework recovered established results [13–16].

In Chapters 6 and 7, we examined in detail an $SU(2)$-invariant system as a concrete example. We analyzed particular cases to illustrate the differences between the G-local and K-local notions of entropy (see Fig. 6.1). We derived the exact average entanglement entropy and its variance for random symmetry-resolved states (Chapter 6) and then analyzed the probability distribution for S_{GA} and compared it to that for S_{KA}. We plotted the Page curve in Fig. 6.2 for the exact average entanglement entropy and observed an asymmetry in the curve. This was confirmed when we discussed the thermodynamic limit (Chapter 7) for this system. At $O(1)$ in the thermodynamic limit, an asymmetry under subsystem exchange emerged, $f \not\leftrightarrow (1-f)$, where $f = V_A/V$ denotes the subsystem volume fraction. This new feature of non-Abelian symmetry-resolved entanglement was discussed in Sec. 5.4 for a general group G and was illustrated in (6.79) for small systems and in (7.32) for many-body systems in the thermodynamic limit. As observed in the Abelian case, a global non-Abelian symmetry such as $SU(2)$ also produces a leading volume-law entanglement entropy along with a square-root-volume correction at half-system size, as first reported in [99] and derived in Chapter 7 through asymptotic analysis of the exact formulas (see (7.3) for comparison). The coefficient in the volume-law scaling, defined in (7.3), depends on the spin density j/V and can be generalized to densities q_k/V for the non-Abelian charges, namely the rank(G) Casimir operators of a general compact semisimple Lie group G.

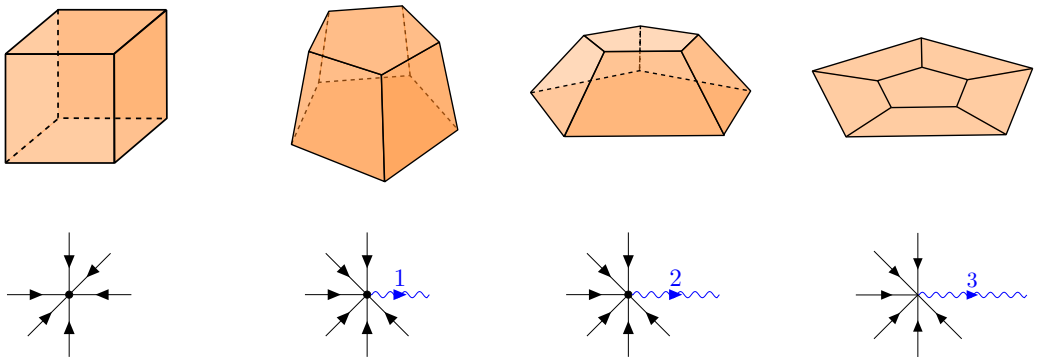

Figure 8.1. Quantum polyhedra provide a concrete example of $SU(2)$ symmetry-resolved states that can be probed only using G-local observables that measure their intrinsic geometry. Each spin corresponds to a quantum plane of fixed area, and the $SU(2)$ invariance in the coupling of angular momenta corresponds to the closure of the faces of the polyhedron.

8.2 Future Research Directions

8.2.1 Quantum Gravity and Quantum Polyhedra

In the quantization of gravity, physical states can exist as superpositions of quanta of geometric regions, which can be understood as quantum polyhedra [92, 93, 101]. Analogous to a classical polyhedron where the normal area vectors of its N faces sum to zero, a quantum polyhedron is visualized as a system of N spins constrained so that their total spin is zero. G-local observables are central to the study of quantum geometry in polyhedral models [92, 93], where operators such as $\vec{S}_a \cdot \vec{S}_b$ (illustrated in Fig. 1.1) measure the angles between the faces of a quantum polyhedron, as depicted in Fig. 8.1 for various spin j sectors. Unlike the uncorrelated faces of a classical polyhedron, the faces in a quantum polyhedron, represented by spins, are inherently correlated. This correlation prompts the question of *how to quantify the entanglement between one region of the polyhedron and the rest*. Equivalently, *how is one region of space entangled with another in quantum gravity?* Conventional entanglement measures falter here due to the system's constraints altering the accessible Hilbert space. To overcome this, we propose using the redefined entanglement measures obtained in this thesis.

Additionally, in the thermodynamic limit of many faces the quantum polyhedron approximates a spherical region, and semiclassical states are suitable here for studying quantum fluctuations of the classical metric. Here, entanglement scaling between regions is conjectured to serve as a probe of the state's nature [69,102–104]: it scales with the volume (number of spins) of a region in truly quantum states, and with the area in semiclassical states. The observation of these entanglement characteristics have important consequences in the context of the thermalization of isolated systems [13], which is why an analogous study of such states in the context of quantum gravity will shed light on the thermodynamic properties of geometric regions of space.

8.2.2 Symmetries, Locality and Non-Abelian ETH

The Eigenstate Thermalization Hypothesis (ETH) [1–3] describes how isolated quantum systems reach thermal equilibrium through their own unitary dynamics, a phenomenon not immediately intuitive given the nature of quantum mechanics. Recently, preliminary ideas regarding quantum thermodynamics and ETH in systems having a non-Abelian symmetry have been laid out in [98, 100, 105–108]. By means of work carried out in this thesis, we conjecture that the distribution $P(S_{GA})$, with its average and variance as given in (3.32)–(3.33)–(4.25) (see Fig. 6.1(a)), corresponds to the entanglement entropy distribution of energy eigenstates of quantum-chaotic Hamiltonians with a non-Abelian symmetry G, when restricted to G-local subsystems. Testing this conjecture numerically—by extending exact diagonalization studies [17–20] to quantum-chaotic Hamiltonians with a non-Abelian symmetry, such as the random Heisenberg model (1.2) and lattice-based Heisenberg models with local interactions [67] (as in [98,99])—would be highly significant in the context of emerging insights in non-Abelian eigenstate thermalization [98, 99, 108], thermodynamics with noncommuting conserved charges [100, 105–107], and quantum many-body scars [109, 110]. As the ETH is formulated in terms of the expectation values of operators, understanding non-Abelian ETH through this framework will enable a deeper understanding of the interplay between symmetries and thermalization. Additionally, ETH makes an assumption about the locality of the operators which undergo thermalization, which makes it interesting to see how the notions of K-locality and G-locality laid out

in in our work can be distinguished on the basis of the influence they have on eigenstate thermalization.

8.2.3 Page Curve and Entanglement Purification

This avenue of research is also relevant to black hole physics, specifically concerning the Page Curve hypothesis [4] presented in Chapter 2. Quantum mechanical toy models with unitary dynamics governed by random Hamiltonians have been employed to model this behavior, but they typically fail to replicate the decreasing phase of the entanglement entropy, as the entanglement entropy merely saturates rather than declines. However, this challenge was recently overcome for a particular setup involving a free fermion chain [111]. This discrepancy leads to critical questions: *what properties should such toy models have for the entanglement entropy to decrease in time after reaching a maximum value? Under which conditions can the entanglement decrease at a faster rate? Can these models be extended to open quantum systems? And can such systems help address the problem of decoherence in practical setups?* We believe these questions can be answered through methods developed in Appendix B by fine tuning the initial state as well as well as the parameters of the random Hamiltonians.

8.2.4 Other Directions

- We derived the average and variance of the probability distribution $P(S_{GA})$ and compared it to the average and variance of the numerically obtained distribution. Similarly, deriving exact expressions for the average and variance of the probability distribution $P(S_{KA})$ for K-local observables (see Fig. 6.1) would be insightful.

- Our framework can be directly applied to lattice systems with a gauge symmetry [80–82, 112] and spin-network systems in loop quantum gravity [96, 97, 113–116]. Finding new phenomena in these systems through the lens of non-abelian, symmetry-resolved subsystems and entanglement will be worthwhile.

- Another promising direction is extending our framework to study systems with a infinite-dimensional Hilbert space, like those encountered in quan-

tum field theory [69, 76–78, 117, 118]. While our analysis has been carried out within a finite-dimensional Hilbert space, the results apply directly to each symmetry-resolved sector even when these sectors are finite-dimensional subspaces of an infinite-dimensional Hilbert space.

Appendix A
Laplace approximation and discontinuities

In this section, we review the asymptotic expansion of integrals using the Laplace method [119] and extend this method to the presence of discontinuities. We derive an asymptotic expansion for $N \gg 1$ of integrals of the form

$$I = \int_K h(x)\, \mathrm{e}^{Ng(x)}\, \mathrm{d}x\,, \tag{A.1}$$

where $K \subset \mathbb{R}$ and $h(x)$ and $g(x)$ are two real-valued functions defined on K such that the integral is well defined for large enough N. We first assume that the functions h and g are smooth on K. Then, we present the formula for the case with h continuous but with a discontinuous first derivative at a point. We assume that the function g has a global maximum at x_0 in K where the gradient vanishes, $g'(x_0) = 0$, and the function also vanishes at the maximum $g(x_0) = 0$. The integral is approximated asymptotically by

$$I = h(x_0) \sqrt{-\frac{2\pi}{N g''(x_0)}} \left(1 + \frac{C_1}{N} + o\left(\frac{1}{N}\right)\right)\,, \tag{A.2}$$

where

$$C_1 = -\frac{1}{2}\frac{h''(x_0)}{h(x_0)g''(x_0)} + \frac{1}{8}\frac{g''''(x_0)h(x_0)}{h(x_0)g''(x_0)^2} + \frac{1}{2}\frac{g'''(x_0)h'(x_0)}{h(x_0)g''(x_0)^2} - \frac{5}{24}\frac{g'''(x_0)^2 h(x_0)}{h(x_0)g''(x_0)^3}\,. \tag{A.3}$$

The approximation (A.2) relies on three main observations.

1. Only the immediate neighborhood of x_0 contributes to the integral.

2. We expand the function $g(x)$ around x_0, and we approximate the exponential part of the integrand with a narrow Gaussian $e^{-\frac{N}{2}g''(x_0)(x-x_0)^2}$. This confirms the first assumption.

3. We expand the remaining part of the integrand around x_0 and extend the integral to the whole real line.

The integrals of terms of the expansion with the Gaussian (x_0 is a maximum, so $g''(x_0) < 0$) are given by

$$M^{(p)} = \int_{-\infty}^{\infty} (x-x_0)^p \, \mathrm{e}^{N\frac{g''(x_0)}{2}(x-x_0)^2} \mathrm{d}x = \begin{cases} 0 & p \text{ odd}, \\ \sqrt{2\pi}(p-1)!! \left(-\frac{1}{Ng''(x_0)}\right)^{\frac{p+1}{2}} & p \text{ even}. \end{cases} \tag{A.4}$$

If we are interested in the leading order or (A.2), expanding the integrand up to order $O(1)$ and combining with M_0 is sufficient

$$h(x_0)M^{(0)} = h(x_0)\sqrt{-\frac{2\pi}{Ng''(x_0)}} \, . \tag{A.5}$$

However, to compute the next-to-leading order (A.3), we have to expand the integrand up to order $O(x-x_0)^6$. The relevant terms are

$$\begin{aligned} h''(x_0)M^{(2)} &= -\tfrac{1}{N}\tfrac{1}{2}\frac{h''(x_0)}{g''(x_0)}\sqrt{-\tfrac{2\pi}{Ng''(x_0)}} \, , \\ N\left(\tfrac{1}{24}g''''(x_0)h(x_0) + \tfrac{1}{6}g'''(x_0)h'(x_0)\right)M^{(4)} &= \tfrac{1}{N}\left(\tfrac{1}{8}\frac{g''''(x_0)}{g''(x_0)^2} + \tfrac{1}{2}\frac{g'''(x_0)h'(x_0)}{h(x_0)g''(x_0)^2}\right)\sqrt{-\tfrac{2\pi}{Ng''(x_0)}} \, , \\ N^2\frac{1}{72}g'''(x_0)^2h(x_0)M^{(6)} &= -\tfrac{1}{N}\tfrac{5}{24}\frac{g'''(x_0)^2}{g''(x_0)^3}\sqrt{-\tfrac{2\pi}{Ng''(x_0)}} \, . \end{aligned}$$

Collecting them together, we obtain (A.3).

In the derivations in Chapter 7, we need to compute integrals of the form (A.1) with a function h that is not continuous in x_0. For simplicity, we will assume that $g(x)$ is still smooth in x_0. We follow the same strategy, expanding the integrand around x_0 and separating the integrals in $x < x_0$ and $x > x_0$. The split Gaussian

integrals are such that

$$\int_{x_0}^{\infty}(x-x_0)^p\,\mathrm{e}^{N\frac{g''(x_0)}{2}(x-x_0)^2}\mathrm{d}x=(-1)^p\int_{-\infty}^{x_0}(x-x_0)^p\,\mathrm{e}^{N\frac{g''(x_0)}{2}(x-x_0)^2}\mathrm{d}x\ , \tag{A.6}$$

and

$$\tilde{M}^{(p)}=\int_{x_0}^{\infty}(x-x_0)^p\,\mathrm{e}^{N\frac{g''(x_0)}{2}(x-x_0)^2}\mathrm{d}x=\begin{cases}\frac{1}{2}\sqrt{2\pi}(\frac{p-1}{2})!\left(-\frac{1}{Ng''(x_0)}\right)^{\frac{p+1}{2}} & p\text{ odd},\\ \frac{1}{2}\sqrt{2\pi}(p-1)!!\left(-\frac{1}{Ng''(x_0)}\right)^{\frac{p+1}{2}} & p\text{ even}.\end{cases} \tag{A.7}$$

The leading order of the Laplace approximation is similar to the one found earlier,

$$\big(h(x_0^-)+h(x_0^+)\big)\,\tilde{M}^{(0)}=\frac{h(x_0^-)+h(x_0^+)}{2}\sqrt{-\frac{2\pi}{Ng''(x_0)}}\ . \tag{A.8}$$

Here, we denote with $h(x_0^\pm)$ the right/left limit of the function h in x_0. If h is continuous in x_0, the formula (A.8) reduces to (A.5). The next-to-leading order term is

$$\big(h'(x_0^-)-h'(x_0^+)\big)\,\tilde{M}^{(1)}=\frac{h'(x_0^-)-h'(x_0^+)}{2}\sqrt{2\pi}\frac{-1}{Ng''(x_0)}\ , \tag{A.9}$$

which is, in general, non-vanishing if the first derivative of h is discontinuous in x_0. The calculation for the next-to-next-leading order term is similar. To summarize, if the function h is discontinuous at the maximum x_0 of g, the Laplace approximation for the integral (A.1) is

$$I=\frac{h(x_0^-)+h(x_0^+)}{2}\sqrt{-\frac{2\pi}{Ng''(x_0)}}\left(1+\frac{\tilde{C}_{1/2}}{\sqrt{N}}+\frac{\tilde{C}_1}{N}+o\left(\frac{1}{N}\right)\right)\ , \tag{A.10}$$

where

$$\tilde{C}_{1/2}=\frac{h'(x_0^-)-h'(x_0^+)}{h(x_0^-)+h(x_0^+)}\sqrt{-\frac{2}{N\pi g''(x_0)}}\ , \tag{A.11}$$

and

$$\tilde{C}_1=\frac{h(x_0^-)C_1(x_0^-)+h(x_0^+)C_1(x_0^+)}{h(x_0^-)+h(x_0^+)}\ , \tag{A.12}$$

where we denote by $C_1(x_0^\pm)$ the expression (A.3) computed (as a limit) in $x_0^\pm$. Thus, a discontinuity results in a $O(1/\sqrt{N})$ correction in the asymptotic expansion.

Appendix B
Entanglement Entropy Evolution and Random Matrices

B.1 Introduction

In this chapter, we discuss the time-evolution of the entanglement entropy in an isolated quantum system prepared in a factorized state. We focus on random-matrix Hamiltonians from the GUE ensemble, and compare the entropy of the average density matrix to the probability distribution of the entropy over the ensemble of random Hamiltonians. While the first captures correctly the saturation value of the entropy only at the leading order, the second captures also sub-leading orders, fluctuations around the average and the short time behavior of the entanglement entropy. We discuss also the relation to other random matrix ensembles, such as GOE. We also derive analogous results for gaussian states of random quadratic fermionic systems, which have been recently studied in [120].

B.2 EE Evolution: Random Matrix Hamiltonians

B.2.1 Entanglement Entropy of Eigenstates of a Random Matrix Hamiltonian

Let $|\psi_n\rangle$ be one eigenstate of a random matrix Hamiltonian H. We define $\rho_{A,n} = \mathrm{Tr}_B|\psi_n\rangle\langle\psi_n|$ to be a normalized $d_A \times d_A$ density matrix. It is helpful to separate this density matrix into diagonal and non-diagonal parts by writing it as $\rho_{A,n} = \left(\frac{I}{d_A} +$

$\epsilon X_{A,n}\Big) + \epsilon Y_{A,n}$, where $\frac{I}{d_A} + \epsilon X_{A,n}$ is the diagonal part and $\epsilon Y_{A,n}$ is the non-diagonal part of $\rho_{A,n}$. Here we use ϵ as a yet to be calculated small parameter, to help identify the leading order terms in susbsequent calculations. $\mathrm{Tr}(Y_{A,n}) = 0$ by construction, and using the normalization of the density matrix we can conclude that $\mathrm{Tr}(X_{A,n}) = 0$. Then using statistics of eigenvector components (see Appendices C and D),

$$\left\langle \frac{I}{d_A} + \epsilon X_{A,n} \right\rangle = \left\langle (\rho_{A,n})_{ii} \right\rangle = \sum_b^{d_B} \left\langle |c_{nib}|^2 \right\rangle = d_B . \frac{1}{d_A d_B} = \frac{1}{d_A},$$

$$\left\langle \epsilon Y_{A,n} \right\rangle = \left\langle (\rho_{A,n})_{ij} \right\rangle_{i \neq j} = \sum_b^{d_B} \left\langle c_{nib} c^*_{njb} \right\rangle_{i \neq j} = 0.$$

To calculate the average entanglement entropy for an eigenstate, we need to calculate the ensemble average of

$$\mathrm{Tr}(\rho^2_{A,n}) = \frac{1}{d_A} + \epsilon^2 \mathrm{Tr}(X^2_{A,n}) + \epsilon^2 \mathrm{Tr}(Y^2_{A,n}) + \epsilon^2 \mathrm{Tr}(X_{A,n} Y_{A,n})$$

Now,

$$\epsilon^2 \mathrm{Tr}(X_{A,n} Y_{A,n}) = \sum_{i,j}^{d_A} \sum_{b,c}^{d_B} |c_{nib}|^2 c_{njc} c^*_{nic} \delta_{ij} (1 - \delta_{ji}) = 0,$$

while the following averages can be calculated using properties derived in Appendix D

$$\left\langle \frac{1}{d_A} + \epsilon^2 \mathrm{Tr}(X^2_{A,n}) \right\rangle = \sum_{i}^{d_A} \sum_{b,c}^{d_B} \langle |c_{nib}|^2 |c_{nic}|^2 \rangle = \begin{cases} \frac{d_B+2}{d_A d_B+2} & GOE \\ \frac{d_B+1}{d_A d_B+1} & GUE \end{cases},$$

and

$$\epsilon^2 \langle \mathrm{Tr}(Y^2_{A,n}) \rangle = \sum_{i,j;i \neq j}^{d_A} \sum_{b}^{d_B} \langle |c_{nib}|^2 |c_{njb}|^2 \rangle = \begin{cases} \frac{d_A-1}{d_A d_B+2} & GOE \\ \frac{d_A-1}{d_A d_B+1} & GUE \end{cases}.$$

This gives the average purity of an eigenstate of a random Hamiltonian as

$$\langle \mathrm{Tr}(\rho^2_{A,n}) \rangle = \begin{cases} \frac{d_A+d_B+1}{d_A d_B+2} & GOE \\ \frac{d_A+d_B}{d_A d_B+1} & GUE \end{cases}. \tag{B.1}$$

The variance around this average purity can also be calculated. Following a detailed derivation, we obtain

$$(\Delta(\mathrm{Tr}[\rho_{A,n}^2]))^2 = \begin{cases} \frac{2(d_A-1)(d_B-1)(d_Ad_B+4d_A+4d_B+6)}{(d_Ad_B+2)^2(d_Ad_B+4)(d_Ad_B+6)} & GOE \\ \frac{2(d_A^2-1)(d_B^2-1)}{(d_Ad_B+1)^2(d_Ad_B+2)(d_Ad_B+3)} & GUE \end{cases} \tag{B.2}$$

For comparison, the variance for a Haar-random state was calculated in [69] as

$$\langle \left(\mathrm{Tr}(\rho^2)\right)^2 \rangle_{\mathrm{Haar}} - \langle \mathrm{Tr}(\rho^2) \rangle_{\mathrm{Haar}}^2 = \frac{2\,(d_A^2-1)(d_B^2-1)}{(d_Ad_B+1)^2\,(d_Ad_B+2)\,(d_Ad_B+3)} \tag{B.3}$$

The average entanglement entropy, $\langle S(\rho_{A,n}) \rangle = -\mathrm{Tr}(\rho_{A,n} \log \rho_{A,n})$, follows from the average purity using

$$\langle S(\rho_{A,n}) \rangle = \log(d_A) + \frac{1}{2} - \frac{d_A}{2} \langle \mathrm{Tr}(\rho_{A,n}^2) \rangle + O(\epsilon^3),$$

which gives us,

Ensemble	$\langle S(\rho_{A,n}) \rangle$	$\langle \mathrm{Tr}(\rho_{A,n}^2) \rangle$
GOE	$\log(d_A) - \frac{d_A^2+d_A-2}{2d_Ad_B} + O\left(\frac{1}{d_B^2}\right)$	$\frac{d_A+d_B+1}{d_Ad_B+2}$
GUE	$\log(d_A) - \frac{d_A^2-1}{2d_Ad_B} + O\left(\frac{1}{d_B^2}\right)$	$\frac{d_A+d_B}{d_Ad_B+1}$

We observe that the formula for the typical entanglement entropy in the GUE case is the same as that of Page [21] upto an order of $O\left(\frac{1}{d_B^2}\right)$, but the corresponding formula in the GOE case is different at this orde. We can now assert that the small parameter ϵ can be defined through

$$\epsilon^2 = \frac{1}{d_B}. \tag{B.4}$$

The variance around the average entanglement entropy of $\rho_{A,n}$ can be calculated as

$$(\Delta S(\rho_{A,n}))^2 \approx \frac{d_A^2}{4} \left[\left\langle (\mathrm{Tr}[\rho_{A,n}^2])^2 \right\rangle - \left\langle \mathrm{Tr}[\rho_{A,n}^2] \right\rangle^2 \right] = \frac{d_A^2}{4} (\Delta(\mathrm{Tr}[\rho_{A,n}^2]))^2 \tag{B.5}$$

$$= \begin{cases} \frac{d_A^2(d_A-1)(d_B-1)(d_Ad_B+4d_A+4d_B+6)}{2(d_Ad_B+2)^2(d_Ad_B+4)(d_Ad_B+6)} & GOE \\ \frac{d_A^2(d_A^2-1)(d_B^2-1)}{2(d_Ad_B+1)^2(d_Ad_B+2)(d_Ad_B+3)} & GUE \end{cases} \tag{B.6}$$

$$= \frac{d_A^2 - 1}{2d_A^2 d_B^2} + +O\left(\frac{1}{d_B^3}\right), \tag{B.7}$$

with

$$\Delta(S(\rho_{A,n})) = \sqrt{\frac{d_A^2 - 1}{2d_A^2}} \frac{1}{d_B} + O\left(\frac{1}{d_B^2}\right). \tag{B.8}$$

This formula matches the variance for typical entanglement in Haar-random states calculated in in [69].

B.2.2 Entropy Evolution of the Average Density Matrix

We consider a system with Hilbert space $\mathcal{H} = \mathcal{H}_A \otimes \mathcal{H}_B$ and a random matrix Hamiltonian H. We assume without loss of generality that $d_A (= dim(A)) < d_B (= dim(B))$. Given a pure state $|\psi_0\rangle$ of the system, its time evolution is $|\psi_t\rangle = e^{-iHt/\hbar}|\psi_0\rangle$ and the reduced density matrix of subsystem A is $\rho_A(t) = \mathrm{Tr}_B |\psi_t\rangle\langle\psi_t|$. We now work towards characterizing the evolution of the ensemble averaged density matrix,

We study the entanglement entropy $S_A(t) = -\mathrm{Tr}_A(\rho_A(t) \log \rho_A(t))$ for a state that is initially un-entangled, i.e., $|\psi_0\rangle = |\phi_A\rangle|\chi_B\rangle$.

B.2.2.1 Average density matrix

We compute the reduced state of the system, $\langle \rho_A(t)_{aa'} \rangle$, averaged over the GUE, using the correlations derived in Appendix D

$$\begin{aligned}
\langle \rho_A(t)_{aa'} \rangle &= \sum_{n,m}^{d_A d_B} \sum_{b}^{d_B} \langle \mathrm{e}^{-\mathrm{i}(E_n - E_m)t} \rangle \langle c_{n00} c^*_{m00} c^*_{nab} c_{ma'b} \rangle \\
&= \frac{1}{d_A d_B + 1} [(d_B + 1)\delta_{a0}\delta_{a'0} + d_B \delta_{aa'}(1 - \delta_{a0})] \\
&\quad + \frac{\langle \mathrm{e}^{-\mathrm{i}(E_n - E_m)t} \rangle}{d_A d_B + 1} [(d_A d_B - d_B)\delta_{a0}\delta_{a'0} - d_B \delta_{aa'}(1 - \delta_{a0})],
\end{aligned}$$

where

$$\langle \mathrm{e}^{-\mathrm{i}(E_n - E_m)t} \rangle = \frac{1}{N(N-1)} \int_{-\infty}^{\infty} dx \int_{-\infty}^{\infty} dy \mathrm{e}^{-\mathrm{i}(x-y)t} (\sigma_N(x,x)\sigma_N(y,y) - \sigma_N^2(x,y)), \tag{B.9}$$

with $N = d_A d_B$ and $\sigma_N(x,y)$ are the cluster functions of the GUE ensemble

$$\sigma_N(x,y) = \sum_{p=0}^{N-1} H_p(x) H_p(y). \tag{B.10}$$

$H_n(x)$ are the Hermite polynomials. Using properties of Hermite polynomials, we can obtain the following expression for the average time-evolution coefficient

$$\langle \mathrm{e}^{-\mathrm{i}(E_n - E_m)t} \rangle = \frac{1}{N(N-1)} \sum_{m=0}^{N-1} \sum_{n=0}^{N-1} (s_{m,m}(t) s^*_{n,n}(t) - |s_{m,n}(t)|^2), \tag{B.11}$$

where

$$s_{m,n}(t) = \int_{-\infty}^{\infty} H_n(x) H_m(x) \mathrm{e}^{-itx} dx = \mathrm{e}^{-\frac{t^2}{4}} \sum_{j=0}^{min(n,m)} \frac{\sqrt{m!n!}}{j!(m-j)!(n-j)!} \left(-\frac{\mathrm{i}}{\sqrt{2}} t \right)^{n+m-2j}, \tag{B.12}$$

Note that these formulas are for the GUE case in which the variance of Hamiltonian elements $\{\langle |H_{nn}|^2 \rangle = 1,\ \langle |H_{mn}|^2 = \frac{1}{2} \rangle\}$. For the general case with $\{\langle |H_{nn}|^2 \rangle = \gamma^2,\ \langle |H_{mn}|^2 \rangle = \frac{\gamma^2}{2} \rangle\}$, we have

$$s_{m,n}(t) = \mathrm{e}^{-\frac{\gamma^2 t^2}{4}} \sum_{j=0}^{min(n,m)} \frac{\sqrt{m!n!}}{j!(m-j)!(n-j)!} \left(-\frac{\mathrm{i}}{\sqrt{2}} \gamma t \right)^{n+m-2j}, \tag{B.13}$$

As we are interested in the early and late time characteristics of the entanglement entropy, the important limits to evaluate are:

1. At $t \to 0$: To evaluate average density matrix near $t = 0$, we note that only $s_{n,n}(t)$ and $s_{n+1,n}(t)$ contribute to the $O(t^2)$ terms. This enables us to obtain

$$\langle \mathrm{e}^{-\mathrm{i}(E_n - E_m)t} \rangle = 1 - \frac{N+1}{2} \gamma^2 t^2 + O(t^4).$$

This gives the average density matrix close to $t = 0$ as

$$\langle \rho_A(t = 0^+)_{aa'} \rangle = \delta_{a0} \delta_{a'0} \left[1 - \frac{d_B(d_A - 1)}{2} \gamma^2 t^2 \right] - \delta_{aa'}(1 - \delta_{a0}) \frac{d_B}{2} \gamma^2 t^2 + O(t^4). \tag{B.14}$$

2. At $t \to \infty$:

$$\lim_{t\to\infty} \langle \mathrm{e}^{-\mathrm{i}(E_n - E_m)t} \rangle = 0,$$

which gives us the average density matrix at late times as

$$\lim_{t\to\infty} \langle \rho_A(t)_{aa'} \rangle = \frac{1}{N+1}[(d_B+1)\delta_{a0}\delta_{a'0} + d_B\delta_{aa'}(1-\delta_{a0})]. \tag{B.15}$$

B.2.2.2 Purity and von Neumann of the average

Once we have the expression for the average density matrix at early and late times, it is straightforward to calculate the corresponding limits for the purity and the entanglement entropy of this average density matrix. We can evaluate the entanglement entropy for the average state as

$$\begin{aligned} S(\langle \rho_A(t) \rangle) = &- \frac{(d_A-1)d_B}{d_A d_B+1} \langle \mathrm{e}^{-\mathrm{i}(E_n-E_m)t} \rangle \log\left(\frac{d_B \langle \mathrm{e}^{-\mathrm{i}(E_n-E_m)t} \rangle}{d_A d_B+1} \right) \\ &- \left(1 - \frac{d_B(d_A-1)}{d_A d_B+1} \langle \mathrm{e}^{-\mathrm{i}(E_n-E_m)t} \rangle \right) \log\left(1 - \frac{d_B(d_A-1)}{d_A d_B+1} \langle \mathrm{e}^{-\mathrm{i}(E_n-E_m)t} \rangle \right). \end{aligned}$$

Then,

1. At $t \to 0$:

$$\mathrm{Tr}[\langle \rho_A(t) \rangle^2] = 1 - d_B(d_A-1)\gamma^2 t^2 + O(t^4),$$

and

$$S(\langle \rho_A(t) \rangle) = -\frac{(d_A-1)d_B}{2}\gamma^2 t^2 \log\left(\frac{d_B}{2\mathrm{e}}\gamma^2 t^2\right) + O(t^4) \tag{B.16}$$

.

2. At $t \to \infty$:

$$\lim_{t\to\infty} \mathrm{Tr}[\langle \rho_A(t) \rangle^2] = \frac{d_B}{d_A d_B+1} + \frac{d_B+1}{(d_A d_B+1)^2} = \frac{d_A+d_B}{d_A d_B+1} + \frac{d_B+1-d_A(d_A d_B+1)}{(d_A d_B+1)^2},$$

and

$$\lim_{t\to\infty} S(\langle \rho_A(t) \rangle) = \log(d_A) - \frac{d_A-1}{2d_A^2 d_B^2} + O\left(\frac{1}{d_B^3}\right). \tag{B.17}$$

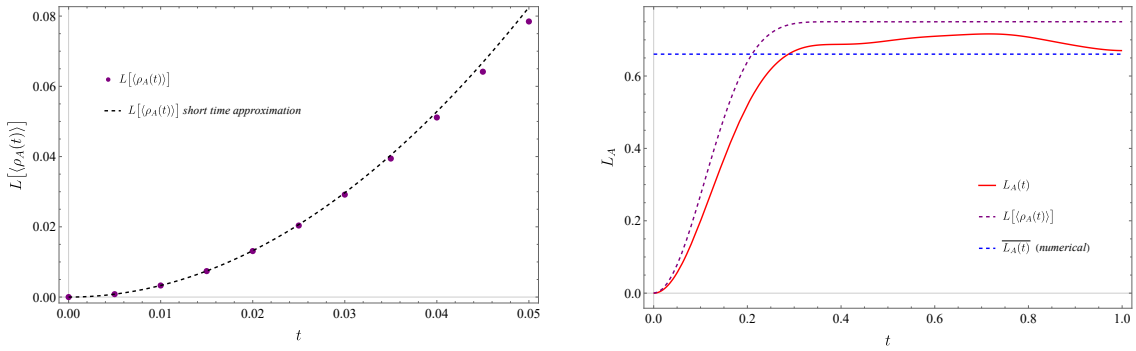

Figure B.1. Average Linear Entropy vs time. The blue curve represents the linear entropy of the average density matrix and the black dashed line denotes the analytical formula for the same at early times.

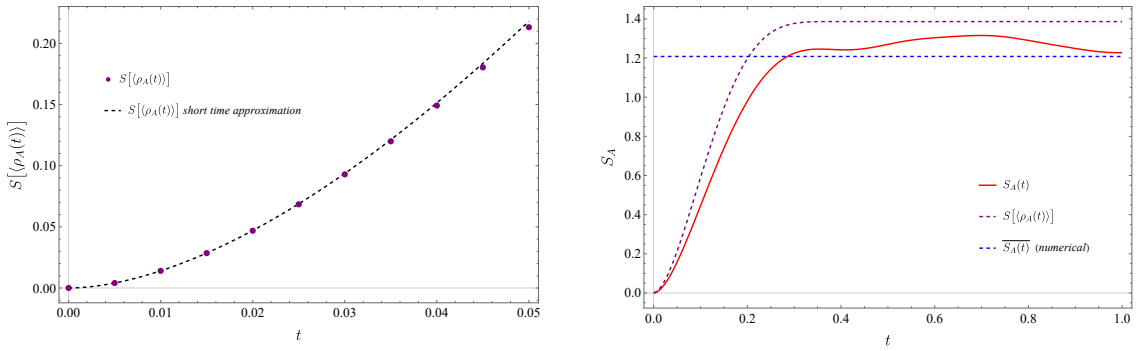

Figure B.2. Average Entanglement Entropy vs time. The blue curve represents the entanglement entropy of the average density matrix and the black dashed line denotes the analytical formula for the same at early times.

B.2.3 Typical Purity: Late Times

We now move towards our main objective, characterizing the early and late evolution of the purity and entanglement entropy of a system in an initially pure and factorized state and governed by a random matrix Hamiltonian.

B.2.3.1 Purity: Long-time Behavior

We begin by splitting the time-dependent reduced density matrix into time-independent and time-dependent parts,

$$\rho_A(t) = \frac{I}{d_A} + \epsilon(X_A + Y_A(t)), \tag{B.18}$$

where

$$\frac{I}{d_A} + \epsilon X_A = \sum_n |c_{n00}|^2 \ \mathrm{Tr}_B(|\psi_n\rangle\langle\psi_n|), \tag{B.19}$$

$$\epsilon Y_A(t) = \sum_{n\neq m} c_{n00}c^*_{m00} \ \mathrm{e}^{-\mathrm{i}(E_n-E_m)t} \ \mathrm{Tr}_B(|\psi_n\rangle\langle\psi_m|). \tag{B.20}$$

Following a detailed derivation, we obtain the average purity at long times as

$$\langle \mathrm{Tr}(\overline{\rho_A^2(t)})\rangle = \begin{cases} \frac{d_A+d_B}{d_Ad_B+1} + \frac{(d_A-1)(d_B-1)(9d_Ad_B+48)}{(d_Ad_B+1)(d_Ad_B+2)(d_Ad_B+4)(d_Ad_B+6)} & GOE \\ \frac{d_A+d_B}{d_Ad_B+1} + \frac{2(d_A-1)(d_B-1)}{d_Ad_B(d_Ad_B+1)(d_Ad_B+3)} & GUE \end{cases}, \tag{B.21}$$

along with the variance about this mean value

$$\Delta(\mathrm{Tr}[\rho_A^2(t)]) = \sqrt{2\frac{d_A^2-1}{d_A^4}}\frac{1}{d_B} + O\left(\frac{1}{d_B^2}\right). \tag{B.22}$$

Here we have made the assertion that our small parameter can be defined as

$$\epsilon^2 = \frac{1}{d_B} \tag{B.23}$$

B.2.3.2 Linear Entropy: Short-time Behavior

The time dependence of the d_A eigenvalues of $\rho_A(t)$ can be written in the form

$$\lambda_i(t) = \begin{cases} 1 - \alpha\frac{t^2}{2!} - \beta\frac{t^3}{3!} - ... & i = 1 \\ \alpha_i\frac{t^2}{2!} + \beta_i\frac{t^3}{3!} + ... & i = 2, 3, ..., d_A \end{cases},$$

where

$$\sum_{i=2}^{d_A}\alpha_i = \alpha; \ \sum_{i=2}^{d_A}\beta_i = \beta; ... \tag{B.24}$$

We can calculate α as

$$\alpha \ = \ -\mathrm{Tr}[\rho_A(0)\ddot{\rho}_A(0) + \dot{\rho}_A^2(0)] \ = \ \frac{2}{\hbar^2}\big[\langle H^2\rangle + \langle H\rangle^2 - \langle HP_AH\rangle - \langle HP_BH\rangle\big], \tag{B.25}$$

where, $P_A = |\phi_A\rangle\langle\phi_A| \otimes \mathcal{I}_B$ and $P_B = \mathcal{I}_A \otimes |\phi_B\rangle\langle\phi_B|$. First, we see that the expression for α is symmetric in $A \longleftrightarrow B$. Secondly, for a non-interacting Hamiltonian

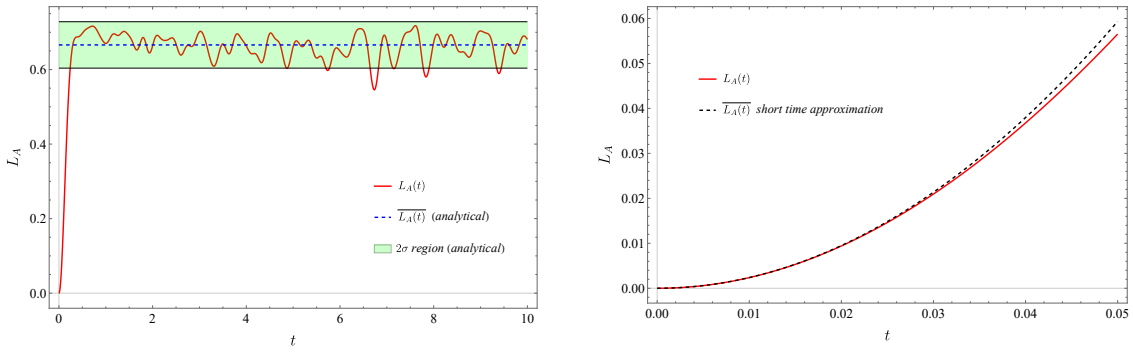

Figure B.3. Average Linear Entropy vs time.

$(H = H_A + H_B)$, $\alpha = 0$, which is the expected result.

Then

$$\mathrm{Tr}[\rho_A^2(t)] = \sum_i \lambda_i^2(t) = 1 - \alpha t^2 + O(t^3). \tag{B.26}$$

B.2.4 Typical Entanglement Entropy: Late Times

B.2.4.1 Entanglement Entropy: Long-time Behavior

We can calculate

$$-\mathrm{Tr}(\rho_A(t)\log\rho_A(t)) = \log(d_A) + \frac{1}{2} - \frac{d_A}{2}\mathrm{Tr}\left(\rho_A^2(t)\right) + O(\epsilon^3), \tag{B.27}$$

which gives us,

$$\langle\overline{S_A(t)}\rangle = \log(d_A) + \frac{1}{2} - \frac{d_A}{2}\langle\mathrm{Tr}\left(\overline{\rho_A^2(t)}\right)\rangle + O(\epsilon^3). \tag{B.28}$$

Using the results of the previous section, we can show that

$$\langle\overline{S_A(t)}\rangle = \begin{cases} \log(d_A) - \frac{d_A^2-1}{2(d_Ad_B+1)} - \frac{d_A(d_A-1)(d_B-1)(9d_Ad_B+48)}{2(d_Ad_B+1)(d_Ad_B+2)(d_Ad_B+4)(d_Ad_B+6)} + O(\epsilon^3) & GOE \\ \log(d_A) - \frac{d_A^2-1}{2(d_Ad_B+1)} - \frac{d_A(d_A-1)(d_B-1)}{d_Ad_B(d_Ad_B+1)(d_Ad_B+3)} + O(\epsilon^3) & GUE \end{cases}, \tag{B.29}$$

which can be simplified to

$$\langle\overline{S_A(t)}\rangle = \log(d_A) - \frac{d_A^2-1}{2d_Ad_B} + O\left(\frac{1}{d_B^2}\right), \tag{B.30}$$

for both the GOE and the GUE. We can also calculate the standard deviation about this mean value as

$$\Delta S_A \approx \frac{d_A}{2}\Delta(\mathrm{Tr}[\rho_A^2(t)])) = \sqrt{\frac{d_A^2-1}{2d_A^2}}\frac{1}{d_B} + O\Big(\frac{1}{d_B^2}\Big). \tag{B.31}$$

We observe that the formula for the time-averaged entanglement entropy and its variance for both the GUE and GOE cases is the same as that for Haar-random states [21, 69] upto an order of $O\Big(\frac{1}{d_B^2}\Big)$.

B.2.4.2 Short Time Behavior

By construction, the entanglement entropy at the initial time vanishes, $S_A(0) = 0$. Determining the behavior of $S_A(t)$ for small t as a function of the Hamiltonian H and the initial state can provide useful information on the time-scale τ of entanglement production. One might expect that a Taylor expansion $S_A(t) = \dot{S}_A(0)\,t + \frac{1}{2}\ddot{S}_A(0)\,t^2 + \ldots$ around $t = 0$ would provide a detailed description of the early-time behavior of the entanglement entropy and an estimate of the time-scale τ of early entanglement production. It is easy to show that the first order vanishes, $\dot{S}_A(0) = 0$. However the second derivative of the entanglement entropy turns out to diverge, $\ddot{S}_A(0) = \infty$, and the function $S_A(t)$ is not analytic at $t = 0$. Because of that, we take an alternative route and study the time dependence of the spectrum of the density matrix $\rho_A(t)$.

We can expand the entanglement entropy as a function of time,

$$S_A(t) \;=\; -\sum_{i=1}^{d_A}\lambda_i(t)log(\lambda_i(t)) \;=\; \left[(1+log2)\alpha - \sum_{i=2}^{d_A}\alpha_i log(\alpha_i)\right]\frac{t^2}{2} - \alpha t^2 logt + O(t^3),$$

where

$$\sum_{i=2}^{d_A}\alpha_i log(\alpha_i) \;=\; \sum_{i=2}^{d_A}\left(\alpha_i log\Big(\frac{\alpha_i}{\alpha}\Big) + \alpha_i log\alpha\right) \;=\; \alpha log\alpha + \alpha.\sum_{i=2}^{d_A}\Big(\frac{\alpha_i}{\alpha}\Big)log\Big(\frac{\alpha_i}{\alpha}\Big).$$

It is not possible to get an exact expression for (6) in terms of H and $\rho(0)$. However, we can obtain a bound on $S_A(t)$ as $t \to 0$, given by $S_A^{\min}(t) \le S_A(t) \le S_A^{\max}(t)$,

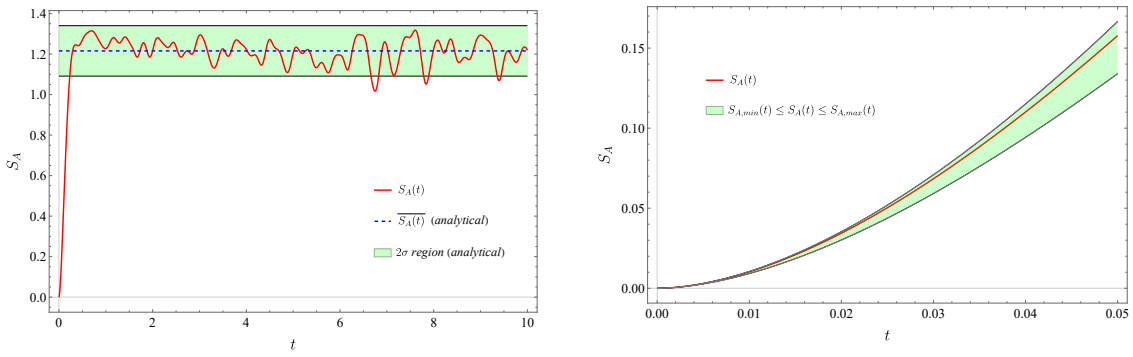

Figure B.4. Average Entanglement Entropy vs time.

where

$$S_A^{\max}(t) = \frac{\alpha\, t^2}{2} \log\left((d_A - 1)\frac{2\,e}{\alpha\, t^2}\right) + O(t^3)\,, \tag{B.32}$$

$$S_A^{\min}(t) = \frac{\alpha\, t^2}{2} \log\left(\frac{2\,e}{\alpha\, t^2}\right) + O(t^3)\,. \tag{B.33}$$

For systems governed by random Hamiltonians, we can define the timescale of entanglement, τ, as the point in time for which $S_A^{max}(t)$ first equals S_{Page}, we find its expression as

$$\tau = \left[\frac{-2\langle\overline{S_A(t)}\rangle}{\alpha.W_{-1}\big(-\frac{\langle\overline{S_A(t)}\rangle}{e.d_A}\big)}\right]^{\frac{1}{2}}. \tag{B.34}$$

B.3 EE Evolution: Random Quadratic Fermionic Hamiltonians

We consider a fermionic system with Hilbert space $\mathcal{H} = \mathcal{H}_A \otimes \mathcal{H}_B$ and a quadratic, fermionic, random matrix Hamiltonian H. The dimensions of the subspaces A and B are respectively $d_A = 2^{N_A}$ and $d_B = 2^{N_B}$ where N_A and N_B are the number of fermions in systems A and B. Given a factorized gaussian state $|\psi_0\rangle$ of the system, its time evolution is $|\psi_t\rangle = e^{-iHt/\hbar}|\psi_0\rangle$ and the reduced density matrix of subsystem A is $\rho_A(t) = \mathrm{tr}_B|\psi_t\rangle\langle\psi_t|$. This fermionic system can also be written in the Fock space given by $\mathcal{H}_{Fock} = \bigoplus_{i=1}^{N} \mathcal{H}_i$ where $N = N_A + N_B$ is the total number of fermions in the composite system. In this Fock space, the state of the system can be represented by a complex structure $\mathcal{J}$ satisfying $\mathcal{J}^2 = -\mathcal{I}$. The

Hamiltonian in this picture can be written as

$$H = \frac{1}{2} h_{ab} \xi^a \xi^b, \tag{B.35}$$

where h is a $2N \times 2N$ antisymmetric matrix. The dynamics of the system, in terms of the initial state $\mathcal{J}_0$ can be written as $\mathcal{J}(t) = M(t)\mathcal{J}_0 M^{-1}(t)$ where $M(t) = \mathrm{e}^{ht}$ is time evolution operator. The reduced complex structure for the subsystem A is denoted by $\mathcal{J}_A$ which is defined through the block structure of $\mathcal{J}$ as follows

$$\mathcal{J} = \left(\begin{array}{c|c} \mathcal{J}_A & \mathcal{J}_{AB} \\ \hline \mathcal{J}_{BA} & \mathcal{J}_B \end{array} \right). \tag{B.36}$$

The entanglement entropy of the subsystem A is then given by

$$S_A = \frac{1}{2} \sum_{i=1}^{2N_A} \Big[-\Big(\frac{1+x_i}{2}\Big) log\Big(\frac{1+x_i}{2}\Big) - \Big(\frac{1-x_i}{2}\Big) log\Big(\frac{1-x_i}{2}\Big) \Big], \tag{B.37}$$

where x_i's are the singular values of $\mathcal{J}_A(t)$.

B.3.1 Preliminaries

Let $\{\psi_m\}$ be the eigenvectors of h_{ab} with eigenvalues $\mathrm{i}E_m$ and $\{\phi_m\}$ be the eigenvectors of the initial factorised state $\mathcal{J}_0$ with eigenvalues $\mathrm{i}P_m$ where P_m takes the values ± 1. These can be expanded in the computational basis $\{e_m\}$ as

$$\psi_m = \sum_i c_{mi} e_i \quad ; \quad \phi_m = \sum_i d_{mi} e_i. \tag{B.38}$$

As h_{ab} and $\mathcal{J}_0$ are both $2N \times 2N$ antisymmetric matrices, the following properties are satisfied

$$E_{2n-1} = -E_n \ ; \ E_{2n} = +E_n \ ; \ \psi_{2n-1} = \psi^*_{2n}, \tag{B.39}$$

$$P_{2n-1} = -1 \ ; \ P_{2n} = +1 \ ; \ \phi_{2n-1} = \phi^*_{2n}. \tag{B.40}$$

The set of eigenvectors $\{\psi_m\}_{m=1}^{2N}$ and $\{\phi_m\}_{m=1}^{2N}$ can therefore be expressed as $\{\psi_m, \psi_m^*\}_{m=1}^{N}$ and $\{\phi_m, \phi_m^*\}_{m=1}^{N}$ respectively. The following equations can then

be derived using orthogonality of eigenvectors:

$$\langle \psi_m^*, \psi_m \rangle = \sum_i c_{mi}^2 = 0, \tag{B.41}$$

$$\langle \psi_m, \psi_m^* \rangle = \sum_i c_{mi}^{*2} = 0, \tag{B.42}$$

$$\langle \phi_m^*, \phi_m \rangle = \sum_i d_{mi}^2 = 0, \tag{B.43}$$

$$\langle \phi_m, \phi_m^* \rangle = \sum_i d_{mi}^{*2} = 0. \tag{B.44}$$

Then, we can write the eigendecomposition of h_{ab} and the initial state $\mathcal{J}_0$ as

$$h_{ij} = \sum_{n=1}^{N} \left[(\mathrm{i}E_n) c_{2n,i} c_{2n,j}^* + (-\mathrm{i}E_n) c_{2n,i}^* c_{2n,j} \right], \tag{B.45}$$

$$(\mathcal{J}_0)_{ij} = \sum_{n=1}^{N} \left[(\mathrm{i}) d_{2n,i} d_{2n,j}^* + (-\mathrm{i}) d_{2n,i}^* d_{2n,j} \right]. \tag{B.46}$$

It is also possible to write down the following useful inner products

$$\langle \psi_m, \phi_n \rangle = \langle \phi_n^*, \psi_m^* \rangle = \sum_i d_{ni} c_{mi}^* = b_{mn}, \tag{B.47}$$

$$\langle \psi_m, \phi_n^* \rangle = \langle \phi_n, \psi_m^* \rangle = \sum_i d_{ni}^* c_{mi}^* = b_{m\bar{n}}, \tag{B.48}$$

$$\langle \psi_m^*, \phi_n \rangle = \langle \phi_n^*, \psi_m \rangle = \sum_i d_{ni} c_{mi} = b_{\bar{m}n} = b_{m\bar{n}}^*, \tag{B.49}$$

$$\langle \psi_m^*, \phi_n^* \rangle = \langle \phi_n, \psi_m \rangle = \sum_i d_{ni}^* c_{mi} = b_{\bar{m}\bar{n}} = b_{mn}^*. \tag{B.50}$$

B.3.2 Average Fermionic Gaussian State and its EE

Assuming $d_A \leq d_B$, we compute the reduced state of the system, $\langle \mathcal{J}(t)_{ij} \rangle$, averaged over the ensemble of gaussian distributed real, antisymmetric matrices. To do that

it would helpful to first note that the initial state $\mathcal{J}_0$ can be written as

$$(\mathcal{J}_0)_{ij} = \sum_{k=1}(\mathrm{i}P_k)d_{ki}d^*_{kj} = -\sum_{k=1}(\mathrm{i}P_k)d_{kj}d^*_{ki}. \tag{B.51}$$

Then we find,

$$\begin{aligned}\langle\mathcal{J}(t)_{ij}\rangle &= \sum_{n,m,q}^{N}(\mathrm{i}P_q)\langle \mathrm{e}^{\mathrm{i}(E_m-E_n)t}\rangle\langle b_{mp}b^*_{np}c_{mi}c^*_{nj}\rangle \\ &= \frac{1}{2N-1}\Big[1+2(N-1)\langle \mathrm{e}^{\mathrm{i}(E_m-E_n)t}\rangle_{m\neq n,\bar{n}}\Big](\mathcal{J}_0)_{ij},\end{aligned}$$

where

$$\langle \mathrm{e}^{-\mathrm{i}(E_n-E_m)t}\rangle = \frac{1}{N(N-1)}\int_{-\infty}^{\infty}dx\int_{-\infty}^{\infty}dy\mathrm{e}^{-\mathrm{i}(x-y)t}(\sigma_{2N}(x,x)\sigma_{2N}(y,y)-\sigma^2_{2N}(x,y)), \tag{B.52}$$

with $\sigma_{2N}(x,y)$ given as in (Mehta & Rosenzweig 1967)

$$\sigma_{2N}(x,y) = \sum_{p=0}^{N-1}H_{2p}(x)H_{2p}(y). \tag{B.53}$$

$H_n(x)$ are the Hermite polynomials. Using the product formula

$$H_m(x)H_n(x) = \sum_{j=0}^{min(m,n)} j!\binom{m}{j}\binom{n}{j}H_{m+n-2j}(x), \tag{B.54}$$

and the formula,

$$H_n(x+y) = \sum_{j=0}^{n}\binom{n}{j}H_j(x)(2y)^{n-j}, \tag{B.55}$$

we can show

$$s_{m,n}(t) = \int_{-\infty}^{\infty}H_n(x)H_m(x)\mathrm{e}^{-itx}dx = \mathrm{e}^{-\frac{t^2}{4}}\sum_{j=0}^{min(n,m)}\frac{\sqrt{m!n!}}{j!(m-j)!(n-j)!}\left(-\frac{\mathrm{i}}{\sqrt{2}}t\right)^{n+m-2j}, \tag{B.56}$$

and

$$\langle \mathrm{e}^{-\mathrm{i}(E_n-E_m)t}\rangle = \frac{1}{N(N-1)}\sum_{m=0}^{N-1}\sum_{n=0}^{N-1}(s_{2m,2m}(t)s^*_{2n,2n}(t) - |s_{2m,2n}(t)|^2) \tag{B.57}$$

Note that these formulas are for the case in which the variance of Hamiltonian elements $\langle |H_{mn}|^2\rangle = 1$. For the general case with $\langle |H_{mn}|^2\rangle = \gamma^2$, we have

$$s_{m,n}(t) = \mathrm{e}^{-\frac{\gamma^2 t^2}{4}}\sum_{j=0}^{min(n,m)}\frac{\sqrt{m!n!}}{j!(m-j)!(n-j)!}\Big(-\frac{\mathrm{i}}{\sqrt{2}}\gamma t\Big)^{n+m-2j}, \tag{B.58}$$

To evaluate average density matrix near $t=0$, we use

$$s_{n,n}(t) = \mathrm{e}^{-\frac{\gamma^2 t^2}{4}}\sum_{j=0}^{n}\frac{n!}{j!(n-j)!(n-j)!}\Big(-\frac{\mathrm{i}}{\sqrt{2}}\gamma t\Big)^{2n-2j} = 1-\frac{2n+1}{4}\gamma^2t^2+O(t^4), \tag{B.59}$$

Some important cases are:

1. At $t\to 0$:

$$\begin{aligned}\langle \mathrm{e}^{-\mathrm{i}(E_n-E_m)t}\rangle &= \frac{1}{N(N-1)}\Bigg[\sum_{n,m=0;n\neq m}^{N-1} s_{2m,2m}(t)s^*_{2n,2n}(t)+O(t^4)\Bigg]\\ &= \frac{1}{N(N-1)}\Bigg[\sum_{n,m=0;n\neq m}^{N-1}\Big(1-\frac{4m+1}{4}\gamma^2t^2\Big)\Big(1-\frac{4n+1}{4}\gamma^2t^2\Big)+O(t^4)\Bigg]\\ &= 1-\frac{1}{2}\gamma^2t^2-\frac{1}{N(N-1)}\sum_{n,m=0;n\neq m}^{N-1}(m+n)\gamma^2t^2+O(t^4)\\ &= 1-\frac{2N-1}{2}\gamma^2t^2+O(t^4)\end{aligned}$$

   This gives us at t close to 0

$$\langle \mathcal{J}(t)_{ij}\rangle = \Big[1-(N-1)\gamma^2t^2\Big](\mathcal{J}_0)_{ij} \tag{B.60}$$

2. At $t\to\infty$:

$$\lim_{t\to\infty}\langle \mathrm{e}^{-\mathrm{i}(E_n-E_m)t}\rangle = 0 \quad \textit{and} \quad \lim_{t\to\infty}\langle \mathcal{J}(t)_{ij}\rangle = \frac{1}{2N-1}(\mathcal{J}_0)_{ij}$$

B.3.2.1 Entanglement entropy of the average state

The entanglement entropy is given by the von Neumann entropy of the average state $\langle \mathcal{J}_A(t) \rangle$ of subsystem A with singular values $a(t)$

$$S\Big(\langle \mathcal{J}_A(t) \rangle\Big) = \frac{1}{2} \sum_{i=1}^{2N_A} \Big[- \Big(\frac{1+a(t)x_{i0}}{2}\Big) log\Big(\frac{1+a(t)x_{i0}}{2}\Big) - \Big(\frac{1-a(t)x_{i0}}{2}\Big) log\Big(\frac{1-a(t)x_{i0}}{2}\Big)\Big],$$

where $x_{i0} = 1$ for an initially factorised state. For early times, $t \to 0$, we have $a(t) = 1 - (N-1)\gamma^2 t^2$ which gives us

$$S\Big(\langle \mathcal{J}_A(t) \rangle\Big) = N_A \frac{N-1}{2} \gamma^2 t^2 \left[1 - \log\left(\frac{N-1}{2} \gamma^2 t^2 \right) \right] + O(t^4). \tag{B.61}$$

B.3.3 Typical Entanglement Entropy and Variance: Late Times

The entanglement entropy for fermionic gaussian states can be expressed as [120, 121]

$$S_{A.f} = N_A \log 2 - \sum_{n=1}^{\infty} \frac{\mathrm{Tr}\big[(\mathrm{i}\mathcal{J}_A)^{2n}\big]}{4n(2n-1)},$$

where the series converges absolutely. For a fermionic system with a random quadratic Hamiltonian, the the entanglement entropy as a function of time can be written as

$$S_{A.f}(t) = N_A \log 2 - \sum_{n=1}^{\infty} \epsilon^{2n} \frac{\mathrm{Tr}\big[(\mathrm{i}\mathcal{J}_A(t))^{2n}\big]}{4n(2n-1)},$$

where ϵ is a small, yet to be determined parameter. The series can then be truncated at the lowest order which gives us

$$S_{A.f}(t) = N_A \log 2 + \epsilon^2 \frac{\mathrm{Tr}\big[\mathcal{J}_A^2(t)\big]}{4} + O(\epsilon^4). \tag{B.62}$$

We begin by noting that the time-dependent reduced fermionic state can be split into two parts, one time-independent one, and the other time-dependent,

$$\mathcal{J}_A(t) = \mathcal{J}X_A + \mathcal{J}Y_A(t), \tag{B.63}$$

where

$$(\mathcal{J}X_A)_{ij} = \sum_{n,m=1}^{2N} \mathrm{i}P_m |b_{nm}|^2 c_{ni} c_{nj}^*, \tag{B.64}$$

$$(\mathcal{J}Y_A)_{ij}(t) = \sum_{n,m;n\neq m}^{2N} \sum_{q=1}^{2N} \mathrm{i}P_q b_{mq} b_{nq}^* c_{mi} c_{nj}^* \mathrm{e}^{\mathrm{i}(E_m - E_n)t}. \tag{B.65}$$

The average of any function, $f(t) = f(\mathcal{J}_A(t))$, for a system governed by a random matrix Hamiltonian is given by

$$\langle \overline{f(t)} \rangle = \left\langle \overline{f(\mathrm{e}^{-iHt}|\psi_0\rangle)} \right\rangle = \left\langle \lim_{t\to\infty} \frac{1}{T} \int_0^T f(\mathcal{J}_A(t)) dt \right\rangle, \tag{B.66}$$

where the average is evaluated both over time and over the random matrix ensemble. Then,

$$\left\langle \mathrm{Tr}\big(\overline{\mathcal{J}_A^2(t)}\big) \right\rangle = \left\langle \mathrm{Tr}\big(\mathcal{J}X_A^2\big) \right\rangle + \left\langle \mathrm{Tr}\big(\overline{\mathcal{J}Y_A^2(t)}\big) \right\rangle. \tag{B.67}$$

Following a long derivation where we use the statistical properties of components of eigenvectors of random matrices we find,

$$\left\langle \mathrm{Tr}\big(\overline{\mathcal{J}Y_A^2(t)}\big) \right\rangle = -\frac{N_A(2N_A-1)}{N} + O\left(\frac{1}{N^2}\right), \tag{B.68}$$

$$\left\langle \mathrm{Tr}\big(\mathcal{J}X_A^2\big) \right\rangle = O\left(\frac{1}{N^2}\right), \tag{B.69}$$

which leads us to

$$\left\langle \overline{S_{A.f}(t)} \right\rangle = N_A \log 2 - \frac{N_A(2N_A-1)}{4N} + O\left(\frac{1}{N^2}\right). \tag{B.70}$$

We can also calculate the variance of the purity as

$$\begin{aligned} \Delta^2(S_{A,f}(t)) &= \left\langle \overline{(S_{A,f}(t))^2} \right\rangle - \left\langle \overline{S_{A,f}(t)} \right\rangle^2 \\ &= \frac{\epsilon^4}{16} \left[\left\langle \overline{(\mathrm{Tr}[\mathcal{J}Y_A^2(t)])^2} \right\rangle - \left\langle \overline{\mathrm{Tr}[\mathcal{J}Y_A^2(t)]} \right\rangle^2 \right] + O(\epsilon^6). \end{aligned}$$

Following a detailed derivation, we obtain

$$\Delta^2(S_{A,f}(t)) = \frac{N_A^2}{4N^2}\left(1 - \frac{1}{2N_A}\right) + O\left(\frac{1}{N^3}\right). \tag{B.71}$$

B.3.4 Entanglement entropy: Short-time behavior

We prepare the system in the state $|0\rangle_A \otimes |0\rangle_B$. The time dependence of the N_A singular values of $\mathcal{J}_A(t)$ can be written in the form

$$j_i(t) = 1 - A\frac{t^2}{2!} - B\frac{t^3}{3!} - ...$$

Then, using (B.37), we find the expression for the entanglement entropy at small times as

$$S_A(t) = \left[(1 + log2)\sum_{i=1}^{N_A}\frac{A_i}{2} - \sum_{i=1}^{N_A}\frac{A_i}{2}log\Big(\frac{A_i}{2}\Big)\right]\frac{t^2}{2} - \sum_{i=1}^{N_A}\frac{A_i}{2}t^2 logt + O(t^3),$$

Comparing with B.25 we find that

$$\sum_{i=1}^{N_A}\frac{A_i}{2} = \alpha. \tag{B.72}$$

Moreover, similar to the procedure in the previous section, we can obtain a bound on $S_A(t)$ as $t \to 0$, given by $S_A^{\min}(t) \leq S_A(t) \leq S_A^{\max}(t)$, where

$$S_A^{\max}(t) = \frac{\alpha\, t^2}{2}\log\left(N_A\frac{2\,e}{\alpha\, t^2}\right) + O(t^3)\,, \tag{B.73}$$

$$S_A^{\min}(t) = \frac{\alpha\, t^2}{2}\log\left(\frac{2\,e}{\alpha\, t^2}\right) + O(t^3)\,. \tag{B.74}$$

To help with the computations, we define a structure $C_{\mu,\nu}$ as

$$C_{\mu,\nu} = \frac{1}{2}\big(\delta_{\mu,\nu} + i\Omega_{\mu,\nu}\big), \tag{B.75}$$

where $\delta_{\mu,\nu}$ is the $2N \times 2N$ identity matrix, and $\Omega_{\mu,\nu}$ is the $2N \times 2N$ fundamental sympletic matrix,

$$\Omega_{\mu,\nu} = \bigoplus_{i=1}^{N} \left(\begin{array}{c|c} 0 & 1 \\ \hline -1 & 0 \end{array}\right). \tag{B.76}$$

It should be noted that $C_{\mu,\nu} = \langle \xi_\mu \xi_\nu \rangle$, is a correlation matrix for the fermionic operator, ξ_μ, in the initial state. Then, in terms of this structure, using (B.25) we can get the expression for α as

$$\alpha = 2 \sum_{\mu,\rho \in A} \sum_{\nu,\sigma \in B} h_{\mu,\nu} h_{\rho,\sigma} C_{\mu,\rho} C_{\nu,\sigma}. \tag{B.77}$$

For a random, quadratic, fermionic, matrix Hamiltonian $h_{\mu,\nu}$ with $\langle h_{\mu,\nu} \rangle_{random\ h} = \Delta^2$ for $\mu \neq \nu$ and $\langle h_{\mu,\nu} \rangle_{random\ h} = 0$, we can compute

$$\langle \alpha \rangle_{random\ h} = 2\Delta^2 N_A N_B. \tag{B.78}$$

Defining the timescale of entanglement, τ, as the point in time for which $S_A^{max}(t)$ first equals S_{Gauss}, we find its expression as

$$\tau = \left[\frac{-2S_{Gauss}}{\alpha . W_{-1}\big(-\frac{S_{Gauss}}{e.N_A}\big)} \right]^{\frac{1}{2}}. \tag{B.79}$$

Appendix C
Exact PDF for Eigenvectors of GUE and GOE Random Matrices

The probability distribution function, $P_{M,d}(v_1, \ldots, v_d)$, of d out of the M independent components of one eigenvector, v, of a random matrix has been well studied. For instance,

$$P_{M,d}(v_1, \ldots, v_d) = \frac{1}{\pi^{\frac{d}{2}}} \frac{\Gamma(\frac{M}{2})}{\Gamma(\frac{M-d}{2})} (1 - v_1^2 - \ldots - v_d^2)^{\frac{M-d-2}{2}},$$

where $M = N$ for the GOE ensemble, $M = 2N$ for the GUE and GSE ensembles. However, the PDF corresponding to the components of two or more eigenvectors of a random matrix has not been studied in detail. In the following discussion, we aim to calculate the PDF of the components of two eigenvectors, $P(\bar{v}, \bar{w})$, of random matrices belonging to various ensembles.

C.1 GOE

For the GOE ensemble, $P(\bar{v}, \bar{w})$ has the form

$$P^{GOE}(\bar{v}, \bar{w}) = C_N \delta(1 - \bar{v}^2)\delta(1 - \bar{w}^2)\delta(\bar{v}.\bar{w}) \tag{C.1}$$

$$= C_N \oint \frac{ds_1}{2\pi \mathrm{i}} \mathrm{e}^{+s_1 t_1} \oint \frac{ds_2}{2\pi \mathrm{i}} \mathrm{e}^{+s_2 t_2} \oint \frac{ds_3}{2\pi \mathrm{i}} \mathrm{e}^{+s_3 t_3} \mathrm{e}^{-|\bar{v}^2| s_1} \mathrm{e}^{-|\bar{w}^2| s_2} \mathrm{e}^{-\bar{v}.\bar{w} s_3} \tag{C.2}$$

where C_N is the normalization constant, $t_1 = t_2 = 1$ and $t_3 = 0$. The first task is to calculate C_N. Normalisation of this PDF requires that

$$\begin{aligned} 1 &= \int d^N v \int d^N w P^{GOE}(\bar{v}, \bar{w}) \\ &= C_N \int d^N v \int d^N w \oint \frac{ds_1}{2\pi \mathrm{i}} \mathrm{e}^{+s_1 t_1} \oint \frac{ds_2}{2\pi \mathrm{i}} \mathrm{e}^{+s_2 t_2} \oint \frac{ds_3}{2\pi \mathrm{i}} \mathrm{e}^{+s_3 t_3} \mathrm{e}^{-|\bar{v}^2| s_1} \mathrm{e}^{-|\bar{w}^2| s_2} \mathrm{e}^{-\bar{v}.\bar{w} s_3}. \end{aligned}$$

Expressing $|\bar{v}^2| s_1 + |\bar{w}^2| s_2 + \bar{v}.\bar{w} s_3 = \bar{V}^T M \bar{V}$ where M is a $2N \times 2N$ matrix of the form

$$M = \left(\begin{array}{c|c} s_1 \mathrm{I} & \frac{s_3}{2} \mathrm{I} \\ \hline \frac{s_3}{2} \mathrm{I} & s_2 \mathrm{I} \end{array} \right). \tag{C.3}$$

This gives us

$$\int d^{2N} V \mathrm{e}^{-\bar{V}^T M \bar{V}} = \frac{\pi^{\frac{2N}{2}}}{\sqrt{det(M)}} = \frac{\pi^N}{(s_1 s_2 - \frac{s_3^2}{4})^{\frac{N}{2}}}.$$

Then, the normalisation condition simplifies to

$$\begin{aligned} 1 &= C_N \oint \frac{ds_1}{2\pi \mathrm{i}} \mathrm{e}^{+s_1 t_1} \frac{1}{(s_1 - \frac{s_3^2}{4 s_2})^{\frac{N}{2}}} \oint \frac{ds_2}{2\pi \mathrm{i}} \mathrm{e}^{+s_2 t_2} \oint \frac{ds_3}{2\pi \mathrm{i}} \mathrm{e}^{+s_3 t_3} \frac{\pi^N}{s_2^{\frac{N}{2}}} \\ &= C_N \oint \frac{ds_2}{2\pi \mathrm{i}} \mathrm{e}^{+s_2 t_2} \oint \frac{ds_3}{2\pi \mathrm{i}} \mathrm{e}^{+s_3 t_3} \frac{\pi^N}{s_2^{\frac{N}{2}}} \frac{1}{\Gamma(\frac{N}{2})} t_1^{\frac{N}{2}-1} \mathrm{e}^{\frac{s_3^2}{4 s_2}} \theta(t_1), \end{aligned}$$

where $\theta(x)$ is the heaviside function. Setting $t_1 = 1$ in eq(1),

$$\begin{aligned} 1 &= \frac{C_N \pi^N}{\Gamma(\frac{N}{2})} \oint \frac{ds_2}{2\pi \mathrm{i}} \mathrm{e}^{+s_2 t_2} \frac{1}{s_2^{\frac{N}{2}}} \oint \frac{ds_3}{2\pi \mathrm{i}} \mathrm{e}^{+s_3 t_3} \mathrm{e}^{\frac{s_3^2}{4 s_2}} \\ &= \frac{C_N \pi^N}{\Gamma(\frac{N}{2})} \oint \frac{ds_2}{2\pi \mathrm{i}} \mathrm{e}^{+s_2 t_2} \frac{1}{s_2^{\frac{N}{2}}} \sqrt{4\pi s_2} \\ &= \frac{C_N \pi^{N-\frac{1}{2}}}{\Gamma(\frac{N}{2}) \Gamma(\frac{N-1}{2})}, \end{aligned}$$

which gives us

$$C_N = \frac{\Gamma(\frac{N}{2}) \Gamma(\frac{N-1}{2})}{\pi^{N-\frac{1}{2}}}. \tag{C.4}$$

C.1.1 4-component PDF

The main PDF of interest to us is, $P^{GOE}(x_1, x_2, y_1, y_2)$, where $x_i = |v_i|^2$ and $y_i = |w_i|^2$.

$$\begin{aligned}
&P^{GOE}(x_1, x_2, y_1, y_2) \\
&= C_N \int d^N v \; d^N w \oint \frac{ds_1}{2\pi \mathrm{i}} \mathrm{e}^{+s_1 t_1} \oint \frac{ds_2}{2\pi \mathrm{i}} \mathrm{e}^{+s_2 t_2} \oint \frac{ds_3}{2\pi \mathrm{i}} \mathrm{e}^{+s_3 t_3} \mathrm{e}^{-|\bar{v}^2| s_1 - |\bar{w}^2| s_2 - \bar{v}.\bar{w} s_3} \\
&\times \delta(x_1 - |v_1|^2) \delta(x_2 - |v_2|^2) \delta(y_1 - |w_1|^2) \delta(y_2 - |w_2|^2).
\end{aligned}$$

Writing $\bar{v}_\perp = (v_3, \ldots, v_N)$ and $\bar{w}_\perp = (w_3, \ldots, w_N)$,

$$\begin{aligned}
&P^{GOE}(x_1, x_2, y_1, y_2) \\
&= C_N \oint \frac{ds_1}{2\pi \mathrm{i}} \mathrm{e}^{+s_1 t_1} \oint \frac{ds_2}{2\pi \mathrm{i}} \mathrm{e}^{+s_2 t_2} \oint \frac{ds_3}{2\pi \mathrm{i}} \mathrm{e}^{+s_3 t_3} \int d\bar{v}_\perp \; d\bar{w}_\perp \mathrm{e}^{-|\bar{v}_\perp^2| s_1 - |\bar{w}_\perp^2| s_2 - \bar{v}_\perp.\bar{w}_\perp s_3} \\
&\times \frac{\mathrm{e}^{-s_1(x_1+x_2) - s_2(y_1+y_2)} (\mathrm{e}^{-s_3\sqrt{x_1 y_1}} + \mathrm{e}^{s_3\sqrt{x_1 y_1}})(\mathrm{e}^{-s_3\sqrt{x_2 y_2}} + \mathrm{e}^{s_3\sqrt{x_2 y_2}})}{4\sqrt{x_1 y_1 x_2 y_2}}.
\end{aligned}$$

Using the same method as in the previous section, we simplify this to

$$\begin{aligned}
&P^{GOE}(x_1, x_2, y_1, y_2) \\
&= \frac{C_N}{4\sqrt{x_1 y_1 x_2 y_2}} \oint \frac{ds_1}{2\pi \mathrm{i}} \mathrm{e}^{+s_1(1-x_1-x_2)} \oint \frac{ds_2}{2\pi \mathrm{i}} \mathrm{e}^{+s_2(1-y_1-y_2)} \oint \frac{ds_3}{2\pi \mathrm{i}} \mathrm{e}^{+s_3 t_3} \\
&\times (\mathrm{e}^{-s_3\sqrt{x_1 y_1}} + \mathrm{e}^{s_3\sqrt{x_1 y_1}})(\mathrm{e}^{-s_3\sqrt{x_2 y_2}} + \mathrm{e}^{s_3\sqrt{x_2 y_2}}) \\
&= \frac{C_N \pi^{N-2}}{\Gamma(\frac{N}{2} - 1)} \frac{(1 - x_1 - x_2)^{\frac{N-4}{2}}}{4\sqrt{x_1 y_1 x_2 y_2}} \theta(1 - x_1 - x_2) \oint \frac{ds_2}{2\pi \mathrm{i}} \frac{\mathrm{e}^{+s_2(1-y_1-y_2)}}{s_2^{\frac{N-2}{2}}} \oint \frac{ds_3}{2\pi \mathrm{i}} \mathrm{e}^{+s_3 t_3} \\
&\times (\mathrm{e}^{-s_3\sqrt{x_1 y_1}} + \mathrm{e}^{s_3\sqrt{x_1 y_1}})(\mathrm{e}^{-s_3\sqrt{x_2 y_2}} + \mathrm{e}^{s_3\sqrt{x_2 y_2}}) \mathrm{e}^{\frac{s_3^2}{4 s_2}(1-x_1-x_2)} \\
&= frac C_N \pi^{N-2} \Gamma(\frac{N}{2} - 1) \frac{(1 - x_1 - x_2)^{\frac{N-5}{2}}}{2\sqrt{x_1 y_1 x_2 y_2}} \theta(1 - x_1 - x_2) \oint \frac{ds_2}{2\pi \mathrm{i}} \frac{\mathrm{e}^{+s_2(1-y_1-y_2)}}{s_2^{\frac{N-3}{2}}} \\
&\times (\mathrm{e}^{-s_2 \frac{(\sqrt{x_1 y_1} + \sqrt{x_1 y_1})^2}{1-x_1-x_2}} + \mathrm{e}^{-s_2 \frac{(\sqrt{x_1 y_1} - \sqrt{x_1 y_1})^2}{1-x_1-x_2}}),
\end{aligned}$$

finally giving us the 4-component PDF as

$$P^{GOE}(x_1, x_2, y_1, y_2) = \frac{\Gamma(\frac{N}{2})\Gamma(\frac{N-1}{2})}{\Gamma(\frac{N-2}{2})\Gamma(\frac{N-3}{2})} \frac{1}{2\pi^2 \sqrt{x_1 y_1 x_2 y_2}} \theta(1 - x_1 - x_2)$$

$$\times \Bigg[\Big(1 - x_1 - x_2 - y_1 - y_2 + (\sqrt{x_1 y_2} - \sqrt{x_2 y_1})^2\Big)^{\frac{N-5}{2}} \times \theta\Big(1 - x_1 - x_2 - y_1 - y_2 + (\sqrt{x_1 y_2} - \sqrt{x_2 y_1})^2\Big) + \Big(1 - x_1 - x_2 - y_1 - y_2 + (\sqrt{x_1 y_2} + \sqrt{x_2 y_1})^2\Big)^{\frac{N-5}{2}} \times \theta\Big(1 - x_1 - x_2 - y_1 - y_2 + (\sqrt{x_1 y_2} + \sqrt{x_2 y_1})^2\Big)\Bigg].$$

C.1.2 4-Point Correlations

$$\begin{aligned}
&\langle x_1\, x_2\, y_1\, y_2\rangle_{GOE} \\
&= \int dx_1 dx_2 dy_1 dy_2\; x_1 x_2 y_1 y_2 P^{GOE}(x_1, x_2, y_1, y_2) \\
&= C_N \int dx_1 dx_2 dy_1 dy_2\; x_1 x_2 y_1 y_2 \oint \frac{ds_1}{2\pi \mathrm{i}} \mathrm{e}^{+s_1 t_1} \oint \frac{ds_2}{2\pi \mathrm{i}} \mathrm{e}^{+s_2 t_2} \oint \frac{ds_3}{2\pi \mathrm{i}} \mathrm{e}^{+s_3 t_3} \\
&\quad \times \mathrm{e}^{-|\bar{v}^2| s_1 - |\bar{w}^2| s_2 - \bar{v}.\bar{w} s_3} \delta(x_1 - |v_1|^2) \delta(x_2 - |v_2|^2) \delta(y_1 - |w_1|^2) \delta(y_2 - |w_2|^2) \\
&= C_N \oint \frac{ds_1}{2\pi \mathrm{i}} \mathrm{e}^{+s_1 t_1} \oint \frac{ds_2}{2\pi \mathrm{i}} \mathrm{e}^{+s_2 t_2} \oint \frac{ds_3}{2\pi \mathrm{i}} \mathrm{e}^{+s_3 t_3} \frac{\pi^{N-2}}{(s_1 s_2 - \frac{s_3^2}{4})^{\frac{N-2}{2}}} \times \frac{\pi^2}{64} \frac{(2 s_1 s_2 + s_3^2)^2}{(s_1 s_2 - \frac{s_3^2}{4})^5} \\
&= \frac{C_N \pi^N}{16} (I_1 + I_2 + I_3).
\end{aligned}$$

Here

$$I_1 = \oint \frac{ds_1}{2\pi \mathrm{i}} \mathrm{e}^{+s_1 t_1} \oint \frac{ds_2}{2\pi \mathrm{i}} \mathrm{e}^{+s_2 t_2} \oint \frac{ds_3}{2\pi \mathrm{i}} \mathrm{e}^{+s_3 t_3} \frac{1}{(s_1 s_2 - \frac{s_3^2}{4})^{\frac{N+4}{2}}} = \frac{\pi^{-\frac{1}{2}}}{\Gamma(\frac{N+3}{2}) \Gamma(\frac{N+4}{2})} \quad \text{(C.5)}$$

$$I_2 = \oint \frac{ds_1}{2\pi \mathrm{i}} \mathrm{e}^{+s_1 t_1} \oint \frac{ds_2}{2\pi \mathrm{i}} \mathrm{e}^{+s_2 t_2} \oint \frac{ds_3}{2\pi \mathrm{i}} \mathrm{e}^{+s_3 t_3} \frac{3 s_3^2}{2(s_1 s_2 - \frac{s_3^2}{4})^{\frac{N+6}{2}}} = \frac{-3\pi^{-\frac{1}{2}}}{\Gamma(\frac{N+3}{2}) \Gamma(\frac{N+6}{2})} \quad \text{(C.6)}$$

$$I_3 = \oint \frac{ds_1}{2\pi \mathrm{i}} \mathrm{e}^{+s_1 t_1} \oint \frac{ds_2}{2\pi \mathrm{i}} \mathrm{e}^{+s_2 t_2} \oint \frac{ds_3}{2\pi \mathrm{i}} \mathrm{e}^{+s_3 t_3} \frac{9 s_3^4}{16(s_1 s_2 - \frac{s_3^2}{4})^{\frac{N+8}{2}}} = \frac{27\pi^{-\frac{1}{2}}}{4\Gamma(\frac{N+3}{2}) \Gamma(\frac{N+8}{2})}. \quad \text{(C.7)}$$

This gives us

$$\langle x_1\, x_2\, y_1\, y_2\rangle_{GOE} = \frac{1}{N^2-1}\frac{N^2+4N+15}{N(N+2)(N+4)(N+6)}. \tag{C.8}$$

C.2 GUE

For the GUE ensemble, $P(\bar{v},\bar{w}) = P(\bar{v}_R,\bar{v}_I,\bar{w}_R,\bar{w}_I)$ has the form

$$\begin{aligned}
P^{GUE}(\bar{v},\bar{w}) &= C_N\delta(1-\bar{v}_R^2-\bar{v}_I^2)\delta(1-\bar{w}_R^2-\bar{w}_I^2)\delta(\bar{v}_R.\bar{w}_R+\bar{v}_I.\bar{w}_I)\delta(\bar{v}_R.\bar{w}_I-\bar{v}_I.\bar{w}_R)\\
&= C_N\oint\frac{ds_1}{2\pi\mathrm{i}}\mathrm{e}^{+s_1t_1}\oint\frac{ds_2}{2\pi\mathrm{i}}\mathrm{e}^{+s_2t_2}\oint\frac{ds_3}{2\pi\mathrm{i}}\mathrm{e}^{+s_3t_3}\oint\frac{ds_4}{2\pi\mathrm{i}}\mathrm{e}^{+s_4t_4}\\
&\quad\times\mathrm{e}^{-(\bar{v}_R^2+\bar{v}_I^2)s_1}\mathrm{e}^{-(\bar{w}_R^2+\bar{w}_I^2)s_2}\mathrm{e}^{-(\bar{v}_R.\bar{w}_R+\bar{v}_I.\bar{w}_I)s_3}\mathrm{e}^{-(\bar{v}_R.\bar{w}_I-\bar{v}_I.\bar{w}_R)s_4},
\end{aligned}$$

where C_N is the normalization constant, $t_1 = t_2 = 1$ and $t_3 = t_4 = 0$. The first task is to calculate C_N. Normalisation of this PDF requires that

$$\begin{aligned}
1 &= \int d^{2N}v\int d^{2N}wP^{GOE}(\bar{v},\bar{w})\\
&= C_N\int d^{2N}v\int d^{2N}w\oint\frac{ds_1}{2\pi\mathrm{i}}\mathrm{e}^{+s_1t_1}\oint\frac{ds_2}{2\pi\mathrm{i}}\mathrm{e}^{+s_2t_2}\oint\frac{ds_3}{2\pi\mathrm{i}}\mathrm{e}^{+s_3t_3}\oint\frac{ds_4}{2\pi\mathrm{i}}\mathrm{e}^{+s_4t_4}\\
&\quad\times\mathrm{e}^{-(\bar{v}_R^2+\bar{v}_I^2)s_1}\mathrm{e}^{-(\bar{w}_R^2+\bar{w}_I^2)s_2}\mathrm{e}^{-(\bar{v}_R.\bar{w}_R+\bar{v}_I.\bar{w}_I)s_3}\mathrm{e}^{-(\bar{v}_R.\bar{w}_I-\bar{v}_I.\bar{w}_R)s_4}\\
&= C_N\int d^{4N}V\oint\frac{ds_1}{2\pi\mathrm{i}}\mathrm{e}^{+s_1t_1}\oint\frac{ds_2}{2\pi\mathrm{i}}\mathrm{e}^{+s_2t_2}\oint\frac{ds_3}{2\pi\mathrm{i}}\mathrm{e}^{+s_3t_3}\oint\frac{ds_4}{2\pi\mathrm{i}}\mathrm{e}^{+s_4t_4}\mathrm{e}^{-\bar{V}^TM\bar{V}}.
\end{aligned}$$

Here M is a $4N\times 4N$ matrix of the form

$$M = \left(\begin{array}{c|c} s_1\mathrm{I}_{2N} & \mathrm{I}_N\otimes A_2 \\ \hline \mathrm{I}_N\otimes A_2^T & s_2\mathrm{I}_{2N}\end{array}\right), \tag{C.9}$$

where

$$A_2 = \left(\begin{array}{c|c} \frac{s_3}{2} & \frac{s_4}{2} \\ \hline -\frac{s_4}{2} & \frac{s_3}{2}\end{array}\right). \tag{C.10}$$

This gives us

$$\int d^{4N}V\mathrm{e}^{-\bar{V}^TM\bar{V}} = \frac{\pi^{\frac{4N}{2}}}{\sqrt{det(M)}} = \frac{\pi^{2N}}{(s_1s_2-\frac{(s_3^2+s_4^2)}{4})^N}.$$

Then, the normalisation condition simplifies to

$$\begin{aligned}1 &= C_N \oint \frac{ds_1}{2\pi \mathrm{i}} \mathrm{e}^{+s_1 t_1} \frac{1}{(s_1 - \frac{(s_3^2+s_4^2)}{4s_2})^N} \oint \frac{ds_2}{2\pi \mathrm{i}} \mathrm{e}^{+s_2 t_2} \oint \frac{ds_3}{2\pi \mathrm{i}} \mathrm{e}^{+s_3 t_3} \oint \frac{ds_4}{2\pi \mathrm{i}} \mathrm{e}^{+s_4 t_4} \frac{\pi^{2N}}{s_2^N} \\ &= C_N \oint \frac{ds_2}{2\pi \mathrm{i}} \mathrm{e}^{+s_2 t_2} \oint \frac{ds_3}{2\pi \mathrm{i}} \mathrm{e}^{+s_3 t_3} \oint \frac{ds_4}{2\pi \mathrm{i}} \mathrm{e}^{+s_4 t_4} \frac{\pi^{2N}}{s_2^N} \frac{1}{\Gamma(N)} t_1^{N-1} \mathrm{e}^{\frac{(s_3^2+s_4^2)}{4s_2}} \theta(t_1).\end{aligned}$$

Setting $t_1 = 1$,

$$\begin{aligned}1 &= \frac{C_N \pi^{2N-1}}{\Gamma(N)} \oint \frac{ds_2}{2\pi \mathrm{i}} \mathrm{e}^{+s_2} \frac{1}{s_2^{N-1}} \\ &= \frac{C_N \pi^{2N-1}}{\Gamma(N)\Gamma(N-1)},\end{aligned}$$

which gives us

$$C_N = \frac{\Gamma(N)\Gamma(N-1)}{\pi^{2N-1}}. \tag{C.11}$$

C.2.1 4-Point Correlations

$$\begin{aligned}&\langle x_1\, x_2\, y_1\, y_2 \rangle_{GUE} \\ &= \int dx_1 dx_2 dy_1 dy_2 \; x_1 x_2 y_1 y_2 P^{GUE}(x_1, x_2, y_1, y_2) \\ &= C_N \int dx_1 dx_2 dy_1 dy_2 \; x_1 x_2 y_1 y_2 \oint \frac{ds_1}{2\pi \mathrm{i}} \mathrm{e}^{+s_1 t_1} \oint \frac{ds_2}{2\pi \mathrm{i}} \mathrm{e}^{+s_2 t_2} \oint \frac{ds_3}{2\pi \mathrm{i}} \mathrm{e}^{+s_3 t_3} \oint \frac{ds_4}{2\pi \mathrm{i}} \mathrm{e}^{+s_4 t_4} \\ &\quad \times \mathrm{e}^{-(\bar{v}_R^2 + \bar{v}_I^2)s_1} \mathrm{e}^{-(\bar{w}_R^2 + \bar{w}_I^2)s_2} \mathrm{e}^{-(\bar{v}_R . \bar{w}_R + \bar{v}_I . \bar{w}_I)s_3} \mathrm{e}^{-(\bar{v}_R . \bar{w}_I - \bar{v}_I . \bar{w}_R)s_4} \\ &\quad \times \delta(x_1 - v_1^2) \delta(x_2 - |v_2|^2) \delta(y_1 - |w_1|^2) \delta(y_2 - |w_2|^2) \\ &= C_N \oint \frac{ds_1}{2\pi \mathrm{i}} \mathrm{e}^{+s_1 t_1} \oint \frac{ds_2}{2\pi \mathrm{i}} \mathrm{e}^{+s_2 t_2} \oint \frac{ds_3}{2\pi \mathrm{i}} \mathrm{e}^{+s_3 t_3} \oint \frac{ds_4}{2\pi \mathrm{i}} \mathrm{e}^{+s_4 t_4} \\ &\quad \times \frac{\pi^{2N-4}}{(s_1 s_2 - \frac{(s_3^2+s_4^2)}{4})^{N-2}} \times \pi^4 \frac{(s_1 s_2 + \frac{(s_3^2+s_4^2)}{4})^2}{(s_1 s_2 - \frac{(s_3^2+s_4^2)}{4})^6} \\ &= C_N \pi^{2N} (I_1 + I_2 + I_3).\end{aligned}$$

Here

$$I_1 = \oint \frac{ds_1}{2\pi \mathrm{i}} \mathrm{e}^{+s_1 t_1} \oint \frac{ds_2}{2\pi \mathrm{i}} \mathrm{e}^{+s_2 t_2} \oint \frac{ds_3}{2\pi \mathrm{i}} \mathrm{e}^{+s_3 t_3} \oint \frac{ds_4}{2\pi \mathrm{i}} \mathrm{e}^{+s_4 t_4} \frac{1}{(s_1 s_2 - \frac{(s_3^2+s_4^2)}{4})^{N+2}}$$

$$= \frac{\pi^{-1}}{\Gamma(N+1)\Gamma(N+2)}$$

$$I_2 = \oint \frac{ds_1}{2\pi \mathrm{i}} \mathrm{e}^{+s_1 t_1} \oint \frac{ds_2}{2\pi \mathrm{i}} \mathrm{e}^{+s_2 t_2} \oint \frac{ds_3}{2\pi \mathrm{i}} \mathrm{e}^{+s_3 t_3} \oint \frac{ds_4}{2\pi \mathrm{i}} \mathrm{e}^{+s_4 t_4} \frac{(s_3^2 + s_4^2)}{(s_1 s_2 - \frac{(s_3^2+s_4^2)}{4})^{N+3}}$$

$$= \frac{-4\pi^{-1}}{\Gamma(N+1)\Gamma(N+3)}$$

$$I_3 = \oint \frac{ds_1}{2\pi \mathrm{i}} \mathrm{e}^{+s_1 t_1} \oint \frac{ds_2}{2\pi \mathrm{i}} \mathrm{e}^{+s_2 t_2} \oint \frac{ds_3}{2\pi \mathrm{i}} \mathrm{e}^{+s_3 t_3} \oint \frac{ds_4}{2\pi \mathrm{i}} \mathrm{e}^{+s_4 t_4} \frac{(s_3^2 + s_4^2)^2}{4(s_1 s_2 - \frac{(s_3^2+s_4^2)}{4})^{N+4}}$$

$$= \frac{8\pi^{-1}}{4\Gamma(N+1)\Gamma(N+4)}.$$

This gives us

$$\langle x_1\, x_2\, y_1\, y_2 \rangle_{GUE} = \frac{N^2 + N + 2}{(N-1)N^2(N+1)(N+2)(N+3)}. \tag{C.12}$$

Appendix D
Eigenvector Statistics of a Random Hamiltonian

The eigenvectors of a random Hamiltonian $H = \sum_n^N E_n|\psi_n\rangle\langle\psi_n|$ can be written in terms of a known or preferred basis, $\{|ab\rangle\}$, of the hilbert space, $\mathcal{H}_A \otimes \mathcal{H}_B$, of the composite system $A + B$. Then we can write $|\psi_n\rangle = \sum_{n,a,b} c_{nab}|ab\rangle$. The statistics of the components c_{nab} can then be obtained for various random matrix ensembles. We will derive some of these statistics for the GOE and GUE ensembles. Using the PDF of the components of one eigenvector, we can calculate

$$\langle |c_{ma}|^{2r} \rangle = \begin{cases} \frac{\Gamma(r+\frac{1}{2})\Gamma(\frac{N}{2})}{\sqrt{\pi}\Gamma(\frac{N}{2}+r)} & GOE \\ \frac{\Gamma(r+1)\Gamma(N)}{\Gamma(N+r)} & GUE \end{cases}, \tag{D.1}$$

$$\langle (|c_{ma}|^2 + |c_{mb}|^2)^r \rangle = \begin{cases} \frac{\Gamma(r+1)\Gamma(\frac{N}{2})}{\Gamma(\frac{N}{2}+r)} & GOE \\ \frac{\Gamma(r+2)\Gamma(N)}{\Gamma(N+r)} & GUE \end{cases}, \tag{D.2}$$

$$\langle (|c_{ma}|^2 + |c_{mb}|^2 + |c_{mc}|^2)^r \rangle = \begin{cases} \frac{2\Gamma(r+\frac{3}{2})\Gamma(\frac{N}{2})}{\sqrt{\pi}\Gamma(\frac{N}{2}+r)} & GOE \\ \frac{\Gamma(r+3)\Gamma(N)}{2\Gamma(N+r)} & GUE \end{cases}. \tag{D.3}$$

From these results, we can derive the following averages,

$$\langle |c_{ma}|^2 |c_{mb}|^2 \rangle = \begin{cases} \frac{1}{N(N+2)} & GOE \\ \frac{1}{N(N+1)} & GUE \end{cases}, \tag{D.4}$$

$$\langle |c_{ma}|^2 |c_{mb}|^4 \rangle = \begin{cases} \frac{3}{N(N+2)(N+4)} & GOE \\ \frac{2}{N(N+1)(N+2)} & GUE \end{cases}, \tag{D.5}$$

$$\langle |c_{ma}|^2 |c_{mb}|^2 |c_{mc}|^2 \rangle = \begin{cases} \frac{1}{N(N+2)(N+4)} & GOE \\ \frac{1}{N(N+1)(N+2)} & GUE \end{cases}, \tag{D.6}$$

$$\langle |c_{ma}|^2 |c_{mb}|^6 \rangle = \begin{cases} \frac{15}{N(N+2)(N+4)(N+6)} & GOE \\ \frac{6}{N(N+1)(N+2)(N+3)} & GUE \end{cases}, \tag{D.7}$$

$$\langle |c_{ma}|^4 |c_{mb}|^4 \rangle = \begin{cases} \frac{9}{N(N+2)(N+4)(N+6)} & GOE \\ \frac{4}{N(N+1)(N+2)(N+3)} & GUE \end{cases}, \tag{D.8}$$

$$\langle |c_{ma}|^4 |c_{mb}|^2 |c_{mc}|^2 \rangle = \begin{cases} \frac{3}{N(N+2)(N+4)(N+6)} & GOE \\ \frac{2}{N(N+1)(N+2)(N+3)} & GUE \end{cases}. \tag{D.9}$$

Moreover, from the result obtained in Appendix C, we can calculate

$$\langle |c_{ma}|^2 |c_{mb}|^2 |c_{na}|^2 |c_{nb}|^2 \rangle = \begin{cases} \frac{N^2+4N+15}{(N-1)N(N+1)(N+2)(N+4)(N+6)} & GOE \\ \frac{N^2+N+2}{(N-1)N^2(N+1)(N+2)(N+3)} & GUE \end{cases}, \tag{D.10}$$

$$\langle |c_{ma}|^2 |c_{mb}|^2 |c_{na}|^2 |c_{nc}|^2 \rangle = \begin{cases} \frac{N^2+6N+9}{(N-1)N(N+1)(N+2)(N+4)(N+6)} & GOE \\ \frac{N+1}{(N-1)N^2(N+2)(N+3)} & GUE \end{cases}, \tag{D.11}$$

From the orthogonality of the two bases, we have

$$\begin{aligned} & \sum_a \left\langle c_{na} c_{ma}^* \right\rangle_{n \neq m} = 0 \\ \Longrightarrow \ & \sum_a \sum_{a'} \left\langle c_{na} c_{ma}^* c_{na'}^* c_{ma'} \right\rangle_{n \neq m} = 0 \\ \Longrightarrow \ & N \left\langle |c_{na}|^2 |c_{ma}|^2 \right\rangle_{n \neq m} + N(N-1) \left\langle c_{na} c_{ma}^* c_{na'}^* c_{ma'} \right\rangle_{a \neq a', m \neq n} = 0 \\ \Longrightarrow \ & \left\langle c_{na} c_{ma}^* c_{na'}^* c_{ma'} \right\rangle_{a \neq a', m \neq n} = \begin{cases} \frac{-1}{(N-1)N(N+2)} & GOE \\ \frac{-1}{(N-1)N(N+1)} & GUE \end{cases}. \end{aligned} \tag{D.12}$$

On similar lines, we can derive

$$\langle |c_{na}|^2 |c_{ma}|^2 c_{na} c_{ma}^* c_{nb}^* c_{mb} \rangle_{a\neq b, m\neq n} = \begin{cases} -\frac{9}{(N-1)N(N+2)(N+4)(N+6)} & GOE \\ -\frac{4}{(N-1)N(N+1)(N+2)(N+3)} & GUE \end{cases}, \quad \text{(D.13)}$$

$$\langle |c_{na}|^2 |c_{ma}|^2 c_{nb} c_{mb}^* c_{nc}^* c_{mc} \rangle_{a\neq b\neq c, m\neq n} = \begin{cases} -\frac{N-3}{(N-1)N(N+1)(N+2)(N+4)(N+6)} & GOE \\ -\frac{1}{N^2(N+1)(N+2)(N+3)} & GUE \end{cases}. \quad \text{(D.14)}$$

Bibliography

[1] Deutsch, J. M. (1991) "Quantum statistical mechanics in a closed system," *Phys. Rev. A*, **43**(4), p. 2046.

[2] Srednicki, M. (1994) "Chaos and Quantum Thermalization," *Phys. Rev. E*, **50**, cond-mat/9403051.

[3] Rigol, M., V. Dunjko, and M. Olshanii (2008) "Thermalization and its mechanism for generic isolated quantum systems," *Nature*, **452**(7189), pp. 854–858, 0708.1324.

[4] Page, D. N. (1993) "Information in black hole radiation," *Phys. Rev. Lett.*, **71**, pp. 3743–3746, hep-th/9306083.

[5] Bianchi, E., P. Dona, and R. Kumar (2024) "Non-Abelian symmetry-resolved entanglement entropy," *SciPost Phys.*, **17**, p. 127.
URL https://scipost.org/10.21468/SciPostPhys.17.5.127

[6] Nielsen, M. A. and I. L. Chuang (2010) *Quantum Computation and Quantum Information: 10th Anniversary Edition*, Cambridge University Press.

[7] Kaufman, A. M., M. E. Tai, A. Lukin, M. Rispoli, R. Schittko, P. M. Preiss, and M. Greiner (2016) "Quantum thermalization through entanglement in an isolated many-body system," *Science*, **353**(6301), p. aaf6725.

[8] Bohigas, O., M. J. Giannoni, and C. Schmit (1984) "Characterization of chaotic quantum spectra and universality of level fluctuation laws," *Phys. Rev. Lett.*, **52**, pp. 1–4.

[9] D'Alessio, L., Y. Kafri, A. Polkovnikov, and M. Rigol (2016) "From quantum chaos and eigenstate thermalization to statistical mechanics and thermodynamics," *Adv. Phys.*, **65**(3), pp. 239–362, 1509.06411.

[10] Mondaini, R. and M. Rigol (2017) "Eigenstate thermalization in the two-dimensional transverse field Ising model. II. Off-diagonal matrix elements of observables," *Phys. Rev. E*, **96**(1), p. 012157.

[11] Richter, J., A. Dymarsky, R. Steinigeweg, and J. Gemmer (2020) "Eigenstate thermalization hypothesis beyond standard indicators: Emergence of random-matrix behavior at small frequencies," *Phys. Rev. E*, **102**(4), p. 042127, 2007.15070.

[12] Schönle, C., D. Jansen, F. Heidrich-Meisner, and L. Vidmar (2021) "Eigenstate thermalization hypothesis through the lens of autocorrelation functions," *Phys. Rev. B*, **103**(23), p. 235137, 2011.13958.

[13] Bianchi, E., L. Hackl, M. Kieburg, M. Rigol, and L. Vidmar (2022) "Volume-Law Entanglement Entropy of Typical Pure Quantum States," *PRX Quantum*, **3**(3), p. 030201, 2112.06959.

[14] Murciano, S., P. Calabrese, and L. Piroli (2022) "Symmetry-resolved Page curves," *Phys. Rev. D*, **106**(4), p. 046015, 2206.05083.

[15] Lau, P. H. C., T. Noumi, Y. Takii, and K. Tamaoka (2022) "Page curve and symmetries," *JHEP*, **10**, p. 015, 2206.09633.

[16] Cheng, Y., R. Patil, Y. Zhang, M. Rigol, and L. Hackl (2023) "Typical entanglement entropy in systems with particle-number conservation," 2310.19862.

[17] Kliczkowski, M., R. Świętek, L. Vidmar, and M. Rigol (2023) "Average entanglement entropy of midspectrum eigenstates of quantum-chaotic interacting Hamiltonians," *Phys. Rev. E*, **107**(6), p. 064119, 2303.13577.

[18] Świętek, R., M. Kliczkowski, L. Vidmar, and M. Rigol (2024) "Eigenstate entanglement entropy in the integrable spin-1/2 XYZ model," *Phys. Rev. E*, **109**(2), p. 024117, 2311.10819.

[19] Rodriguez-Nieva, J. F., C. Jonay, and V. Khemani (2023) "Quantifying quantum chaos through microcanonical distributions of entanglement," 2305.11940.

[20] Langlett, C. M. and J. F. Rodriguez-Nieva (2024) "Entanglement patterns of quantum chaotic Hamiltonians with a scalar U(1) charge," 2403.10600.

[21] Page, D. N. (1993) "Average entropy of a subsystem," *Phys. Rev. Lett.*, **71**, pp. 1291–1294, gr-qc/9305007.

[22] Vidmar, L. and M. Rigol (2017) "Entanglement Entropy of Eigenstates of Quantum Chaotic Hamiltonians," *Phys. Rev. Lett.*, **119**(22), p. 220603, 1708.08453.

[23] Hawking, S. W. (1976) "Breakdown of Predictability in Gravitational Collapse," *Phys. Rev. D*, **14**, pp. 2460–2473.

[24] Marolf, D. (2017) "The Black Hole information problem: past, present, and future," *Rept. Prog. Phys.*, **80**(9), p. 092001, 1703.02143.

[25] Laflorencie, N. and S. Rachel (2014) "Spin-resolved entanglement spectroscopy of critical spin chains and Luttinger liquids," *J. Phys. A*, **2014**(11), p. P11013.

[26] Goldstein, M. and E. Sela (2018) "Symmetry-resolved entanglement in many-body systems," *Phys. Rev. Lett.*, **120**(20), p. 200602, 1711.09418.

[27] Xavier, J. C., F. C. Alcaraz, and G. Sierra (2018) "Equipartition of the entanglement entropy," *Phys. Rev. B*, **98**(4), p. 041106, 1804.06357.

[28] Bartlett, S. D. and H. M. Wiseman (2003) "Entanglement Constrained by Superselection Rules," *Phys. Rev. Lett.*, **91**, p. 097903, quant-ph/0303140.
URL https://link.aps.org/doi/10.1103/PhysRevLett.91.097903

[29] Bartlett, S. D., T. Rudolph, and R. W. Spekkens (2007) "Reference frames, superselection rules, and quantum information," *Rev. Mod. Phys.*, **79**, pp. 555–609, quant-ph/0610030.

[30] Barghathi, H., C. M. Herdman, and A. D. Maestro (2018) "Rényi Generalization of the Accessible Entanglement Entropy," *Phys. Rev. Lett.*, **121**(15), p. 150501, 1804.01114.

[31] Barghathi, H., E. Casiano-Diaz, and A. Del Maestro (2019) "Operationally accessible entanglement of one-dimensional spinless fermions," *Phys. Rev. A*, **100**(2), p. 022324, 1905.03312.

[32] de Groot, C., D. T. Stephen, A. Molnar, and N. Schuch (2020) "Inaccessible entanglement in symmetry protected topological phases," *J. Phys. A*, **53**(33), p. 335302, 2003.06830.

[33] Monkman, K. and J. Sirker (2020) "Operational entanglement of symmetry-protected topological edge states," *Phys. Rev. Res.*, **2**(4), p. 043191, 2005.13026.

[34] Casini, H., M. Huerta, J. M. Magán, and D. Pontello (2020) "Entanglement entropy and superselection sectors. Part I. Global symmetries," *JHEP*, **02**, p. 014, 1905.10487.

[35] Tan, M. T. and S. Ryu (2020) "Particle number fluctuations, Rényi entropy, and symmetry-resolved entanglement entropy in a two-dimensional Fermi gas from multidimensional bosonization," *Phys. Rev. B*, **101**(23), p. 235169, 1911.01451.

[36] Bonsignori, R., P. Ruggiero, and P. Calabrese (2019) "Symmetry resolved entanglement in free fermionic systems," *J. Phys. A*, **52**(47), p. 475302, 1907.02084.

[37] Murciano, S., G. Di Giulio, and P. Calabrese (2020) "Symmetry resolved entanglement in gapped integrable systems: a corner transfer matrix approach," *SciPost Phys.*, **8**, p. 046, 1911.09588.

[38] Azses, D. and E. Sela (2020) "Symmetry-resolved entanglement in symmetry-protected topological phases," *Phys. Rev. B*, **102**(23), p. 235157, 2008.09332.

[39] Murciano, S., P. Ruggiero, and P. Calabrese (2020) "Symmetry resolved entanglement in two-dimensional systems via dimensional reduction," *J. Stat. Mech.*, **2008**, p. 083102, 2003.11453.

[40] Estienne, B., Y. Ikhlef, and A. Morin-Duchesne (2021) "Finite-size corrections in critical symmetry-resolved entanglement," *SciPost Phys.*, **10**(3), p. 054, 2010.10515.

[41] Murciano, S., R. Bonsignori, and P. Calabrese (2021) "Symmetry decomposition of negativity of massless free fermions," *SciPost Phys.*, **10**(5), p. 111, 2102.10054.

[42] Oblak, B., N. Regnault, and B. Estienne (2022) "Equipartition of entanglement in quantum Hall states," *Phys. Rev. B*, **105**(11), p. 115131, 2112.13854.

[43] Neven, A. et al. (2021) "Symmetry-resolved entanglement detection using partial transpose moments," *npj Quantum Inf.*, **7**, p. 152, 2103.07443.

[44] Vitale, V., A. Elben, R. Kueng, A. Neven, J. Carrasco, B. Kraus, P. Zoller, P. Calabrese, B. Vermersch, and M. Dalmonte (2022) "Symmetry-resolved dynamical purification in synthetic quantum matter," *SciPost Phys.*, **12**(3), p. 106, 2101.07814.

[45] Ares, F., S. Murciano, and P. Calabrese (2023) "Entanglement asymmetry as a probe of symmetry breaking," *Nature Commun.*, **14**(1), p. 2036, 2207.14693.

[46] Jones, N. G. (2022) "Symmetry-Resolved Entanglement Entropy in Critical Free-Fermion Chains," *J. Stat. Phys.*, **188**(3), p. 28, 2202.11728.

[47] Piroli, L., E. Vernier, M. Collura, and P. Calabrese (2022) "Thermodynamic symmetry resolved entanglement entropies in integrable systems," *J. Stat. Mech.*, **2022**(7), p. 073102, 2203.09158.
URL https://dx.doi.org/10.1088/1742-5468/ac7a2d

[48] Scopa, S. and D. X. Horváth (2022) "Exact hydrodynamic description of symmetry-resolved Rényi entropies after a quantum quench," *J. Stat. Mech.*, **2208**(8), p. 083104, 2205.02924.

[49] Parez, G. (2022) "Symmetry-resolved Rényi fidelities and quantum phase transitions," *Phys. Rev. B*, **106**(23), p. 235101, 2208.09457.

[50] Rath, A., V. Vitale, S. Murciano, M. Votto, J. Dubail, R. Kueng, C. Branciard, P. Calabrese, and B. Vermersch (2023) "Entanglement Barrier and its Symmetry Resolution: Theory and Experimental Observation," *PRX Quantum*, **4**(1), p. 010318, 2209.04393.

[51] Feldman, N., J. Knaute, E. Zohar, and M. Goldstein (2024) "Superselection-Resolved Entanglement in Lattice Gauge Theories: A Tensor Network Approach," 2401.01942.

[52] Belin, A., L.-Y. Hung, A. Maloney, S. Matsuura, R. C. Myers, and T. Sierens (2013) "Holographic Charged Renyi Entropies," *JHEP*, **12**, p. 059, 1310.4180.

[53] Caputa, P., G. Mandal, and R. Sinha (2013) "Dynamical entanglement entropy with angular momentum and U(1) charge," *JHEP*, **11**, p. 052, 1306.4974.

[54] Feldman, N. and M. Goldstein (2019) "Dynamics of Charge-Resolved Entanglement after a Local Quench," *Phys. Rev. B*, **100**(23), p. 235146, 1905.10749.

[55] Fraenkel, S. and M. Goldstein (2020) "Symmetry resolved entanglement: Exact results in 1D and beyond," *J. Stat. Mech.*, **2003**(3), p. 033106, 1910.08459.

[56] Zhao, S., C. Northe, and R. Meyer (2021) "Symmetry-resolved entanglement in AdS_3/CFT_2 coupled to U(1) Chern-Simons theory," *JHEP*, **07**, p. 030, 2012.11274.

[57] Chen, H.-H. (2021) "Symmetry decomposition of relative entropies in conformal field theory," *JHEP*, **07**, p. 084, 2104.03102.

[58] Horvath, D. X., L. Capizzi, and P. Calabrese (2021) "U(1) symmetry resolved entanglement in free 1+1 dimensional field theories via form factor bootstrap," *JHEP*, **05**, p. 197, 2103.03197.

[59] Gaur, H. and U. A. Yajnik (2023) "Symmetry resolved entanglement entropy in hyperbolic de Sitter space," *Phys. Rev. D*, **107**(12), p. 125008, 2211.11218.

[60] Ghasemi, M. (2023) "Universal thermal corrections to symmetry-resolved entanglement entropy and full counting statistics," *JHEP*, **05**, p. 209, 2203.06708.

[61] Capizzi, L., O. A. Castro-Alvaredo, C. De Fazio, M. Mazzoni, and L. Santamaría-Sanz (2022) "Symmetry resolved entanglement of excited states in quantum field theory. Part I. Free theories, twist fields and qubits," *JHEP*, **12**, p. 127, 2203.12556.

[62] Capizzi, L., C. De Fazio, M. Mazzoni, L. Santamaría-Sanz, and O. A. Castro-Alvaredo (2022) "Symmetry resolved entanglement of excited states in quantum field theory. Part II. Numerics, interacting theories and higher dimensions," *JHEP*, **12**, p. 128, 2206.12223.

[63] Gaur, H. and U. A. Yajnik (2024) "Multi-charged moments and symmetry-resolved Rényi entropy of free compact boson for multiple disjoint intervals," *JHEP*, **01**, p. 042, 2310.14186.

[64] Di Giulio, G. and J. Erdmenger (2023) "Symmetry-resolved modular correlation functions in free fermionic theories," *JHEP*, **07**, p. 058, 2305.02343.

[65] Castro-Alvaredo, O. A. and L. Santamaría-Sanz (2024) "Symmetry Resolved Measures in Quantum Field Theory: a Short Review," 2403.06652.

[66] Sachdev, S. (2023) *Quantum Phases of Matter*, Cambridge University Press.

[67] Tasaki, H. (2020) *Physics and Mathematics of Quantum Many-Body Systems*, Graduate Texts in Physics, Springer Cham.

[68] Iniguez, F. and M. Srednicki (2023) "Microcanonical Truncations of Observables in Quantum Chaotic Systems," 2305.15702.

[69] Bianchi, E. and P. Dona (2019) "Typical entanglement entropy in the presence of a center: Page curve and its variance," *Phys. Rev. D*, **100**(10), p. 105010, 1904.08370.

[70] Foong, S. K. and S. Kanno (1994) "Proof of Page's conjecture on the average entropy of a subsystem," *Phys. Rev. Lett.*, **72**(8), p. 1148.

[71] Sánchez-Ruiz, J. (1995) "Simple proof of Page's conjecture on the average entropy of a subsystem," *Phys. Rev. E*, **52**, pp. 5653–5655.
URL https://link.aps.org/doi/10.1103/PhysRevE.52.5653

[72] Sen, S. (1996) "Average entropy of a subsystem," *Phys. Rev. Lett.*, **77**, pp. 1–3, hep-th/9601132.

[73] Lloyd, S. and H. Pagels (1988) "COMPLEXITY AS THERMODYNAMIC DEPTH," *Annals Phys.*, **188**, p. 186.

[74] Petz, D. (2007) *Quantum Information Theory and Quantum Statistics*, Theoretical and Mathematical Physics, Springer Berlin Heidelberg.

[75] Moretti, V. (2019) *Fundamental Mathematical Structures of Quantum Theory: Spectral Theory, Foundational Issues, Symmetries, Algebraic Formulation*, Springer International Publishing.

[76] Hollands, S. and K. Sanders (2018) *Entanglement measures and their properties in quantum field theory*, SpringerBriefs in Mathematical Physics, Springer Nature Switzerland, 1702.04924.

[77] Witten, E. (2018) "On entanglement properties of quantum field theory," *Rev. Mod. Phys.*, **90**(4), p. 045003, 1803.04993.

[78] Casini, H. and M. Huerta (2023) "Lectures on entanglement in quantum field theory," *PoS*, **TASI2021**, p. 002, 2201.13310.

[79] Sorce, J. (2024) "Notes on the type classification of von Neumann algebras," *Rev. Math. Phys.*, **36**(02), p. 2430002, 2302.01958.

[80] Casini, H., M. Huerta, and J. A. Rosabal (2014) "Remarks on entanglement entropy for gauge fields," *Phys. Rev. D*, **89**(8), p. 085012, 1312.1183.

[81] Huang, X. and C.-T. Ma (2020) "Analysis of the Entanglement with Centers," *J. Stat. Mech.*, **2005**, p. 053101, 1607.06750.

[82] Lin, J. and D. Radičević (2020) "Comments on defining entanglement entropy," *Nucl. Phys. B*, **958**, p. 115118, 1808.05939.

[83] Langenscheidt, S., D. Oriti, and E. Colafranceschi (2024) "Channel-State duality with centers," 2404.16004.

[84] Moudgalya, S. and O. I. Motrunich (2022) "Hilbert Space Fragmentation and Commutant Algebras," *Phys. Rev. X*, **12**, p. 011050, 2108.10324.

[85] ——— (2023) "Numerical methods for detecting symmetries and commutant algebras," *Phys. Rev. B*, **107**(22), p. 224312, 2302.03028.

[86] Nielsen, M. A. and I. L. Chuang (2010) *Quantum Computation and Quantum Information*, Cambridge University Press.

[87] Gilmore, R. (2008) *Lie Groups, Physics, and Geometry: An Introduction for Physicists, Engineers and Chemists*, Cambridge University Press.

[88] Georgi, H. (2018) *Lie algebras in particle physics*, CRC Press, Boca Raton.

[89] Fuchs, J. and C. Schweigert (2003) *Symmetries, Lie algebras and representations: A graduate course for physicists*, Cambridge University Press.

[90] Racah, G. *Group theory and spectroscopy*, CERN, Geneva (1961), Reprinted in: Ergebnisse der exakten Naturwissenschaften, Bd. 37 (1965), Springer Berlin Heidelberg.

[91] Perelomov, A. M. and V. S. Popov (1968) "Casimir operators for semisimple Lie groups," *Mathematics of the USSR-Izvestiya*, **2**(6), p. 1313. URL https://dx.doi.org/10.1070/IM1968v002n06ABEH000731

[92] Bianchi, E., P. Dona, and S. Speziale (2011) "Polyhedra in loop quantum gravity," *Phys. Rev. D*, **83**, p. 044035, 1009.3402.

[93] Bianchi, E. and H. M. Haggard (2011) "Discreteness of the volume of space from Bohr-Sommerfeld quantization," *Phys. Rev. Lett.*, **107**, p. 011301, 1102.5439.

[94] Amico, L., R. Fazio, A. Osterloh, and V. Vedral (2008) "Entanglement in many-body systems," *Rev. Mod. Phys.*, **80**, pp. 517–576, quant-ph/0703044.

[95] Varshalovich, D. A., A. N. Moskalev, and V. K. Khersonskii (1988) *Quantum Theory of Angular Momentum*, World Scientific, Singapore.

[96] Rovelli, C. and F. Vidotto (2014) *Covariant Loop Quantum Gravity*, Cambridge Monographs on Mathematical Physics, Cambridge University Press.

[97] Ashtekar, A. and E. Bianchi (2021) "A short review of loop quantum gravity," *Rept. Prog. Phys.*, **84**(4), p. 042001, 2104.04394.

[98] Noh, J. D. (2023) "Eigenstate thermalization hypothesis in two-dimensional XXZ model with or without SU(2) symmetry," *Phys. Rev. E*, **107**(1), p. 014130, 2210.14589.

[99] Patil, R., L. Hackl, G. R. Fagan, and M. Rigol (2023) "Average pure-state entanglement entropy in spin systems with SU(2) symmetry," *Phys. Rev. B*, **108**(24), p. 245101, 2305.11211.

[100] Majidy, S., A. Lasek, D. A. Huse, and N. Yunger Halpern (2023) "Non-Abelian symmetry can increase entanglement entropy," *Phys. Rev. B*, **107**(4), p. 045102, 2209.14303.

[101] Bianchi, E. and R. C. Myers (2014) "On the architecture of spacetime geometry," *Classical and Quantum Gravity*, **31**(21), p. 214002.
URL https://dx.doi.org/10.1088/0264-9381/31/21/214002

[102] Livine, E. R. and S. Speziale (2007) "New spinfoam vertex for quantum gravity," *Phys. Rev. D*, **76**, p. 084028.
URL https://link.aps.org/doi/10.1103/PhysRevD.76.084028

[103] Bianchi, E., J. Guglielmon, L. Hackl, and N. Yokomizo (2016) "Loop expansion and the bosonic representation of loop quantum gravity," *Phys. Rev. D*, **94**, p. 086009.
URL https://link.aps.org/doi/10.1103/PhysRevD.94.086009

[104] Freidel, L. and E. R. Livine (2010) "The fine structure of SU(2) intertwiners from U(N) representations," *Journal of Mathematical Physics*, **51**(8), p. 082502.
URL https://doi.org/10.1063/1.3473786

[105] Yunger Halpern, N., P. Faist, J. Oppenheim, and A. Winter (2016) "Microcanonical and resource-theoretic derivations of the thermal state of a quantum system with noncommuting charges," *Nature Communications*, **7**, p. 12051.
URL https://doi.org/10.1038/ncomms12051

[106] Yunger Halpern, N., M. E. Beverland, and A. Kalev (2020) "Noncommuting conserved charges in quantum many-body thermalization," *Phys. Rev. E*, **101**(4), p. 042117, 1906.09227.

[107] Majidy, S., W. F. Braasch, A. Lasek, T. Upadhyaya, A. Kalev, and N. Yunger Halpern (2023) "Noncommuting conserved charges in quantum thermodynamics and beyond," *Nature Rev. Phys.*, **5**(11), pp. 689–698, 2306.00054.

[108] Murthy, C., A. Babakhani, F. Iniguez, M. Srednicki, and N. Yunger Halpern (2023) "Non-Abelian Eigenstate Thermalization Hypothesis," *Phys. Rev. Lett.*, **130**(14), p. 140402, 2206.05310.

[109] O'Dea, N., F. Burnell, A. Chandran, and V. Khemani (2020) "From tunnels to towers: quantum scars from Lie Algebras and q-deformed Lie Algebras," *Phys. Rev. Res.*, **2**(4), p. 043305, 2007.16207.

[110] Moudgalya, S., B. A. Bernevig, and N. Regnault (2022) "Quantum many-body scars and Hilbert space fragmentation: a review of exact results," *Rept. Prog. Phys.*, **85**(8), p. 086501, 2109.00548.

[111] Kehrein, S. (2024) "Page curve entanglement dynamics in an analytically solvable model," *Phys. Rev. B*, **109**, p. 224308.
URL https://link.aps.org/doi/10.1103/PhysRevB.109.224308

[112] Ebner, L., A. Schäfer, C. Seidl, B. Müller, and X. Yao (2024) "Entanglement Entropy of (2 + 1)-Dimensional SU(2) Lattice Gauge Theory," 2401.15184.

[113] Bianchi, E. and E. R. Livine "Loop Quantum Gravity and Quantum Information," *in "Handbook of Quantum Gravity" (Eds. C. Bambi, L. Modesto and I.L. Shapiro), Springer Nature, Singapore (2023),*, 2302.05922.

[114] Bianchi, E., L. Hackl, and N. Yokomizo (2015) "Entanglement entropy of squeezed vacua on a lattice," *Phys. Rev. D*, **92**(8), p. 085045, 1507.01567.

[115] Baytaş, B., E. Bianchi, and N. Yokomizo (2018) "Gluing polyhedra with entanglement in loop quantum gravity," *Phys. Rev. D*, **98**(2), p. 026001, 1805.05856.

[116] Bianchi, E., P. Donà, and I. Vilensky (2019) "Entanglement entropy of Bell-network states in loop quantum gravity: Analytical and numerical results," *Phys. Rev. D*, **99**(8), p. 086013, 1812.10996.

[117] Bianchi, E. and A. Satz (2019) "Entropy of a subalgebra of observables and the geometric entanglement entropy," *Phys. Rev. D*, **99**(8), p. 085001, 1901.06454.

[118] Agullo, I., B. Bonga, P. Ribes-Metidieri, D. Kranas, and S. Nadal-Gisbert (2023) "How ubiquitous is entanglement in quantum field theory?" *Phys. Rev. D*, **108**(8), p. 085005, 2302.13742.

[119] Erdélyi, A. (1956) *Asymptotic Expansions*, Dover Books on Mathematics, Dover Publications.

[120] Bianchi, E., L. Hackl, and M. Kieburg (2021) "Page curve for fermionic Gaussian states," *Phys. Rev. B*, **103**(24), p. L241118, 2103.05416.

[121] Vidmar, L., L. Hackl, E. Bianchi, and M. Rigol (2017) "Entanglement Entropy of Eigenstates of Quadratic Fermionic Hamiltonians," *Phys. Rev. Lett.*, **119**(2), p. 020601, 1703.02979.

Vita

Rishabh Kumar

Rishabh joined the Indian Institute of Technology, Delhi (IIT Delhi) for his undergraduate studies in July 2014. He completed a bachelor's degree in Engineering Physics in July 2018, following which he joined The Pennsylvania State University to pursue his graduate studies at the Department of Physics. He worked under the guidance of Prof. Eugenio Bianchi at the Institute for Gravitation and the Cosmos between 2019 and 2025 on topics covering quantum entanglement, symmetries and random Hamiltonians. He defended his dissertation in February 2025.